EVALUATION OF INFILTRATION USING THE GREEN-AMPT MODEL AND RAINFALL-RUNOFF DATA FOR LAGAN AND SAMBRET CATCHMENTS, KERICHO, KENYA

By

JOHN PAUL ODHIAMBO OBIERO

B.Sc. Agric. Eng.

Thesis submitted to the Department of Agricultural Engineering of the University of Nairobi in partial fulfilment of the requirements for the degree of **MASTER OF SCIENCE IN AGRICULTURAL ENGINEERING** (Soil and Water Engineering).

UNIVERSITY OF NAIROBI

1996

DECLARATION

I hereby declare that this thesis is my original work and has not been presented for a degree in any other University. All sources of information have been acknowledged.

....17/6/96.....

J.P.O. Obiero **Date**

This Thesis has been submitted for examination with my approval as University supervisor.

....17/6/96.....

Prof. T.C. Sharma **Date**

Moi University

Eldoret, Kenya

DEDICATION

This Thesis is dedicated to my parents, brothers, sisters, friends and other close relatives for their understanding, encouragement, patience and support during the preparation of this work.

TABLE OF CONTENTS

LIST OF TABLES i

LIST OF FIGURES iii

LIST OF SYMBOLS AND ABBREVIATIONS vi

ACKNOWLEDGEMENTS viii

ABSTRACT ix

1. INTRODUCTION 1

1.1 General Background 1

1.2 Justification 2

1.3 Objectives and Scope of the Study 6

1.4 The Study Area 7

2. LITERATURE REVIEW 12

2.1 Infiltration Related Studies in Kenya 12

2.2 Infiltration Equations and Models 13

2.2.1 Kostiakov Equation (Proposed in 1932) 14

2.2.2 Horton Equation (Proposed in 1940) 15

2.2.3 Richards Equation (Proposed in 1931) 15

2.2.4 Phillips Equation (Proposed in 1957) 16

2.2.5 Holtan Equation (Proposed in 1961) 17

2.2.6 The Green-Ampt Infiltration Model for Ponded Conditions (Proposed in 1911) 18

2.2.7 Application of Green-Ampt Model to Rainfall Infiltration 21

2.2.8 Determination of Green-Ampt Model Parameters 24

2.2.8.1 Hydraulic Conductivity 24

2.2.8.2 Wetting Front Suction 25

2.2.8.3 Effective Porosity 27

2.2.8.4 Antecedent Moisture Content 27

2.3 Measurement of Infiltration 27

2.3.1 Ring Infiltrometers 28

2.3.2 The Sprinkling Infiltrometer 30

2.3.3 Drainage Basin Rainfall-Runoff Analysis . . . 30

2.4 Interception Losses 31

2.5 Depression Storage 31

3. MATERIALS AND METHODS 34

3.1 Data Acquisition 34

3.1.1 Abstraction of Hyetographs 34

3.1.2 Abstraction of Hydrographs 34

3.1.3 Abstraction of Soil Moisture Data 35

3.1.4 Abstraction of Soil Hydraulic Parameters in the Green-Ampt Equation 36

3.2 Data Analysis 44

3.2.1 Determination of Measured Surface Runoff . . 44

3.2.2 Prediction of Surface Runoff (Without Interception 45

3.2.3 Prediction of Surface Runoff (With Interception) 46

3.2.4 Determination of Interception Loss 47

3.2.5 Optimization of the Green-Ampt Model Parameters 51

3.2.6 Validation of the Green-Ampt Model 51

4. RESULTS AND DISCUSSION 53

4.1 Prediction of Surface Runoff Using Parameters in Green and Ampt Model 53

4.1.1 Performance of the Original Green-Ampt Model (Developed for Ponded Conditions 54

4.1.2 Performance of the Modified Green-Ampt Model (Developed for Rainfall Infiltration 60

4.1.3 Suspected Reasons for Overprediction 61

4.2 Optimization of Saturated Hydraulic Conductivity (K_s) 67

4.3 Validation of Hydraulic Conductivity (K_s) 75

4.4 Comparison of Infiltration Characteristics Based on the Original Green-Ampt Model and Cylinder Infiltrometer Measurements 81

5. CONCLUSIONS 87

6. RECOMMENDATIONS 89

7. REFERENCES 91

LIST OF APPENDICES

APPENDIX 1 THE VEGETATION OF THE SAMBRET AND LAGAN EXPERIMENTAL CATCHMENTS. 95

APPENDIX 2 SUMMARY OF SOIL SURVEY OBSERVATIONS ON THE SAMBRET VALLEY. 96

APPENDIX 3 DETERMINATION OF SURFACE RUNOFF FROM RAINFALL USING GREEN-AMPT INFILTRATION MODEL. 97

APPENDIX 4 SOME SOIL CHARACTERISTICS OF KABETE SOILS. 99

APPENDIX 5 COMPUTER PROGRAMS. 100

LIST OF TABLES

Table 1.1 Mean monthly rainfall and temperature data (1958-74) for the Sambret and Lagan catchments. 8

Table 3.1 Rating equations for the gauging stations at the research catchments. 35

Table 3.2 Bulk density and soil moisture data for soils in Sambret catchment. 37

Table 3.3 Soil texture for Sambret catchment. 37

Table 4.1 Surface runoff for Sambret catchment based on the original Green-Ampt model. 55

Table 4.2 Surface runoff for Sambret sub-catchment based on the original Green-Ampt model. 55

Table 4.3 Surface runoff for Lagan catchment based on the original Green-Ampt model 56

Table 4.4 Surface runoff for Sambret catchment based on the modified Green-Ampt model. 61

Table 4.5 Surface runoff for Sambret sub-catchment based on the modified Green-Ampt model. 62

Table 4.6 Surface runoff for Lagan catchment based on the modified Green-Ampt model. 62

Table 4.7 Surface runoff, obtained without considering interception for Sambret catchment. 69

Table 4.8 Variation of objective function (J_{xs}) with saturated hydraulic conductivity. 69

Table 4.9 Surface runoff, obtained considering interception, for Sambret catchment. 70

Table 4.10 Surface runoff, obtained without considering interception, for Sambret sub-catchment. 71

Table 4.11 Surface runoff, obtained considering interception, for Sambret sub-catchment. 71

Table 4.12 Surface runoff, obtained without considering interception, for Lagan catchment. 72

Table 4.13 Surface runoff, obtained considering interception, for Lagan catchment. 72

Table 4.14 Surface runoff at the optimized values of K_s (cm/h) for Sambret catchment. 73

Table 4.15 Surface runoff at the optimized values of K_s (cm/h) for Sambret sub-catchment. 73

Table 4.16 Surface runoff at the optimized values of K_s (cm/h) for Lagan catchment. 74

Table 4.17 Summary of the optimized values of saturated hydraulic conductivity (K_s) for the catchments. . . . 74

Table 4.18 Surface runoff for Sambret catchment during validation. 76

Table 4.19 Surface runoff for Sambret sub-catchment during validation. 76

Table 4.20 Surface runoff for Lagan catchment during validation. 77

Table A1 Intensity distribution of a hypothetical storm. . . . 97

Table A2 Texture and porosity for Kabete soils 99

Table 4.13 Surface runoff, obtained considering interception, for Lagan catchment. 72

Table 4.14 Surface runoff at the optimized values of K_s (cm/h) for Sambret catchment. 73

Table 4.15 Surface runoff at the optimized values of K_s (cm/h) for Sambret sub-catchment. 73

Table 4.16 Surface runoff at the optimized values of K_s (cm/h) for Lagan catchment. 74

Table 4.17 Summary of the optimized values of saturated hydraulic conductivity (K_s) for the catchments. . . . 74

Table 4.18 Surface runoff for Sambret catchment during validation. 76

Table 4.19 Surface runoff for Sambret sub-catchment during validation. 76

Table 4.20 Surface runoff for Lagan catchment during validation. 77

Table A1 Intensity distribution of a hypothetical storm. . . . 97

Table A2 Texture and porosity for Kabete soils 99

LIST OF FIGURES

Fig. 1.1 Location of research catchments in Kenya. 9

Fig. 1.2 Relative positions of Sambret and Lagan catchments. . .9

Fig. 1.3 The Sambret catchment. 10

Fig. 1.4 The Lagan catchment. 11

Fig. 2.1 Definition sketch of Green-Ampt model. 19

Fig. 2.2 Double ring infiltrometer. 29

Fig. 2.3 Single ring infiltrometer. 29

Fig. 3.1 Soil moisture release curve for Sambret. 38

Fig. 3.2 Nomograph for saturated hydraulic conductivity. . . . 39

Fig. 3.3 Nomograph for wetting front suction. 40

Fig. 3.4 Nomograph for effective porosity. 41

Fig. 3.5 Nomograph for water retention at 1/3 bar suction. . 42

Fig. 3.6 Nomograph for water retention at 15 bar suction. . . 43

Fig. 3.7 Hydrograph resulting from the storm that occurred on 10-9-69 in Sambret catchment. 44

Fig. 3.8 Infiltration curve derived from the modified Green-Ampt model. 48

Fig. 3.9 Infiltration curve derived from the original Green-Ampt model. 48

Fig. 3.10 Flow chart of program used in determination of surface runoff from rainfall using original Green-Ampt model 49

Fig. 3.11 Flow chart for program used in determination of surface runoff from rainfall using modified Green-Ampt model 50

Fig. 4.1 Comparison of predicted surface runoff to measured for Sambret catchment based on original Green-Ampt model without interception. 57

Fig. 4.2 Comparison of predicted surface runoff to measured for Sambret catchment based on the original Green-Ampt model with interception. 57

Fig. 4.3 Comparison of predicted surface runoff to measured for Sambret sub-catchment based on the original Green-Ampt model without interception. . . . 58

Fig. 4.4 Comparison of predicted surface runoff to measured for Sambret sub-catchment based on the original Green-Ampt model with interception. 58

Fig. 4.5 Comparison of predicted surface runoff to measured for Lagan catchment based on the original Green-Ampt model without interception. . . . 59

Fig. 4.6 Comparison of predicted surface runoff to measured for Lagan catchment based on the original Green-Ampt model with interception. . . 59

Fig. 4.7 Comparison of predicted surface runoff to measured for Sambret catchment based on the modified Green-Ampt model without interception. . . . 63

Fig. 4.8 Comparison of predicted surface runoff to measured for Sambret catchment based on the modified Green-Ampt model with interception. 63

Fig. 4.9 Comparison of predicted surface runoff to measured for Sambret sub-catchment based on the modified Green-Ampt model without interception. . . . 64

Fig. 4.10 Comparison of predicted surface runoff to measured for Sambret sub-catchment based on the modified Green-Ampt model with interception. 64

Fig. 4.11 Comparison of predicted surface runoff to measured for Lagan catchment based on the modified Green-Ampt model without interception. . . . 65

Fig. 4.12 Comparison of predicted surface runoff to measured for Lagan catchment based on the modified Green-Ampt model with interception. 65

Fig. 4.13 Variation of objective function J_{xs} with saturated hydraulic conductivity assuming negligible interception. 70

Fig. 4.14 Comparison of predicted surface runoff to measured for Sambret catchment during validation without interception. 78

Fig. 4.15 Comparison of predicted surface runoff to measured for Sambret catchment during validation with interception. 78

Fig. 4.16 Comparison of predicted surface runoff to measured for Sambret sub-catchment during validation without interception. 79

Fig. 4.17 Comparison of predicted surface runoff to measured for Sambret sub-catchment during validation with interception. 79

Fig. 4.18 Comparison of predicted surface runoff to measured for Lagan catchment during validation without interception. 80

Fig. 4.19 Comparison of predicted surface runoff to measured for Lagan catchment during validation with interception. 80

Fig. 4.20 Infiltration rate curve for Kabete soils derived from the original Green-Ampt model. 83

Fig. 4.21 Infiltration rate curve for Kabete soils derived from the double ring infiltrometer. 84

Fig. A1 Hyetograph for a hypothetical storm. 97

Fig. A2 Soil moisture characteristic curve for Kabete soils...99

LIST OF SYMBOLS AND ABBREVIATIONS

Symbol/Abbreviation	Meaning
A	Soil transmissivity
a	Storage index of surface connected porosity
E	Average rate of evaporation during a storm
EAAFRO	East African Agricultural and Forestry Research Organization
F	Cumulative infiltration
f_p	Potential infiltration rate
f_c	Final constant infiltration rate
f_o	Initial potential infiltration rate
F_p	Cumulative infiltration at ponding time
g	Acceleration due to gravity
G-A	Green-Ampt
GI	Growth index of crop in percent of maturity
H	Gauge height
H_o	Ponded depth
K	Unsaturated hydraulic conductivity
K_r	Relative conductivity
K_s	Saturated hydraulic conductivity
L	Depth to the wetting front
M	Fillable porosity
q	Discharge
R	Rainfall intensity

Q_o	Observed surface runoff
Q_p	Predicted surface runoff
S	Soil sorptivity
SA	Available storage in the soil surface layer
S_f	Effective suction at the wetting front
S_{av}	Average suction at the wetting front
SAREC	Swedish Agency For Research Cooperation with Developing Countries
t	Time
t_p	Ponding time
t_s	Equivalent time to ponding
USDA-SCS	United States Department of Agriculture-Soil Conservation Service
z	Distance below the soil surface
ß	A soil parameter that controls the infiltration rate.
θ	Moisture content
θ_i	Antecedent soil moisture content
θ_m	Mass water content
θ_s	Saturated soil moisture content
θ_v	Volumetric moisture content
μ	Viscosity of water
η	Total porosity
ρ	Density of water
ρ_b	Dry bulk density
Ψ	Soil water matric potential

ACKNOWLEDGEMENTS

The author wishes to express his sincere gratitude to the supervisor Prof. T.C. Sharma for his consistent assistance and guidance from the initiation to completion of the research project work.

To all the staff at Kenya Agricultural Research Institute, Muguga, who were involved in assisting me acquire journals, soils, rainfall and streamflow data which were quite useful in my research work. To all staff at the Tea Research Foundation involved in assisting me acquire some soils data and other relevant information.

I acknowledge the staff and students of the Department of Agricultural Engineering, University of Nairobi for their constructive criticisms, suggestions and any other useful contributions.

I also wish to thank the relevant authorities at the Ministry of Water Development for allowing me to use some of the information available on rating equations at their headquarters, Nairobi.

Finally I would also wish to thank the Swedish Agency for Research Corporation with Developing Countries (SAREC) for awarding me a scholarship to study for an M.Sc. degree in the Department of Agricultural Engineering, University of Nairobi.

ACKNOWLEDGEMENTS

The author wishes to express his sincere gratitude to the supervisor Prof. T.C. Sharma for his consistent assistance and guidance from the initiation to completion of the research project work.

To all the staff at Kenya Agricultural Research Institute, Muguga, who were involved in assisting me acquire journals, soils, rainfall and streamflow data which were quite useful in my research work. To all staff at the Tea Research Foundation involved in assisting me acquire some soils data and other relevant information.

I acknowledge the staff and students of the Department of Agricultural Engineering, University of Nairobi for their constructive criticisms, suggestions and any other useful contributions.

I also wish to thank the relevant authorities at the Ministry of Water Development for allowing me to use some of the information available on rating equations at their headquarters, Nairobi.

Finally I would also wish to thank the Swedish Agency for Research Corporation with Developing Countries (SAREC) for awarding me a scholarship to study for an M.Sc. degree in the Department of Agricultural Engineering, University of Nairobi.

ABSTRACT

The Green-Ampt model was used to evaluate the infiltration parameters by testing it on Sambret and Lagan catchments of Kericho district, Kenya. The comparison of observed and predicted surface runoff formed the basis for evaluating the parameters in the Green-Ampt infiltration model. The model parameters were obtained from texture based nomographs emanating from United States Department of Agriculture-Soil Conservation Service (USDA-SCS). Values of antecedent soil moisture were obtained from available records. The nomographs have not been previously examined in Kenya. The storm hyetographs and hydrographs provided the necessary hydrologic information in the analysis.

For the selected events in all catchments, surface runoff was overestimated by the model both in its original form, for ponded conditions and the modified form, for predicting rainfall infiltration. This was regardless of the influence of interception which was estimated as a percentage of storm rainfall for each event considered. Poor prediction by the original Green-Ampt model was attributed to its poor representation of infiltration during rainfall events. It assumes immediate ponding at the onset of rain so that surface runoff starts at the moment rainfall commences. The result is an overprediction of surface runoff. Overprediction of surface runoff by the modified Green-Ampt model was attributed to the low values of saturated hydraulic conductivity (K_s) and

effective porosity (θ_s) predicted from the nomographs. A low value of K_s implies that less water is allowed to infiltrate resulting in high surface runoff volume. A low effective porosity (θ_s) means a reduced moisture deficit due to the small difference between the porosity and antecedent soil moisture.

Attempts were made to establish a correct value of K_s for each catchment through an optimization and validation exercise. K_s is the most variable and unpredictable parameter. θ_s is a function of soil texture and varies only slightly with land use changes. The measured value of θ_s (θ_s=0.7cm^3/cm^3) obtained from records was used in the procedure of optimization and validation. Saturated hydraulic conductivity (K_s) for Sambret, Sambret sub-catchment, and Lagan catchments were found to be 0.03, 0.04, and 0.05cm/h respectively. Since these optimized values were those obtained with interception taken into consideration, the results therefore show that interception has a significant effect on the rainfall-infiltration-runoff process in all the catchments studied. These results also show that the nomographs require modifications before they can be used on Kenyan catchments.

The infiltration rate curve derived from the original Green-Ampt model was compared to the curve obtained from double ring infiltrometer measurements. The results indicated that the concentric cylinder measurements yield highly variable and unreliable results which must be used cautiously.

1. INTRODUCTION

1.1 General Background

Infiltration is the term applied to the process of water entry into the soil, generally by downward flow through all or part of the soil surface (Hillel, 1982). In the context of this thesis, a number of terms associated with infiltration are briefly defined. The first term is the instantaneous infiltration rate (f_i) which is defined as the rate at which water moves through the soil surface (mm/h). Another term of interest, the infiltration volume or cumulative infiltration (F), is the total volume of infiltration from the beginning of a rainfall event (mm). The infiltration process is influenced by many soil and hydrologic factors such as the antecedent (initial) soil moisture. Wet soils will absorb less water than dry soils. Another factor is the soil surface condition. Tillage and the presence of cracks may lead to higher infiltration. The soil type also influences infiltration. Soils with coarse texture will have higher infiltration. Vegetation, through retarding velocity, and increasing the time water is resident on the soil surface, increases infiltration. Many other factors influence the infiltration process. These include landslope, soil compaction, surface sealing, temperature, and duration of precipitation among others. The process is, therefore, a complex one that has drawn the attention of many research workers.

There is need to find means by which the infiltration process can

be described by physical analysis based on simplified mathematical procedures. An approach of this nature would enable one to characterize the infiltration process using a model approach in which the concepts can be easily comprehended and where the parameters involved are related to the soil physical properties that influence infiltration. The parameters in such models should be such that they are measurable or can be easily estimated from soil properties related to them.

This study focuses on the role of Green-Ampt infiltration model in determining the infiltration behaviour of soils on selected catchments in Kenya. The model is based on the law of continuity or the conservation of mass to describe water flow into a homogeneous soil (Chow et al., 1988). The model parameters may be easily determined from soil texture. The study further evaluates the validity of texture based nomographs originating from United States Department of Agriculture-Soil Conservation Service (USDA-SCS).

1.2 Justification

In the past, cans, ring infiltrometers, sprinkling infiltrometers, bottle infiltrometers and other techniques have been used to measure infiltration rates. Due to the temporal and spatial variation of infiltration characteristics, these methods have yielded highly variable and unreliable results which cannot be used reliably in agricultural water management activities. Soil features over a given field, however small are never identical. Even if a

particular method were to be used to measure infiltration in a small area such as a field, variation would still be observed in the measured values. Therefore there is a need for developing techniques by which this process may be described adequately based on measurable soil and hydrologic properties. The use of a model approach to prediction of infiltration is therefore advisable. The advantage of using models is that they predict infiltration taking into account soil characteristics that influence the process and therefore provides a better estimation of infiltration as compared to the measurements carried in some specific sites.

Simple, empirically based models, such as those of Kostiakov and Horton are popular because of their simplicity and capability of fitting most infiltration data. These models can give reliable results when calibrated, however they are limited in their ability to incorporate the influence of physical soil properties (e.g. texture, bulk density, and hydraulic conductivity) on infiltration because the model parameters have no physical meaning (Mullem, 1991), and thus cannot be parameterized using these properties. The shortcoming of these empirical models therefore is that they have no physical basis upon which they can be used to describe infiltration. Bradford et al. (1990) point out that the calibration of empirical models is impossible because no hydrological records exist that are representative of changes in catchment soil properties contemplated. Again the models describe the infiltration process under ponded soil conditions which cannot be used to

describe rainfall infiltration which often occurs under unsaturated soil conditions. In view of this, the need to introduce theoretical concepts in predicting infiltration characteristics has become necessary, hence the preferable use of physically based models. Physically based models can in principle be used to simulate future changes in catchment hydrologic response because the plugging of changed values of parameters in the model equations allow such simulation.

Complex models, despite the fact that they provide a physically consistent means of quantifying infiltration in terms of soil properties that govern soil water movement are rarely used in practice. The shortcoming with these models is the elaborate mathematical procedures involved which are of limited use in practice. Also a more severe limitation is the difficulty of obtaining the necessary soil data. Variation of soil properties both with depth and from point to point in the field will require numerous measurements to adequately describe field conditions. Such data are only available for limited soils and the present methods for determining properties are difficult. In light of this, the need to utilize physically based models that use simplified theoretical concepts is required for predicting infiltration behaviour.

The use of simplified concepts based on parameters that can be quantified using measurable soil and hydrologic properties is

required to predict infiltration from consideration of the fact that neither the simple empirical models nor the complex theoretical ones can simplify the determination of infiltration characteristics at minimal cost and time. The Green-Ampt model has in the recent past become widely used because of its applicability in describing infiltration under various modes of water entry into the soil. It is also based on a simplified theoretical concept and the parameters in the model can be easily determined from soil properties that can be measured. Parameter determination for the Green-Ampt model is based on the nomographic technique in which information on texture is used in conjunction with nomographs developed by Rawls and Brakensiek (1983) to estimate the parameters.

Surface runoff may be predicted from rainfall using an infiltration approach. This is based on a hydrologic technique which involves analysis of rainfall and streamflow on a gauged catchment. By prediction of infiltration characteristics using Green-Ampt model and superimposing it on a rainfall hyetograph taking into account other significant abstractions, surface runoff may be predicted. When this is compared with the observed surface runoff derived by hydrograph analysis, an assessment can be made of the parameters involved in the Green-Ampt model. By adjustment of suspect model parameters, an appropriate set of parameters may be established for which the measured and predicted surface runoff compare reasonably well. Thus the hydrologic technique plays a significant role on

evaluation of infiltration characteristics of a catchment. Such an approach for estimating infiltration in Kenyan catchments has not been applied so far. The majority of the infiltration studies in Kenyan catchments are based on concentric ring infiltrometers which at times are known to yield exaggerated values of infiltration rates. It is against this background that the present study is directed to evaluate the infiltration characteristics using the observed rainfall, runoff and soil data from the gauged catchments.

1.3 Objectives and Scope of the Study

The objectives of the study are as follows:

1. To test the applicability of the USDA-SCS texture based nomographs for estimating the Green-Ampt infiltration parameters.
2. To calibrate and validate the Green-Ampt infiltration model using the rainfall-runoff data from the gauged catchments.

The study is intended to evaluate the infiltration process by analyzing the surface runoff predicted from the Green-Ampt infiltration model. The model parameters are to be estimated from textural soil properties using nomographs. The analysis will be based on the available data on rainfall, streamflow and soil moisture from the gauged catchments viz. Sambret and Lagan in Kenya. Good quality data on rainfall, streamflow and soil moisture are available from these catchments for a period of 16 years

(1958-75).

1.4 The Study Area

Two catchments, namely Sambret and Lagan in Kericho district, Kenya were chosen for the study (Fig. 1.1). The catchments are situated in the south west Mau forest reserve in Western Kenya within the Lake Victoria drainage basin (Fig. 1.2).

The catchments consist of two parallel valleys at a mean altitude of 2200m. Figs. 1.3 and 1.4 show the catchments indicating the location of the recording raingauges, river gauging stations, and moisture sampling sites. Before 1958, both catchments were under unbroken forest cover and topographically similar with mean slopes of 4 percent for Lagan and 4.5 percent for Sambret. Following the completion of negotiations in 1957, between the Kenya government, East African Agricultural and Forestry Research Organization (EAAFRO) and the Kenya Tea Company, now Brooke Bond Liebig (Kenya) Limited, a suitable area of forest within the West Mau Forest Reserve was to be made available for a catchment study designed to evaluate the changes in total water yield and its seasonal distribution that might result from replacing natural forest by tea estates. The Sambret catchment was chosen as the experimental catchment. Sambret was originally mostly evergreen forest with montane bamboo appearing at 2300m. The area of the catchment is 702 hectares of which 376 ha became tea estate which include roads and estate buildings as well as stands of tea, 128 ha remained under

forest, and 190 ha contained mixed bamboo with scattered evergreen forest elements. There is also an 8 ha, partially enclosed drainage basin (Fig 1.3) in the upper part of the catchment. Under the experimental programme, Lagan (544 ha) remained as control catchment entirely under moist evergreen high forest. Detailed description of the vegetation of these catchments has been presented by Kerfoot (1962) and is presented in Appendix 1.

The soils in these catchments consist of deep, stone free, clay soils heavily leached and uniform in physical structure to a depth of 6m (Edwards et al., 1979). A summary of soil survey observations in the Sambret catchment is well presented by Scott (1962) and is also shown in Appendix 2. The climatic environment of the two catchments, based on 16 years record, is summarized by meteorological data in Table 1.1.

Table 1.1 Mean monthly rainfall and temperature data (1958-74) for the Sambret and Lagan catchments (adapted from Tea Research Foundation)

Altitude 2073m, Latitude 0° 21'S, Longitude 35° 20'E

	Rainfall (mm)	Temperature (°C)		
	Monthly total	Max.	Min.	Mean
January	92.6	23.9	9.0	16.5
February	104.8	24.1	9.1	16.6
March	171.5	24.1	9.5	16.8
April	264.4	22.8	10.0	16.4
May	282.8	21.9	9.8	15.8
June	209.8	21.3	9.1	15.2
July	197.0	20.5	9.2	14.9
August	213.2	20.8	9.1	15.0
September	181.8	21.9	8.6	15.3
October	172.3	22.3	9.1	15.7
November	151.0	22.3	9.7	16.0
December	98.2	23.0	9.1	16.1

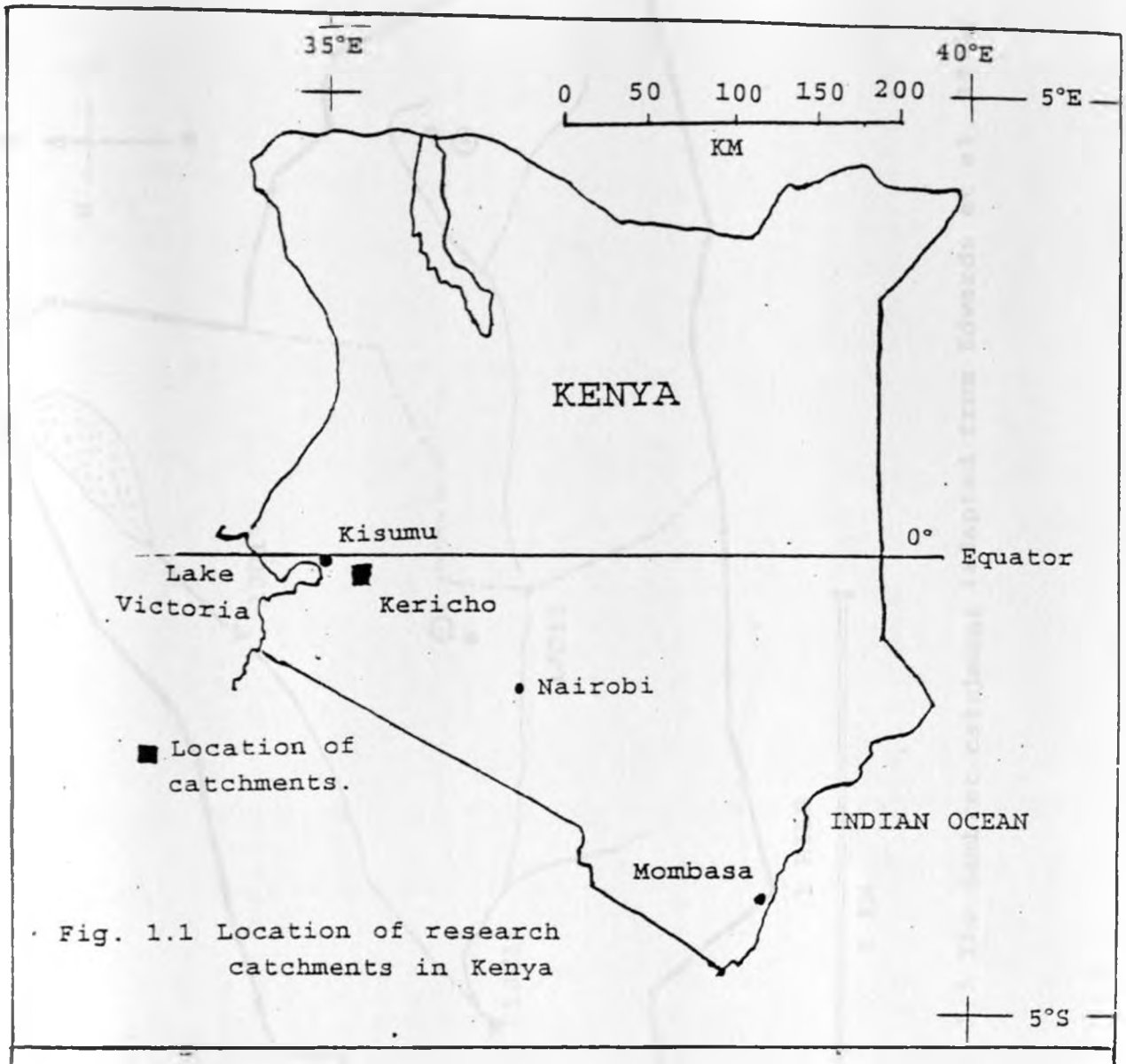

Fig. 1.1 Location of research catchments in Kenya

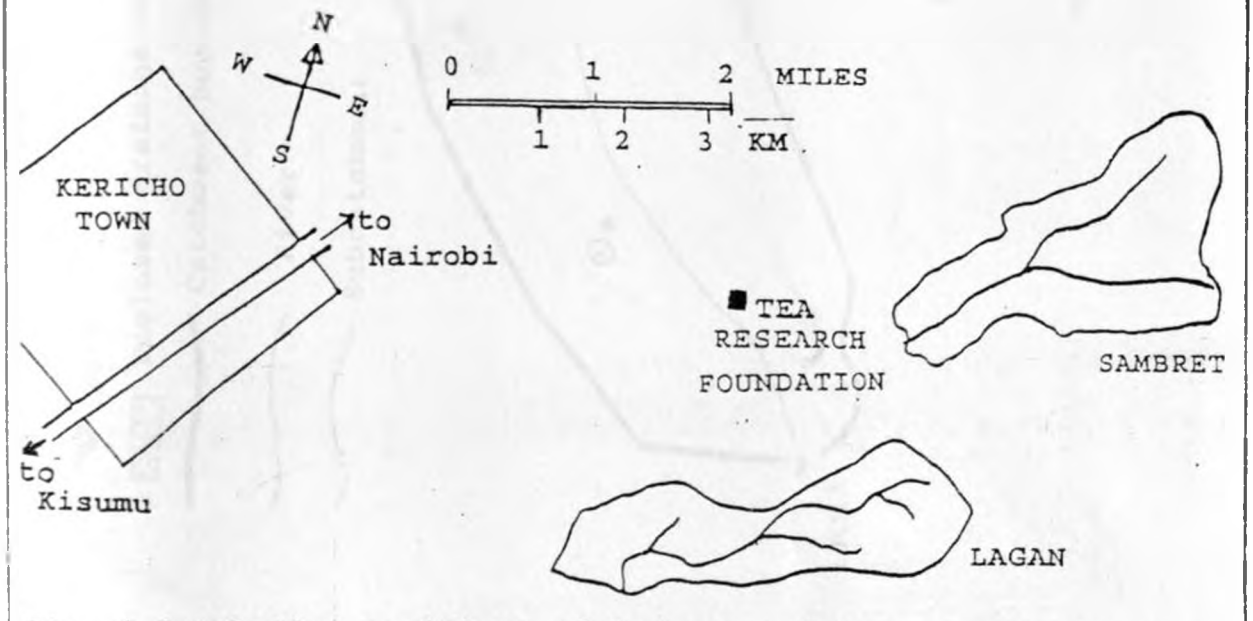

Fig. 1.2 Relative positions of Sambret and Lagan catchments

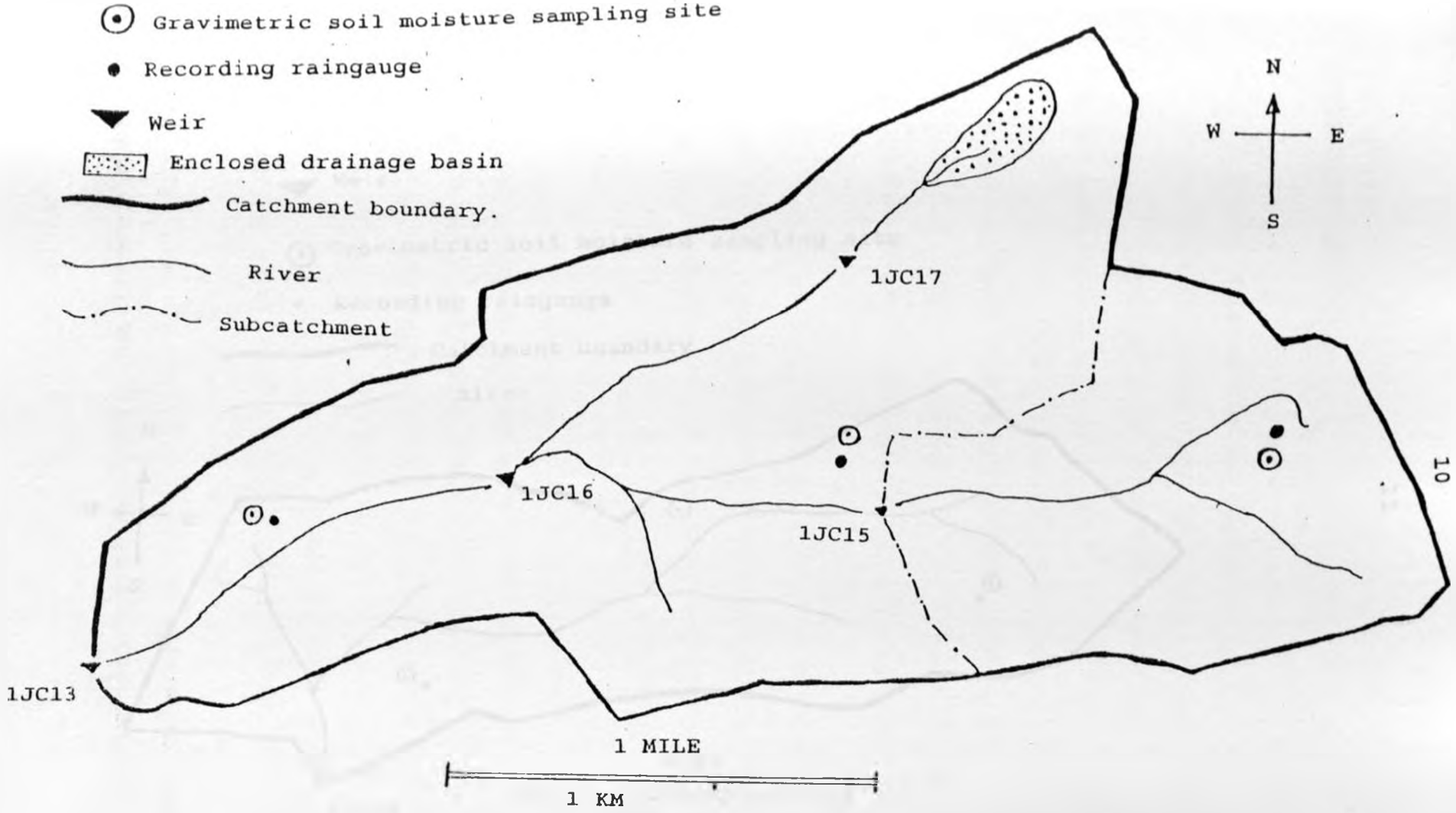

Fig. 1.3 The Sambret catchment (adapted from Edwards et al.,1976)).

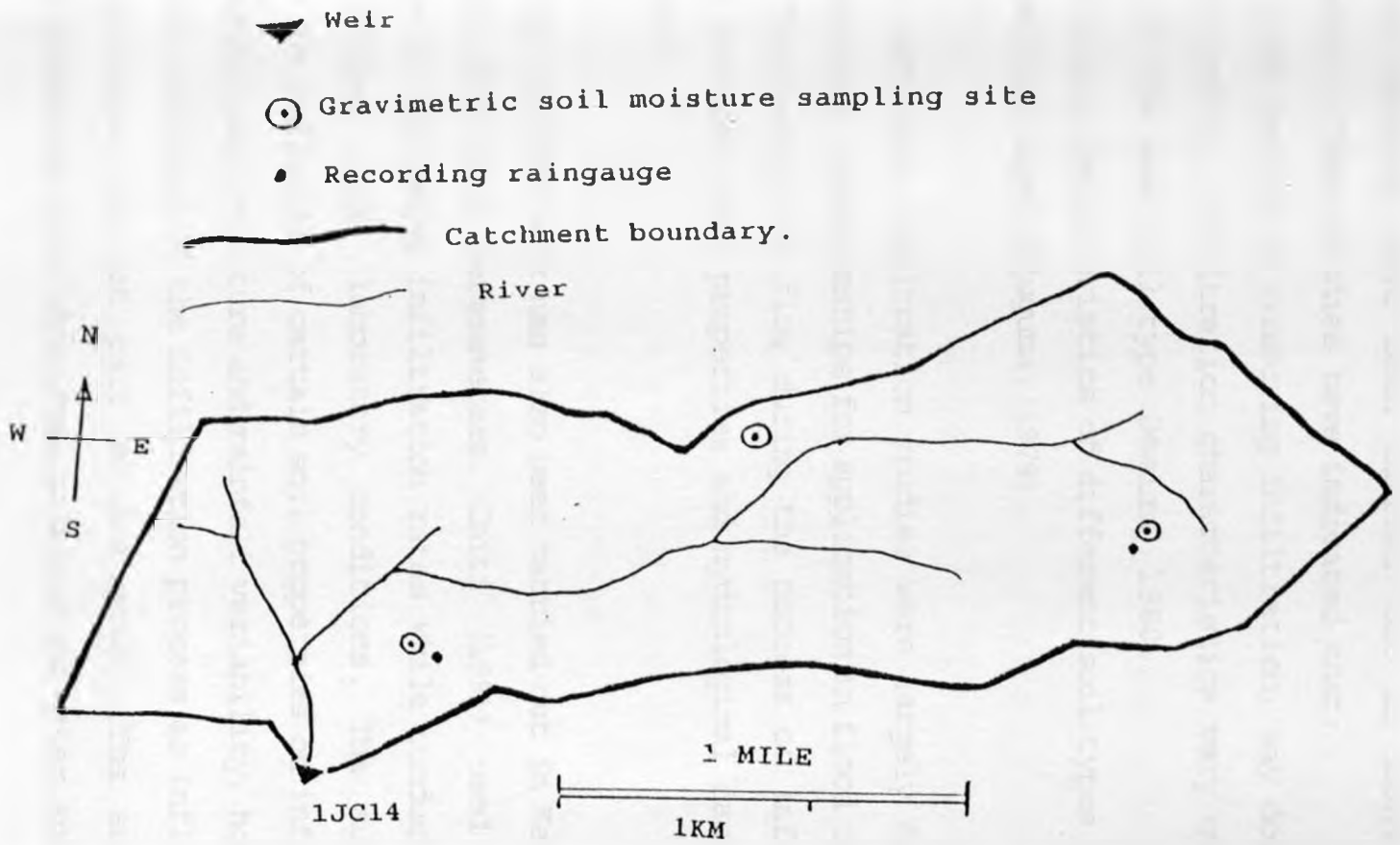

Fig. 1.4 The Lagan catchment (adapted from Edwards et al., 1979).

2. LITERATURE REVIEW

2.1 Infiltration Related Studies in Kenya

Infiltration studies have been carried out in Kenya using infiltrometers. These studies have indicated that:

i) For a given method of measuring infiltration, say double ring infiltrometer, infiltration characteristics vary over space even on the same soil type (Mwaura, 1980).

ii) Infiltration characteristics of different soil types vary with the methods used (Njuguna, 1979).

The above mentioned infiltration studies were largely focused to provide empirical relationships for application in flood irrigation systems. The physics of flow during the process of infiltration using the physical soil properties and hydrological factors were not analyzed.

Infiltration related work has also been carried out in Kenya using rainulators and disc permeameters. Chiti (1991) used rainfall simulators to determine infiltration rates while conducting soil erosion studies under laboratory conditions. The author has mentioned the influence of certain soil properties on infiltration e.g. antecedent soil moisture and rainfall variability, however the mathematical analysis of the infiltration process as influenced by these properties was not part of the study. The author was primarily concerned with the total infiltrated water and not the

description of the infiltration process under water application using the simulators. The use of such simulators does not represent natural rainfall conditions in terms of droplet size and terminal velocity. Gachene (1995) used the disc permeameter to determine steady state infiltration rates as well as unsaturated and ponded hydraulic conductivities while carrying out studies to asses the influence of cumulative soil loss on soil physical and chemical properties of a nitisol in the highlands of central Kenya. Field studies associated with this work were conducted using runoff plots at Kabete campus, Nairobi. These studies in Kenya were not aimed at describing the infiltration process by physical analysis especially on a catchment scale. A study of this nature is one of determining a spatially averaged infiltration rate on the basis of catchment characteristics like landuse, vegetation, soil texture, etc. that influence infiltration. In short, the aforementioned studies in Kenya are of limited physical analysis of water flow into the soil for description of the infiltration process.

2.2 Infiltration Equations and Models

Numerous formulations, some entirely empirical and others theoretically based, have been proposed over the years in repeated attempts to express infiltration rate or cumulative infiltration as a function of time. Models that are strictly empirical require parameters that must be obtained from measured infiltration data or estimated from more approximate procedures. On the other hand theoretically based equations are used to characterize infiltration

by solving the relevant differential equations using numerical methods. These solutions provide a physically consistent means of quantifying infiltration in terms of the soil properties governing the movement of water and air.

Attempts to characterize infiltration for field applications have usually involved simplified concepts which permit the infiltration rate or cumulative infiltration volume to be expressed algebraically in terms of time and certain soil parameters (Skaags and Khaleel, 1982). In developing these approximate models, simplified principles of the soil water movement have been applied. The parameters in such models can be determined from soil water properties when they are available.

Some of the more widely applied equations are presented briefly as follows.

2.2.1 Kostiakov Equation (Proposed in 1932)

This is one of the simplest and among the most commonly used empirical infiltration equations. It is expressed as

$$f_p = at^{-b} \qquad t>0 \qquad (2.1)$$

where

f_p = infiltrability at time t (mm/h)

t = time after infiltration starts (h)

a and b are constants which depend on soil and initial conditions.

The parameters in this equation have no physical interpretation and must be evaluated from experimental data.

2.2.2 Horton Equation (Proposed in 1940)

This is a three parameter infiltration equation which may be written as

$$f_p = f_c + (f_o - f_c)\, e^{-\beta t} \qquad (2.2)$$

where

f_p= infiltrability (mm/h) at time t

f_c = the final infiltration rate (mm/h)

f_o = infiltrability at t = 0 (mm/h), and

ß is a parameter which controls the rate of decrease of infiltration rate. The parameters f_o and ß depend on the initial water content as well as the application rate, and for homogeneous profiles, f_c will be somewhat smaller than the saturated hydraulic conductivity. Again the equation parameters must be evaluated from experimental infiltration data.

2.2.3 Richards Equation (Proposed in 1931)

This is the most theoretically based equation which uses the general equation of flow for unsaturated porous media derived by Richards. It is a second order, non-linear partial differential equation which may be written as,

$$\frac{\partial \theta}{\partial t} = \frac{\partial}{\partial z} K(\theta) \frac{\partial \psi}{\partial z} - \frac{\partial K(\theta)}{\partial z} \qquad (2.3)$$

where

θ = volumetric moisture content (mm^3/mm^3)

z = distance below the soil surface (mm)

ψ = soil water matric potential (mm)

$K(\theta)$ = unsaturated hydraulic conductivity (mm/h) and is dependent on the moisture content.

The equation is derived by combining the Darcy's law with the law of conservation of mass to obtain the general flow equation for water in the soil. Derivation of Richards equation from aforementioned physical laws is documented in Hillel (1982).

2.2.4 Phillips Equation (Proposed in 1957)

Phillips solved Richards equation (Eq. 2.3) for a ponded surface and deep homogeneous soil and proposed the following infiltration equation.

$$F = St^{\frac{1}{2}} + At \qquad (2.4).$$

where

F = volume of infiltration at time t (mm)

S = sorptivity ($mmh^{-1/2}$)

A = transmissivity (mm/h)

S and A are constants depending on soil properties and initial

moisture content. In its differentiated form, the equation may be expressed as

$$f_p = \frac{S}{2} t^{-\frac{1}{2}} + A \qquad (2.5)$$

where f_p is as defined previously.

2.2.5 Holtan Equation (Proposed in 1961)

This is an empirical equation described by Holtan in 1961. Skaags and Khaleel (1982) point out that several modifications from the original form yield the following equation.

$$f_p = GI.a.SA^{1.4} + f_c \qquad (2.6)$$

where

SA = available storage in the surface layer (mm)

GI = growth index of crop in percent of maturity

a = an index (mm/h per $(mm)^{1.4}$ of storage) of surface connected porosity which is a function of surface conditions and the density of plant roots.

f_c = steady state infiltration rate (mm/h)

Detailed description of the above models are well documented in Hillel (1982), Slack and Larson (1981), Skaags and Khaleel (1982) and Chow et al. (1988).

2.2.6 The Green-Ampt Infiltration Model for Ponded Conditions (Proposed in 1911)

Green and Ampt developed an approximate theory that has an exact analytical solution to derive an infiltration model (Chow et al., 1988). The derivation was based on the following assumptions.

- the surface is ponded to a negligible depth.
- soil profile is deep, homogeneous and has a uniform initial moisture.
- diffusion of soil moisture is negligible.

However the equation is by far one of the best models available to describe infiltration during a rainfall event and the prospect for an improved analysis is promising (Chu, 1978). The model has undergone numerous modifications to cater for conditions under which the assumptions do not apply. Bouwer 1969, quoted by Skaags and Khaleel (1982) has shown that the model may also be used for non-uniform initial water content. The Green-Ampt equation has further been used with good results for profiles that become denser with depth, those where hydraulic conductivity increases with depth and also for soils with partially sealed surfaces. The form of equation remains the same when simultaneous movement of both water and air is considered (Skaags and Khaleel, 1982)

The model utilizes Darcy's law and the law of continuity. Water is assumed to enter the soil as slug flow resulting in a sharply defined wetting front which separates a wetted zone from the unwetted one. The simplified picture of infiltration as proposed by

Green and Ampt is shown in Fig. 2.1.

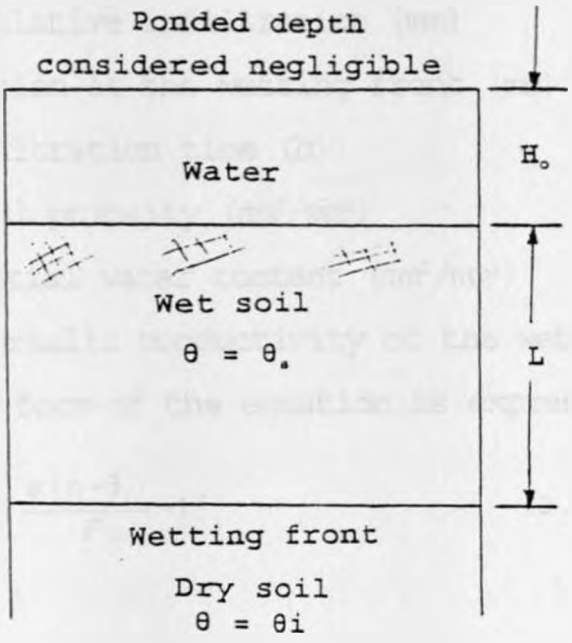

Fig. 2.1 Definition sketch for Green-Ampt Model (adapted from Viessman et al., 1989).

Referring to Fig. 2.1

H_o=ponded depth (mm)

L=depth to the wetting front (mm)

θ_s=water content behind the wetting front (mm^3/mm^3)

θ_i=initial water content (mm^3/mm^3)

Application of Darcy's law and the law of continuity yield the following original form of Green-Ampt equation.

$$F-\psi(\eta-\theta_i)\ln\left(1+\frac{F}{\psi(\eta-\theta_i)}\right)=K_s t \qquad (2.7)$$

where

F = cumulative infiltration (mm)

ψ = suction at the wetting front (mm)

t = infiltration time (h)

η = total porosity (mm^3/mm^3)

θ_i = initial water content (mm^3/mm^3)

K_s = hydraulic conductivity of the wetted zone (mm/h)

The differentiated form of the equation is expressed as

$$f = K_s\left[\frac{\psi(\eta-\theta_i)}{F}+1\right] \qquad (2.8)$$

where

f = infiltration rate (mm/h)

Detailed derivation of equations (2.7) and (2.8) may be found in Chow et al. (1988).

It should be pointed out that the derivation of these equations assume a ponded surface so that infiltration rate is equal to infiltrability all times. The original derivation also assumed total saturation behind the wetting front so that the moisture deficit is given by $(\eta-\theta_i)$, however this requirement has been relaxed (Skaags and Khaleel, 1982) hence the difference between initial and final moisture content becomes $\theta_s - \theta_i$ (fillable porosity). θ_s is constant but not necessarily equal to total porosity. The modified equations thus take the following forms.

$$f = K_s\left[1 + \frac{(\theta_s - \theta_i)\, S_f}{F}\right] \qquad (2.9)$$

and the integrated form

$$K_s t = F - S_{av}[\theta_s - \theta_i] \ln\left[1 + \frac{F}{(\theta_s - \theta_i)\, S_{av}}\right] \qquad (2.10)$$

Where

S_{av} = average suction at the wetting front (mm)

θ_s = actual moisture content behind the wetting front (mm^3/mm^3)

S_f = effective suction at the wetting front (mm)

Other parameters are as previously defined.

2.2.7 Application of Green-Ampt Model to Rainfall Infiltration

The Green-Ampt infiltration model and even the other models discussed in the previous sections are based on assumptions that water is ponded to a small depth on the soil surface so that all the water the soil can infiltrate is available at the surface. However, during a rainfall event, water will pond on the surface only if the rainfall intensity is greater than the infiltrability of the soil. During a rainfall event there are periods of heavy downpour and periods of light drizzle. Under heavy intense rainfall, the soil surface becomes ponded with water. When intensity is light there is no surface ponding. As pointed out by Chu (1978), there are two distinct stages of infiltration during a rainfall event: a stage in which the ground surface is ponded with

water and a stage without surface ponding. Under ponded conditions, infiltration occurs at the maximum rate and is referred to as the infiltrability (f_p). However without surface ponding, all the rainfall infiltrates into the soil and the rate of infiltration equals the rainfall intensity, which is less than the infiltrability. The Green-Ampt equation was originally formulated to describe the infiltration process under a ponded surface. The time that separates the two stages of infiltration should be determined to offset the difficulty of modelling infiltration during a rainfall event. The infiltration for different stages can thus be treated separately.

Mein and Larson (1971) utilized concepts of flow similar to those of Green and Ampt to develop a relationship for predicting infiltration volume prior to surface ponding for the case of an initial uniform moisture profile and constant rainfall rate. At the time of surface ponding, from Eq. (2.9),

$$f=f_p=R=K_s\left(1+\frac{MS_{av}}{F_p}\right) \qquad (2.11)$$

Where

$M = \theta_s - \theta_i$

F_p = cumulative infiltration (mm) at ponding time (t_p)

R = rainfall intensity (mm/h)

Substituting S_{av} for S_f and solving for F_p, the equation may be expressed as,

$$F_p = \frac{S_{av} M}{\frac{R}{K_s} - 1} \qquad (2.12)$$

Prior to surface ponding, f = R

Hence, for steady rainfall, the infiltration rate may be expressed as,

$$f = R \qquad t < t_p \qquad (2.13)$$

and

$$f = f_p = K_s \left(1 + \frac{S_{av} M}{F_p}\right) \qquad t > t_p \qquad (2.14)$$

Where

$$t_p = \frac{F_p}{R} \qquad (2.15)$$

If $R < K_s$, surface ponding will not occur provided the profile is deep and homogeneous as is assumed in the original Green-Ampt equation.

Studies support the use of Green-Ampt equation for unsteady rainfall. A study quoted by Skaags and Khaleel (1982) found out that the potential infiltration rate (f_p) for unsteady rainfall could be approximated as a function of cumulative infiltration (F)

regardless of the application rate versus time history. The Green-Ampt equation expresses f_p as a function of F for steady rainfall, a special case of unsteady rainfall, hence it follows that the equation should hold for unsteady case as well. A comprehensive study of the application of the Green-Ampt equation for unsteady rainfall was carried out by Chu (1978) who found a good agreement between the predicted rainfall excess (based on the modified equation) and measured runoff from a 113-acre watershed. A simplified approach to rainfall infiltration is given by

Skaags and Khaleel (1982), which may be expressed as,

$$K_s(t-t_p+t_s) = F - S_{av}(\theta_s-\theta_i)\ln\left(1+\frac{F}{(\theta_s-\theta_i)S_{av}}\right) \qquad (2.16)$$

where

t_s=equivalent time to ponding (h) i.e. the time to infiltrate volume F_p under initially ponded surface conditions.

2.2.8 Determination of Green-Ampt Model Parameters

2.2.8.1 Hydraulic Conductivity

The accurate determination of K_s poses problems because of its variation over space and time. A number of techniques have been proposed to determine saturated hydraulic conductivity. Field methods of measuring saturated hydraulic conductivity include augerhole and piezometer methods (below the water table). Above water table methods include the shallow well pumping and field

permeameter methods. Saturated hydraulic conductivity may also be determined by laboratory techniques. Laboratory permeameters (constant and variable head permeameters) are used as laboratory techniques. Field techniques present more representative field conditions and hence give better results.

2.2.8.2 Wetting Front Suction

A technique to determine wetting front suction from field measurement is presented by Bouwer (1966). He developed an apparatus to measure the air entry suction of the soil from which an estimate of S_{av} may be made. Mein and Larson (1971) proposed that the average suction at the wetting front S_{av} can be conveniently expressed in terms of relative conductivities as

$$S_{av} = \int_0^1 S dk_r(\theta) \qquad (2.17)$$

$$K_r(\theta) = \frac{K(\theta)}{K(\theta_s)} \qquad (2.18)$$

Where

K_r = relative conductivity

S = soil suction (mm)

$K(\theta)$ = hydraulic conductivity at moisture content (θ) (mm/h)

$K(\theta_s)$ = hydraulic conductivity at saturated soil moisture content (mm/h)

This suggests that S-K relationship for the soil in question is to be known. From Eq. (2.17) the wetting front suction is simply the area under the S-K_r curve. In practice the S-K_r relationship near K_r=0 is hard to define, so, the area in the range K_r = 0.01 to K_r =1.0 may be used (Mein and Larson, 1971).

The theoretical justification for determining the wetting front suction parameter in the Green-Ampt equation is presented in detail by Mein and Farrel (1974). The need for hydraulic conductivity versus capillary conductivity relation for the soil is emphasized. However the authors point out that the S-K relationship for a soil is both tedious and time consuming to determine and hence suggests that things would be simplified if S_{av} could be obtained from S-θ curve (moisture release curve). This may be achieved by making use of equations which relate hydraulic conductivity to pore size distribution so as to permit S_{av} to be estimated from S-θ curve without any measurement of conductivity.

Marshal (1958) presented an appropriate technique for calculating permeability from the curve relating water content to suction. The calculated values were found to agree satisfactorily with measured values over a wide range of permeability. The hydraulic conductivity may be obtained in cm/s from the intrinsic permeability using the formula

$$K = \frac{\rho g k}{\mu} \qquad (2.19)$$

Where

ρ = density of water (g/cm^3)

g = acceleration due to gravity (cm/s^2)

k = intrinsic permeability (cm^2)

μ = viscosity of water ($g\ cm^{-1}\ s^{-1}$)

K = hydraulic conductivity (cm/s).

2.2.8.3 Effective Porosity

According to Ahuja et al. (1988), the effective porosity of a soil may be regarded as the difference between the total porosity and water content at -33 kpa potential.

2.2.8.4 Antecedent Moisture Content

The soil water content prior to a storm, θ_i, should be obtained from soil moisture measurements. However the modeller may select θ_i based on soil texture and antecedent rainfall conditions (Madramootoo and Enright, 1989).

2.3 Measurement of Infiltration

The rate at which water can enter the soil when not limited by the rate of supply is measured in the field with water either ponded on the surface or falling on it as artificial or natural rain at a rate sufficient to cause some runoff (Marshal and Holmes, 1988). Several methods of determining infiltration characteristics may be found in literature, the most common being the double ring

infiltrometer. These methods are discussed briefly as follows.

2.3.1 Ring Infiltrometers

An infiltrometer is a wide short tube or other impervious boundary surrounding an area of soil (Wilson, 1974). In the case of ring infiltrometers, the infiltration characteristics of the soil is determined by ponding in a metal cylinder installed on the field surface and observing the rate at which water lowered in the cylinder. Michael (1987) points out that in earlier studies only a single cylinder was used and many of the data indicated a high degree of variability due to the uncontrolled lateral movement of water from the cylinder after the wetting front reaches the bottom of the cylinder. While the wetting front is in the cylinder, the water subsidence rate corresponds to the infiltration rate. When the wetting front passes below the cylinder, a more or less divergent flow will occur. The lateral movement of water from the cylinder is minimized by ponding in a guard cylinder of buffer area around the cylinder, hence the double ring infiltrometer. The cylinders are usually about 25cm deep and formed from 2mm rolled steel. The inner cylinder, from which the infiltration measurements are taken is usually 30cm in diameter. The outer cylinder, used to form the buffer is about 60cm in diameter. The cylinders are installed about 10cm deep in the soil. Figs. 2.2 and 2.3 show the two types of ring infiltrometer.

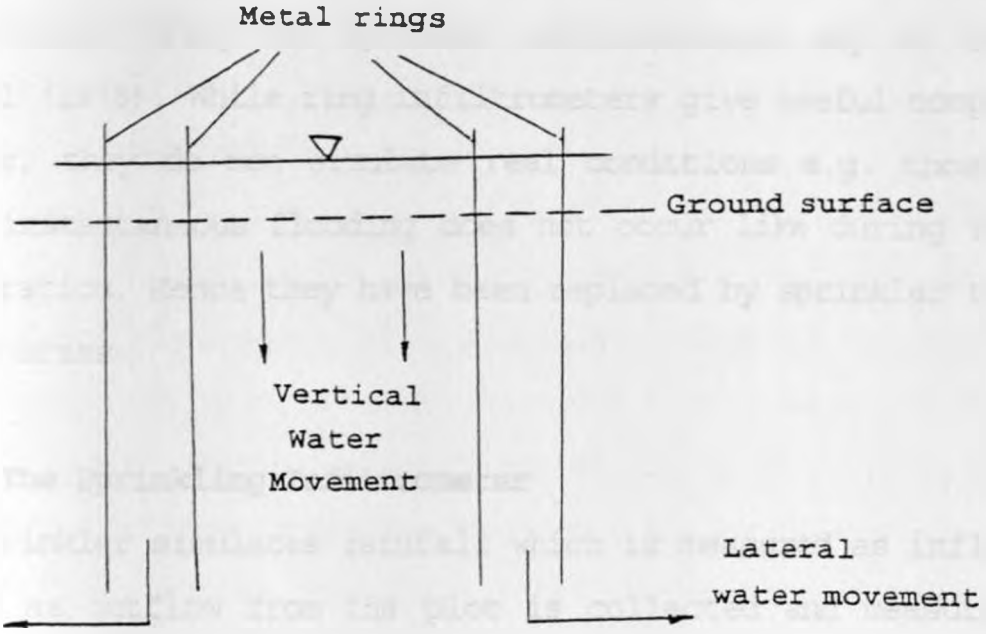

Fig. 2.2 Double ring infiltrometer

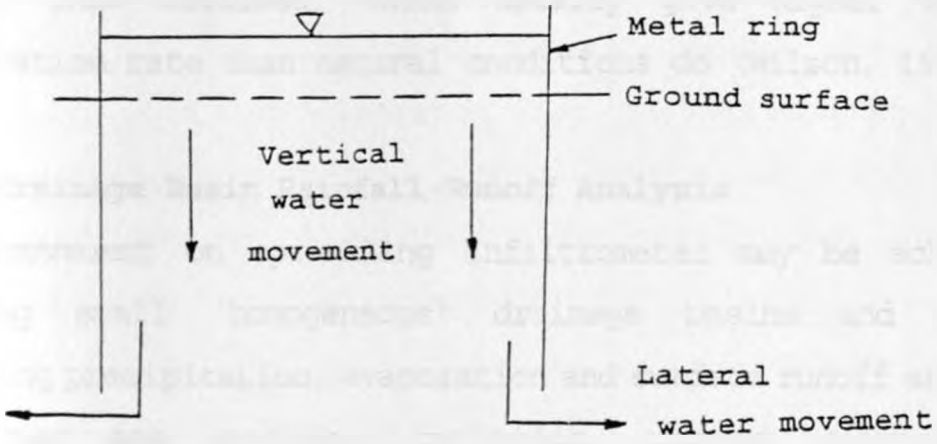

Fig. 2.3 Single ring infiltrometer

Details of the experimental set-up and description of infiltration measurements using the cylinder infiltrometers may be found in Michael (1978). While ring infiltrometers give useful comparative results, they do not simulate real conditions e.g. those under which instantaneous flooding does not occur like during rainfall infiltration. Hence they have been replaced by sprinkler tests on larger areas.

2.3.2 The Sprinkling Infiltrometer

The sprinkler simulates rainfall which is measured as inflow. The runoff as outflow from the plot is collected and measured. The difference between inflow and outflow is assumed to be infiltrated. Despite rain-simulating sprinklers being a good deal more realistic than the flooded rings, there are limitations to the reliability of results thus obtained, which usually give higher values of infiltration rate than natural conditions do (Wilson, 1974).

2.3.3 Drainage Basin Rainfall-Runoff Analysis

An improvement on sprinkling infiltrometer may be achieved by choosing small 'homogeneous' drainage basins and carefully measuring precipitation, evaporation and surface runoff as outflow. Techniques are available by which, through elimination of everything except infiltration, average infiltration rate values may be obtained for such basins (Wilson, 1974). Where interception losses and surface depression storage are significant, these have

to be taken into account together with infiltration before the surface runoff may be predicted accurately. These abstractions are briefly discussed as follows.

2.4 Interception Losses

The precipitation that actually reaches the ground surface is significantly influenced by interception. Factors affecting interception, methods of measuring interception and its significance in water balance have been discussed by Ward and Robinson (1992). Estimated interception losses from selected types of vegetation have also been given. In an attempt to model interception, simple equations that have been developed for calculating interception are based upon the principle factors that influence it and can be found in the text.

From literature revisited on the approach by a number of authors in quantifying interception and depression storage when modelling interception, it is observed that no universally accepted technique was used in doing so. Morel-Seytox (1981) has assumed a value of 1.27mm for interception while modelling infiltration during a variable rainfall event using the Green-Ampt model. The storm was arbitrary and the author does not elaborate how the value was arrived at.

2.5 Depression Storage

The depression storage is closely linked to interception. It

comprises the water retained in hollows and depressions on the ground surface during and after rainfall. The water may be evaporated back directly or used by vegetation or else infiltrate into the soil, so that none of it appears as surface runoff.

Depression storage is commonly thought of as a small scale phenomena related to minor depressions and puddles but may be significant on a larger scale where topographical conditions are particularly favourable, in which case the surface retention storage must be filled before surface runoff can begin. That is, if infiltrability falls below rainfall intensity, water will be ponded on the surface until the ponded depth reaches the maximum value. After this, rainfall in excess of infiltration will be available for runoff. The nature of depressions, as well as their size is largely a function of the original landform and local landuse practices and because of the extreme variability in the nature of depressions, no generalized relation with enough specified parameters is feasible (Viessman et al., 1989). The geometry of land surface is usually complex and thus the depressions vary widely in size, degree of interconnection, and contributing drainage area (Viessman et al., 1989). The aforesaid authors quote depression losses from intense storms as 5.08mm for sand, 3.81mm for loam and 2.5mm for clay. A depth of 6.35mm is quoted for pervious urban areas and 1.59mm for pavements.

Madramootoo and Enright (1989) assumed a value of 1cm depression

storage for a Canadian watershed of 8.13km² area on which they carried out studies on the use of Green-Ampt infiltration model to predict surface runoff. The rural watershed had a variable soil type and landuse described in detail by the authors who also indicated that the aforementioned value of depression storage suits large storms. However for smaller storms the assumed value would be too large. The value to be used for smaller storms was not indicated.

Studies in Kenya have ignored the role of theoretical analysis in determining the infiltration characteristics of soil. It is against this background that the current study is carried out. The study is intended to introduce theoretical concepts in describing the infiltration process. The Green-Ampt model, known for its wide applicability in predicting infiltration rates on a catchment scale has been chosen in the first instance. The model parameters (i.e. saturated hydraulic conductivity, wetting front suction, antecedent soil moisture, and saturated soil moisture content), can either be measured or estimated from related soil properties. The parameters may also be obtained from information available on soil maps and soil survey reports.

3. MATERIALS AND METHODS

3.1 Data Acquisition

The data acquisition for use in the research were basically on soil properties, rainfall and streamflow. Records on the required information were obtained from the archives of Kenya Agricultural Research Institute, Tea Research Foundation, Kericho, and Ministry of Water Development headquarters, Nairobi, Kenya.

3.1.1 Abstraction of Hyetographs

Rainfall charts showing daily rainfall records for the period 1958-74 were acquired. Days were identified for which records on moisture content prior to a storm were available. Bearing in mind that rainfall occurred on the identified days, rainfall hyetographs for the days selected were derived from the rainfall charts.

3.1.2 Abstraction of Hydrographs

The hydrographs resulting from the selected storms were developed from charts showing the stagegraphs. Charts giving the streamflow records for the period 1958-74 were obtained from the archives of Kenya Agricultural Research Institute. Table 3.1 shows the rating equations used to convert the stage graphs to hydrographs resulting from the selected storms.

Table 3.1 Rating equations for the gauging stations at the research catchments

Station No.	Catchment and its Land use	Rating equations
1JC13	Sambret (main outfall) Tea	$q = 2.2344\ H^{1.6264}$ H<=0.1677m
		$q = 1.0797\ H^{1.2191}$ 0.1677m < H <=0.2622m
		$q = 4.5606\ H^{2.2954}$ H>0.2622m
1JC14	Lagan (main outfall) Indigenous forest	$q = 2.243\ H^{1.5}$ for all H
1JC15	Sambret (sub-catchment) Bamboo	$q = 1.343\ H^{2.47}$ H<=0.1373m
		$q = 6.5178\ H^{3.2673}$ H>0.1373m

where,

q= discharge in m^3/s

H= gauge height in m.

By hydrograph analysis surface runoff resulting from selected storms were determined and quantified in mm.

3.1.3 Abstraction of Soil Moisture Data

Measured values of soil moisture content (gravimetric method) were abstracted from available records. The gravimetric moisture content values from the records were available for some days in a month for the period 1965-74 for the catchments selected. The values selected were those which were monitored on days in which storms occurred. Antecedent soil moisture, θ_i (volume basis) is an important parameter in the Green-Ampt model. To convert the mass water contents to volumetric moisture content bulk density measurement is

used. The relationship is as follows:

$$\theta_v = \rho_b \theta_m \qquad (3.1)$$

where

θ_m = mass water content (g water/g soil).

ρ_b = dry bulk density (g/cm^3).

θ_v = volumetric water content (cm^3/cm^3).

The moisture content in most cases is expected to lie between the permanent wilting point and field capacity hence the need to incorporate these parameters in the data collection. Table 3.2 shows the bulk density and moisture contents at the said limits. The saturated soil moisture content for these soils is $0.7 cm^3/cm^3$ for the uppermost soil layer where infiltration takes place.

3.1.4 Abstraction of Soil Hydraulic Parameters in the Green-Ampt Equation

It is cheaper and easier to estimate parameters from soil texture data rather than make detailed measurements of each parameter especially on a catchment scale as this would require a large number of sites. Rawls and Brakensiek (1983) recognizing the desirability of parameter estimation developed a series of equations and nomographs to generate the parameters in the Green-Ampt equation based on soil texture. The latter can be easily measured or evaluated. The data on texture was abstracted from the archives of Tea Research Foundation, Kericho. These were used in conjunction with the nomographs to determine the Green-Ampt

parameters. Since the soils in these areas are uniform, the same texture was used for Lagan and Sambret for analysis. Table 3.3 shows the textural composition of Sambret soils.

Table 3.2 Bulk density and soil moisture data for soils in Sambret catchment (adapted from Tea Research Foundation)

Depth Range (cm)	Bulk Density (g/cm^3)	Moisture Content at 1/3 bar tension (cm^3/cm^3)	Moisture Content at 15 bar tension (cm^3/cm^3)
0-15	0.96	46.00	29.00
15-30	0.92	55.00	30.50
30-60	1.07	52.10	34.50
60-90	1.07	54.60	32.70
90-120	1.13	50.40	34.10
120-150	1.00	52.70	30.20
150-180	1.11	51.60	33.50
180-210	1.15	51.00	34.40
210-240	1.13	48.80	34.20
240-270	1.12	53.30	33.80
270-300	1.07	61.00	51.00

Table 3.3 Soil texture for Sambret catchment

Depth range (cm)	Textural composition of soil			
	% sand	% silt	% clay	Texture
0-15	20	13	67	Clay
15-30	18	17	65	Clay
30-60	14	14	72	Clay
60-90	07	18	75	Clay
90-120	15	12	72	Clay
120-150	14	17	69	Clay
150-180	07	23	70	Clay
180-210	06	20	74	Clay
210-240	04	15	81	Clay
240-270	10	16	74	Clay
270-300	11	19	70	Clay

The soil moisture release curve for Sambret is shown in Fig. 3.1

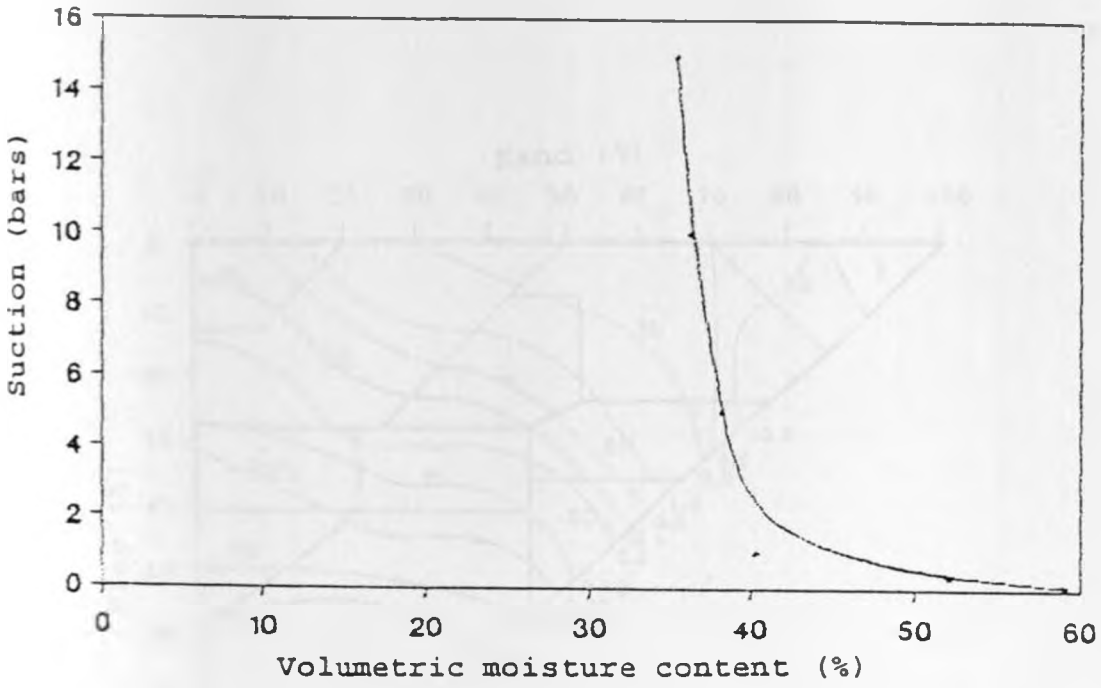

Fig. 3.1 Soil moisture release curve for Sambret (adapted from Tea Research Foundation)

Figs. 3.2-3.6 show the nomographs used in conjunction with texture to obtain the Green and Ampt parameters.

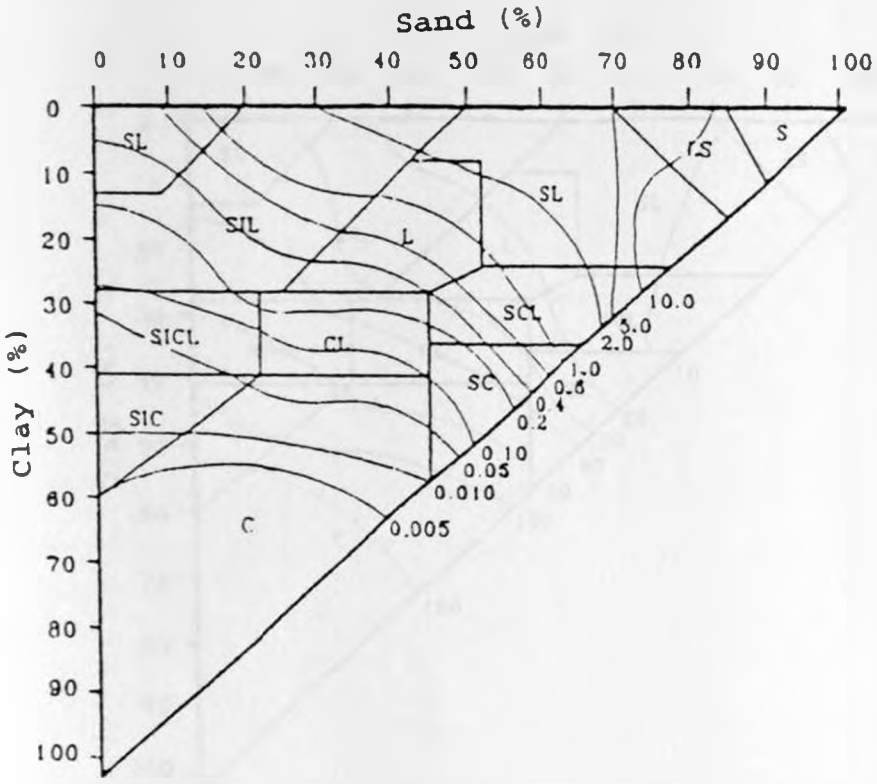

Fig. 3.2 Nomograph for saturated hydraulic conductivity (cm/h) (adapted from Rawls and Brakensiek, 1983)

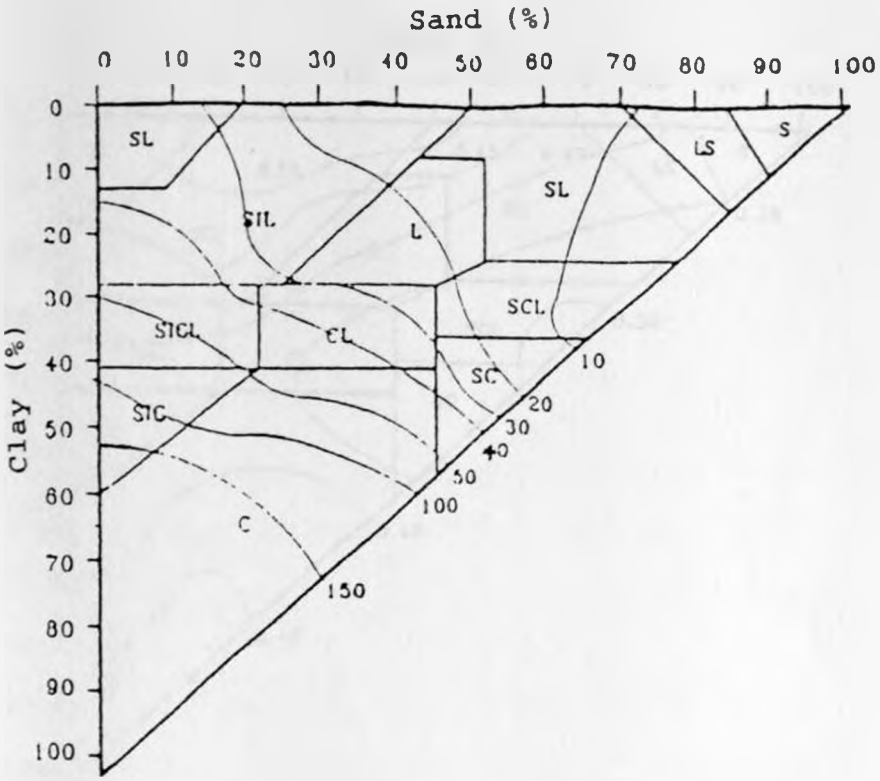

Fig. 3.3 Nomograph for wetting front suction (cm) (adapted from Rawls and Brakensiek, 1983)

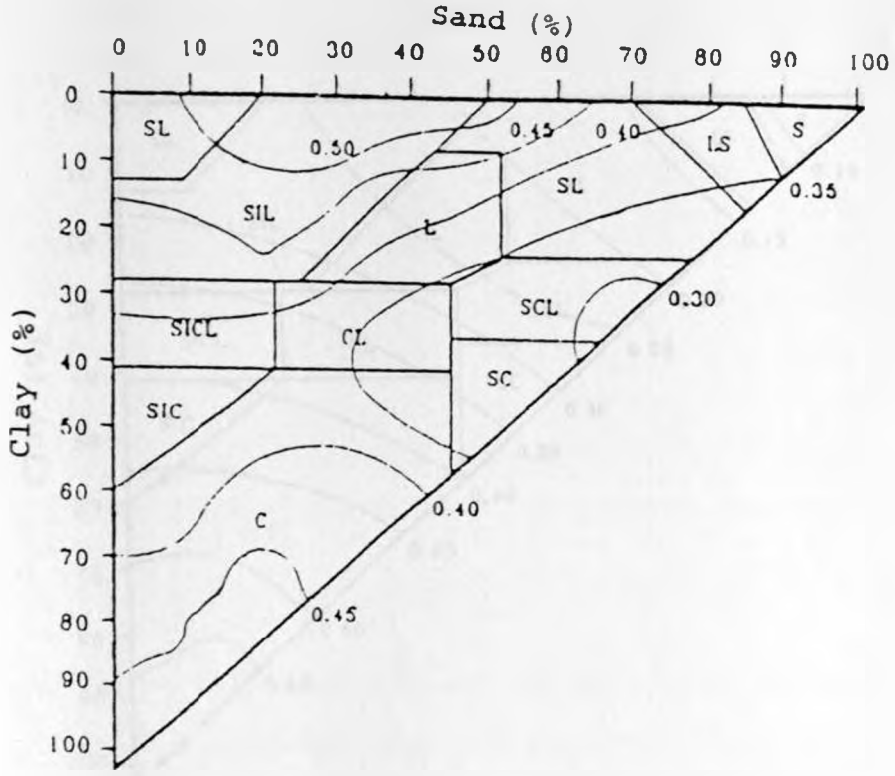

Fig. 3.4 Nomograph for effective porosity (cm^3/cm^3) (adapted from Rawls and Brakensiek, 1983)

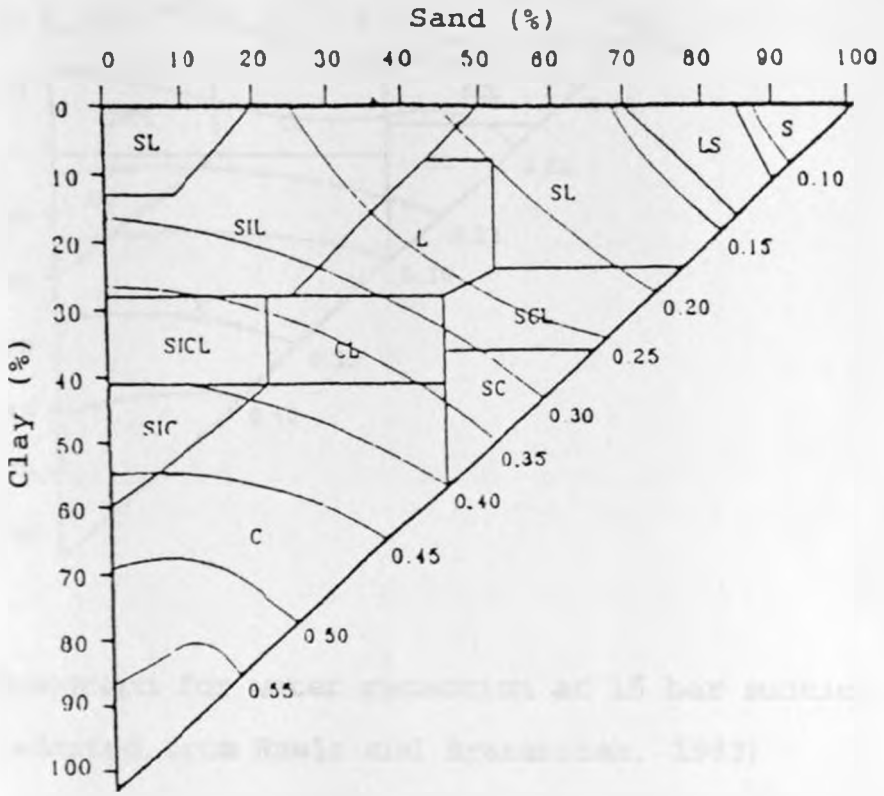

Fig. 3.5 Nomograph for water retention at 1/3 bar suction (cm^3/cm^3) (adapted from Rawls and Brakensiek, 1983)

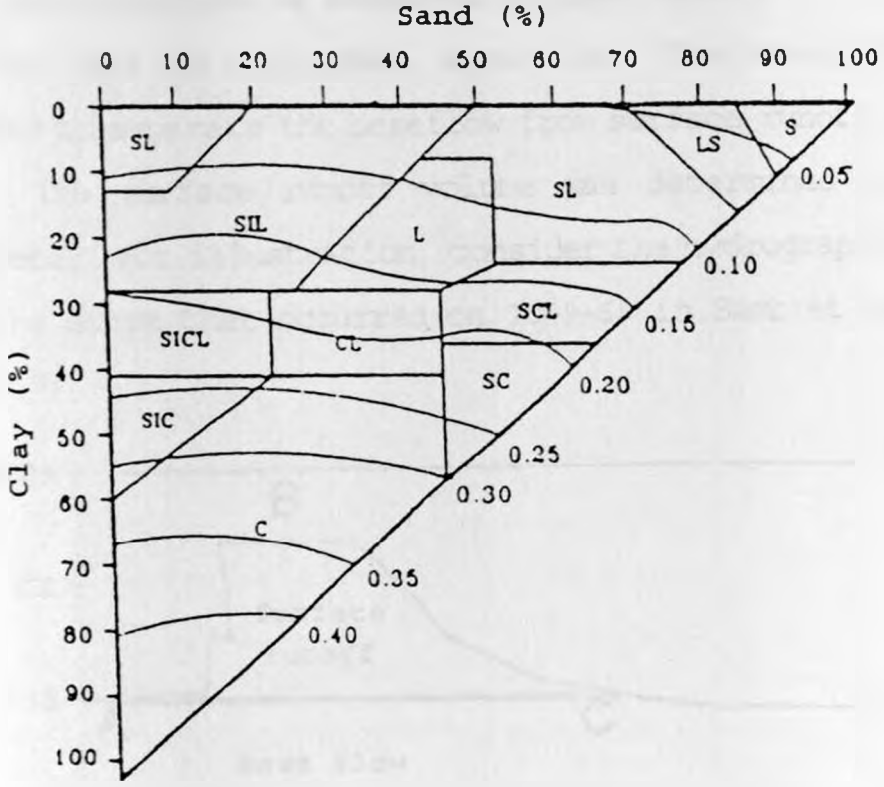

Fig. 3.6 Nomograph for water retention at 15 bar suction (cm^3/cm^3) (adapted from Rawls and Brakensiek, 1983)

The Green-Ampt parameters derived were as follows:

Saturated hydraulic conductivity, K_s=0.005cm/h

Average wetting front suction, S_{av}= 150cm

Saturated soil water content, θ_s=0.45cm^3/cm^3

3.2 Data Analysis

3.2.1 Determination of Measured Surface Runoff

This was done by hydrograph separation. The straight line method was used to separate the baseflow from surface runoff (Chow et al., 1988). The surface runoff volume was determined using the dot planimeter. For illustration, consider the hydrograph that resulted from the storm that occurred on 10-9-69 in Sambret catchment (See Fig. 3.7)

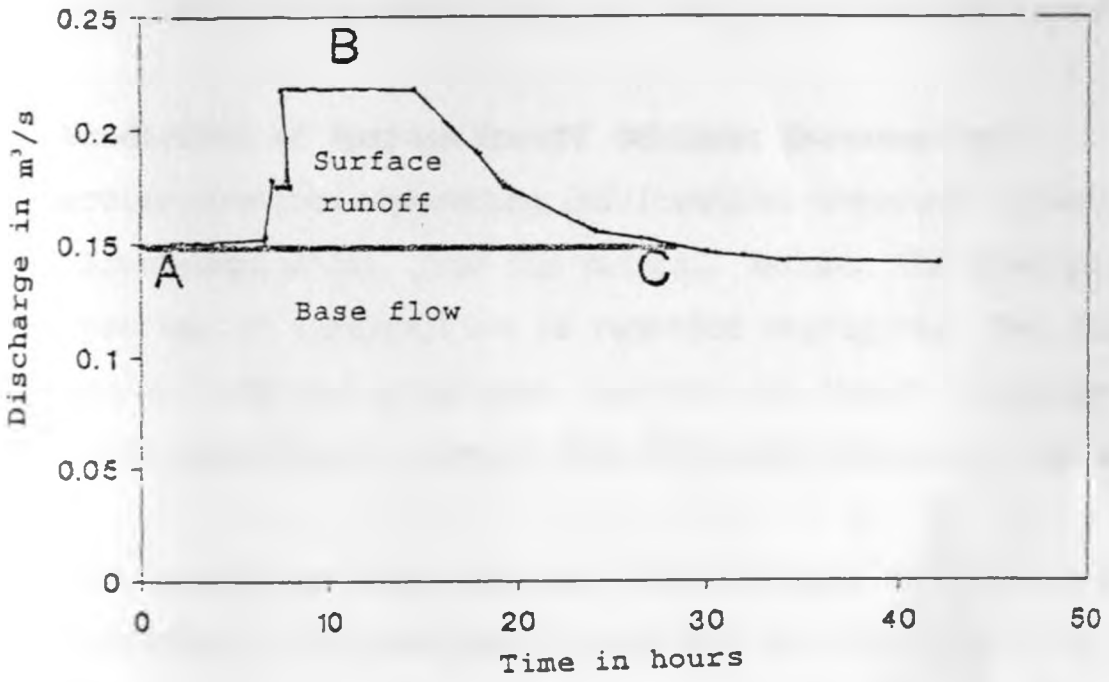

Fig. 3.7 Hydrograph resulting from the storm that occurred on 10-9-69 in Sambret catchment, Kericho, Kenya

Referring to Fig. 3.7 above the line AC separates the baseflow from surface runoff as indicated. The area enclosed under the curve ABC

and the line AB, determined using the dot planimeter gives the measured surface runoff. The hydrograph is indicative of high infiltration capacity in the catchment. This may have been associated with high evapotranspiration losses which reduces soil moisture to a very small value (Wisley and Brater, 1959). Under these conditions, even intense rains falling rarely produce substantial stream rises because most of the water enters the soil and is held there as soil moisture. Also a large proportion of rainfall may have been retained on the irregular ground surface and eventually infiltrated resulting into high infiltration capacity.

3.2.2 Prediction of Surface Runoff (Without Interception)

The exercise involved separating infiltration component, predicted by the Green-Ampt model, from the rainfall amount. The abstraction by the process of interception is regarded negligible. The author developed a computer programme, written in Pascal language to perform the separation, through the following procedure for each event.

i) Model parameters were read into the programme so that the time distribution of infiltration rate may be determined from the model (incorporated in the programme) for any given time interval.

ii) Knowing the intensity distribution of rainfall obtainable from the hyetographs, each intensity and its time interval is entered into the program in the time sequence in which they appear in the hyetograph.

iii) Having entered an intensity and its time interval, the time distribution of infiltration rate is obtained in the interval of the intensity. The area under the resulting infiltration rate curve (infiltrated water) subtracted from the fall (mm) of rain during the intensity interval gives the surface runoff within the interval.

iv) The surface runoff obtained in each of the intensities are summed up to obtain total surface runoff during the event.

A simple illustration of how surface runoff is obtained from the modified and original Green-Ampt models is presented in Figs. 3.8 and 3.9 respectively. These models have been previously described in sections 2.2.6 and 2.2.7. Fig. 3.8 shows the infiltration rate curve derived from the modified form of the model for unsteady rainfall on 10-9-69 in Sambret catchment superimposed on a hyetograph of the same date. Fig. 3.9 shows the infiltration curve derived from the original Green-Ampt model superimposed on the same hyetograph. The area between the hyetograph and the curve gives the predicted surface runoff. The Green-Ampt parameters used to predict infiltration characteristic curves are those based on the USDA-SCS texture based nomographs.

3.2.3 Prediction of Surface Runoff (With Interception)

To determine surface runoff including interception, the intercepted water for an event determined from a given model is subtracted from surface runoff obtained without regard to interception as presented

in the previous section. Figs. 3.10 and 3.11 show the flow charts for the programs used in predicting surface runoff from the original and modified Green-Ampt models respectively. The programs are appended. It should be noted that evapotranspiration losses are being regarded negligible during the storm duration while computing the infiltration. An example on how surface runoff is determined from the Green-Ampt model is appended in Appendix 3.

3.2.4 Determination of Interception Loss

No methods have so far been developed to estimate interception losses for Kenyan catchments. As a result of this, methods developed elsewhere in Europe, America and Asia had to be used. Ward and Robinson (1989) estimated interception for tropical forest in Indonesia, China, Brazil and Puerto Rico as varying from 12 to 54 percent. Interception for heather grass is estimated as varying from 34 to 65 percent. On the basis of this information, interception for the forests in Lagan and Sambret sub-catchment was averagely taken as 30 percent of precipitation taking the forests as being tropical forests. Tea shrubs in Sambret were assumed to have the same interception characteristics as grass and a value of 42 percent of precipitation was assumed.

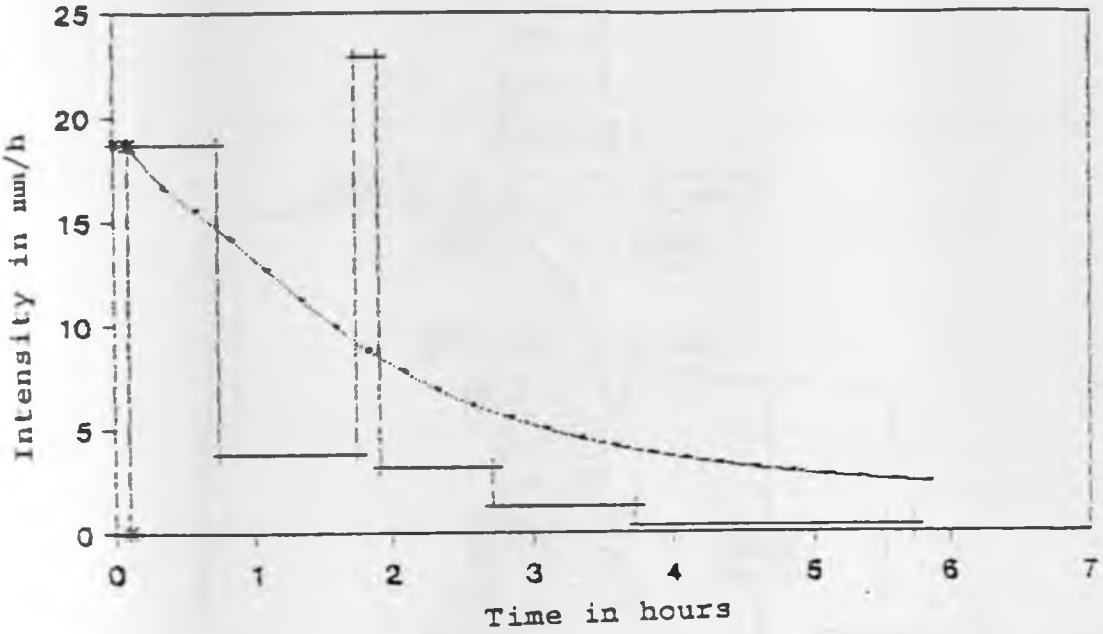

Fig. 3.8 Infiltration curve derived from modified Green-Ampt model superimposed on rainfall hyetograph.

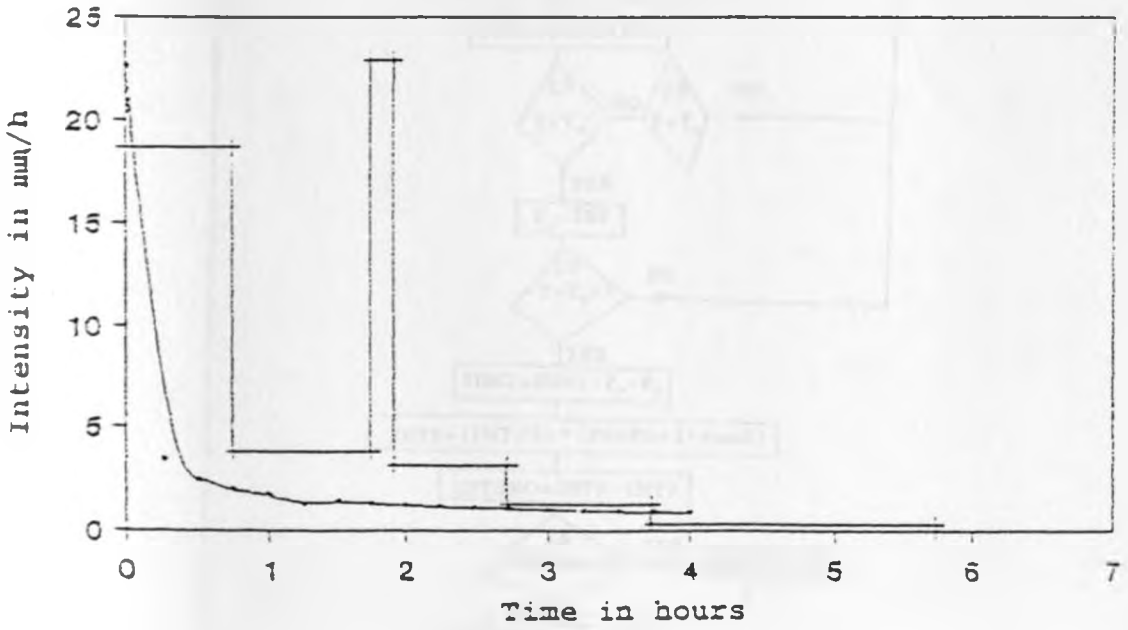

Fig. 3.9 Infiltration curve derived from the original Green-Ampt model superimposed on a rainfall hyetograph

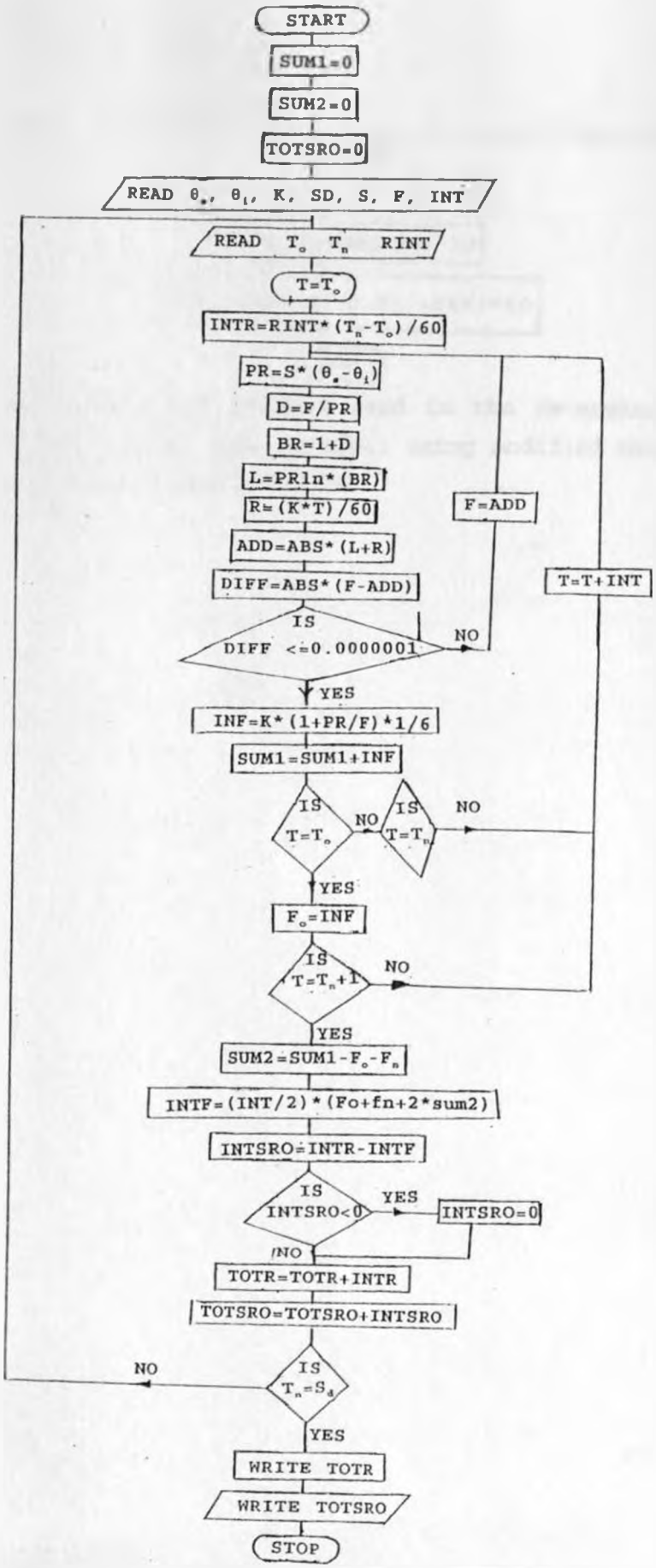

Fig. 3.10 Flow chart of program used in determination of surface runoff from rainfall using original Green-Ampt model for ponded conditions

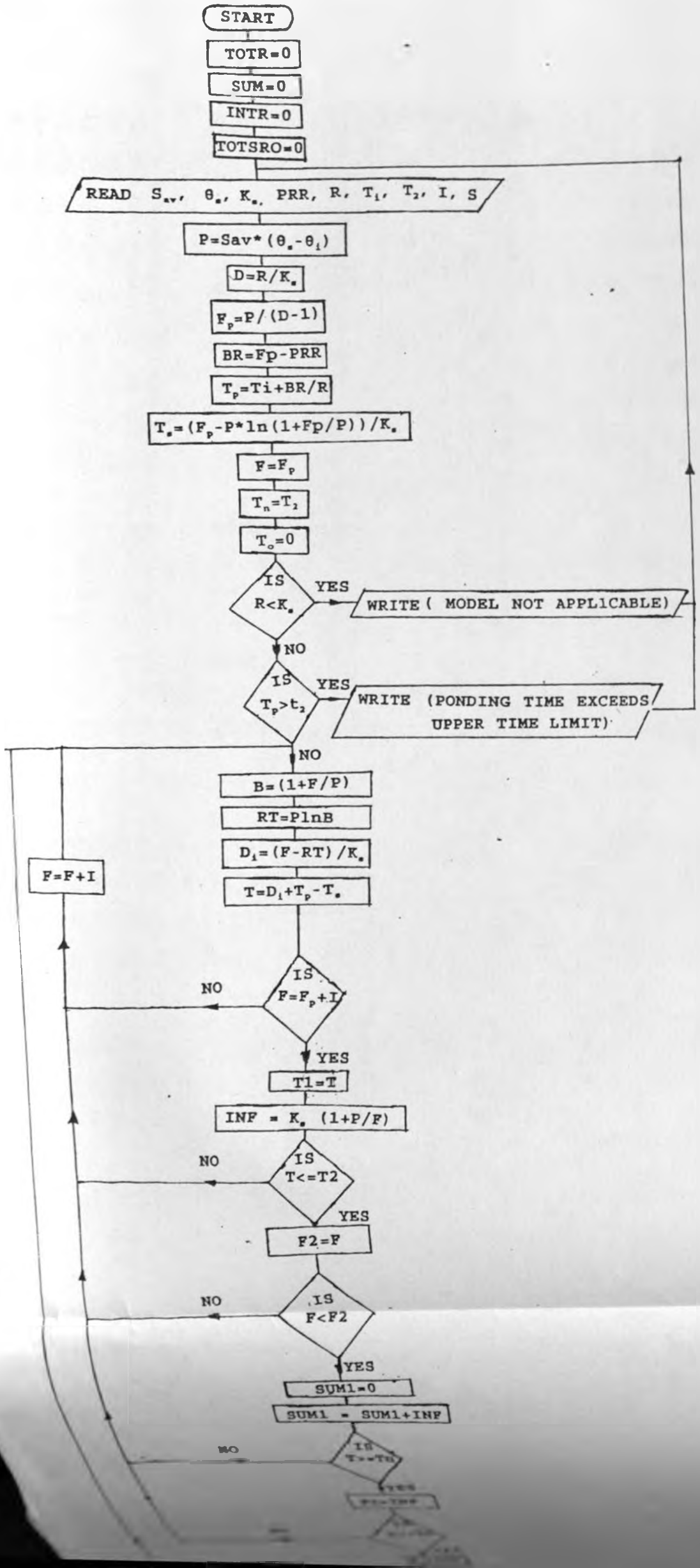
START
TOTR=0
SUM=0
INTR=0
TOTSRO=0
READ S_{av}, θ_s, K_s, PRR, R, T_1, T_2, I, S
P=Sav*(θ_s-θ_i)
D=R/K_s
F_p=P/(D-1)
BR=Fp-PRR
T_p=Ti+BR/R
T_s=(F_p-P*ln(1+Fp/P))/K_s
F=F_p
T_n=T_2
T_o=0
IS R<K_s
YES
WRITE (MODEL NOT APPLICABLE)
NO
IS T_p>t_2
YES
WRITE (PONDING TIME EXCEEDS UPPER TIME LIMIT)
NO
B=(1+F/P)
RT=PlnB
D_i=(F-RT)/K_s
T=D_i+T_p-T_s
F=F+I
IS F=F_p+I
NO
YES
T1=T
INF = K_s (1+P/F)
IS T<=T2
NO
YES
F2=F
IS F<F2
NO
YES
SUM1=0
SUM1 = SUM1+INF

3.2.5 Optimization of the Green-Ampt Model Parameters

The nomograph predicted parameters in the Green-Ampt equation may indicate a disparity in the measured and predicted values of surface runoff, hence the need to optimize them so as to establish an optimal set for which the measured and the predicted values of surface runoff compare reasonably. In a case for which only one parameter is to be optimized, the procedure is to change it systematically while keeping all other parameters constant until a suitable value which makes the predicted surface runoff compare closely to measured value is obtained. The objective function for establishing the correspondence between the measured and predicted surface runoff for a given set of parameters is based on computing a statistic J_{xs} (similar to chisquare) given by the following relationship (Yomota et al., 1993).

$$J_{xs}=\frac{1}{M}\sum \frac{(Q_o-Q_p)^2}{Q_o} \qquad (3.1)$$

Q_o = observed runoff (mm)

Q_p = predicted surface runoff (mm)

M = total number of data points

The best correspondence is achieved when J_{xs} is minimum.

3.2.6 Validation of the Green-Ampt Model

Having established the optimal set of parameters in the model for the catchments under investigation, the model is applied on the

same catchments using a different set of storms. It is on the basis of this validation exercise that model parameters can be said to be applicable to the catchments. In the validation exercise, predicted surface runoff is computed for the selected catchments with the optimized set of parameters. The quality of fit is determined from comparisons between the measured and predicted values about the 1:1 line. The R^2 statistic (coefficient of determination) between predicted and observed surface runoff volume was used as a measure of correspondence between predicted and observed values.

4. RESULTS AND DISCUSSION

4.1 Prediction of Surface Runoff Using Parameters in Green and Ampt Model

Numerical values of the soil parameters in the Green-Ampt model derived from the texture based nomographs were S_{av}=150cm, K_s=0.005cm/h, and θ_s=0.45cm^3/cm^3. The initial moisture content, θ_i, also a parameter in the model was obtained from available records on measured values, at the Kenya Agricultural Research Institute (KARI), Muguga, Kenya. While applying the model in predicting surface runoff, the soil was assumed saturated when θ_i exceeded θ_s, i.e. θ_i was taken as 0.45cm^3/cm^3. It should be borne in mind that the losses through evapotranspiration during a storm have been disregarded in the entire analysis for being very small in magnitude. Likewise, the losses in depression storage have been neglected in view of limited documented information on the behaviour of this process for the vegetated catchments. Using the indicated values of the Green-Ampt model parameters, surface runoff was predicted in Sambret, Lagan and Sambret sub-catchments and the results are discussed below.

4.1.1 Performance of the Original Green-Ampt Model (Developed for Ponded Conditions)

Predicted surface runoff from selected events using the Green-Ampt model for ponded conditions, was compared to the measured with and without taking into account the influence of interception. The values are shown in Table 4.1 through 4.3 for Sambret, Sambret sub-catchment and Lagan catchments respectively. Figs. 4.1 through 4.6 show the comparisons graphically for the said catchments. It is evident that surface runoff was overpredicted for all the events in the three catchments whether interception was assumed negligible or taken into account. Interception reduces the amount of the falling rain that is made available for surface runoff. Some of the rain is intercepted by the leaves and evaporated back to the atmosphere therefore failing to be available for surface runoff. It was therefore felt that the influence of interception be included in testing the performance of the Green-Ampt model. Poor prediction of surface runoff by the original Green-Ampt model is attributed mainly to the fact that the model does not simulate correctly the behaviour of infiltration during rainfall events.

Table 4.1 Measured and predicted surface runoff for Sambret catchment based on the original Green-Ampt model using nomograph parameters

Date	Rainfall mm	Antecedent Moisture Content (cm^3/cm^3)	Interception mm	Surface runoff Measured mm	Predicted Without Interception mm	Predicted With Interception mm
10-9-66	16.30	0.42	6.85	0.36	9.54	2.69
10-2-69	22.86	0.40	9.60	0.22	14.66	5.06
11-7-69	7.37	0.54	3.10	0.21	6.58	3.48
10-9-69	27.43	0.38	11.52	0.40	16.41	4.89
11-10-69	13.97	0.40	5.87	0.02	7.61	1.74
10-2-70	22.85	0.47	9.60	0.16	18.77	9.17
13-5-70	20.57	0.40	8.64	0.20	13.89	5.25
16-1-71	18.90	0.34	7.94	0.31	12.61	4.67
24-4-71	15.20	0.46	6.38	0.18	13.43	7.05
3-5-72	22.30	0.51	9.37	0.33	18.01	8.64
12-2-73	29.40	0.41	12.35	0.50	20.64	8.29

Table 4.2 Measured and predicted surface runoff for Sambret sub-catchment based on the original Green-Ampt model using nomograph parameters

Date	Rainfall mm	Antecedent Moisture Content (cm^3/cm^3)	Interception mm	Surface runoff Measured mm	Predicted Without Interception mm	Predicted With Interception mm
10-2-66	12.20	0.50	3.66	0.12	11.57	7.91
10-3-66	13.30	0.52	3.99	0.30	11.28	7.29
12-4-66	9.40	0.55	2.82	0.13	8.74	5.92
10-2-70	43.18	0.39	12.95	0.70	27.65	14.70
10-4-70	22.35	0.47	6.71	0.26	19.98	13.27
10-4-70	20.40	0.52	6.12	0.21	18.31	12.19
15-1-71	17.60	0.41	5.28	0.18	10.64	5.36
26-5-71	20.80	0.44	6.24	0.23	18.42	12.18
31-1-72	17.50	0.39	5.25	0.21	9.84	4.59
25-10-72	18.40	0.33	5.52	0.22	8.36	2.84
15-1-73	23.20	0.37	6.96	0.30	17.85	10.89

Table 4.3 Measured and predicted surface runoff for Lagan catchment based on the original Green-Ampt model using nomograph parameters

Date	Rainfall mm	Antecedent Moisture Content (cm^3/cm^3)	Interception mm	Surface runoff Measured mm	Predicted Without Interception	Predicted With Interception
21-10-66	14.29	0.49	4.29	0.08	11.20	6.91
21-11-66	19.05	0.43	5.72	0.16	14.47	8.75
5-3-66	17.50	0.42	5.25	0.40	12.42	7.17
21-8-67	21.59	0.39	6.48	0.46	13.64	7.16
22-8-67	27.0	0.49	8.10	0.35	25.64	17.54
21-4-69	12.95	0.53	3.89	0.16	10.46	6.57
21-5-69	27.80	0.44	8.34	0.30	23.42	15.08
21-7-69	15.24	0.51	4.57	0.22	13.61	9.04
29-3-74	17.0	0.42	5.10	0.10	11.64	6.54
30-5-74	11.50	0.46	3.45	0.09	10.99	7.54
29-6-74	17.80	0.39	5.34	0.13	10.64	5.30

The original Green-Ampt model was developed to predict infiltration behaviour under ponded conditions, which assumes potential infiltration rate from the beginning to the end of water application i.e. ponded conditions prevail throughout the period of water application. Under ponded conditions, it is assumed therefore that water is made available for surface runoff immediately at the onset of the rains. This will result into high predicted surface runoff. However during rainfall, infiltration occurs in two stages: the stage without surface ponding and the stage with surface ponding. The stages interchange in a recurrent style depending on the intensity distribution of rainfall. Ponding only occurs when the rainfall intensity exceeds the infiltration capacity of the soil. Should the reverse be true, then no ponding will occur.

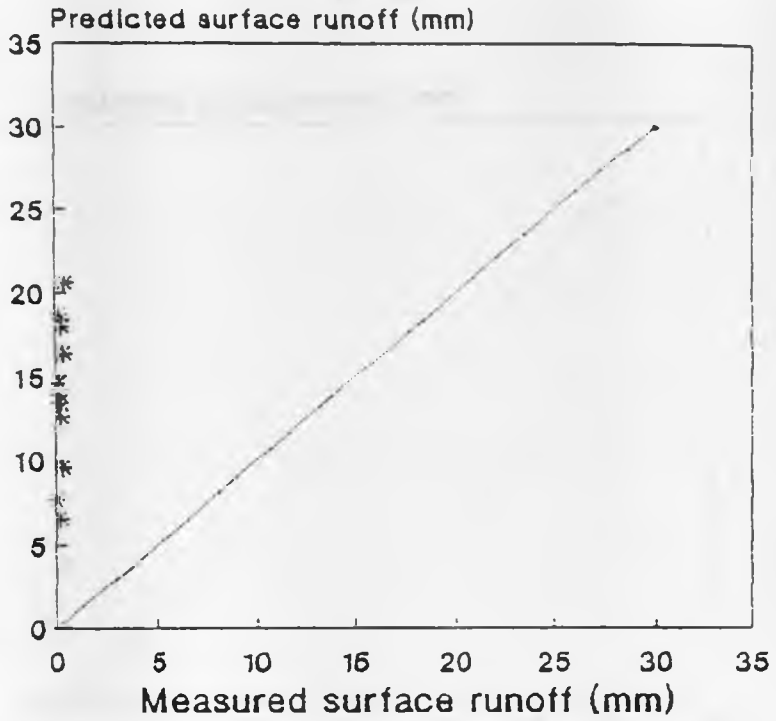

Fig. 4.1 Comparison of predicted surface runoff to measured for Sambret catchment based on the original Green-Ampt model using nomograph parameters and assuming negligible interception

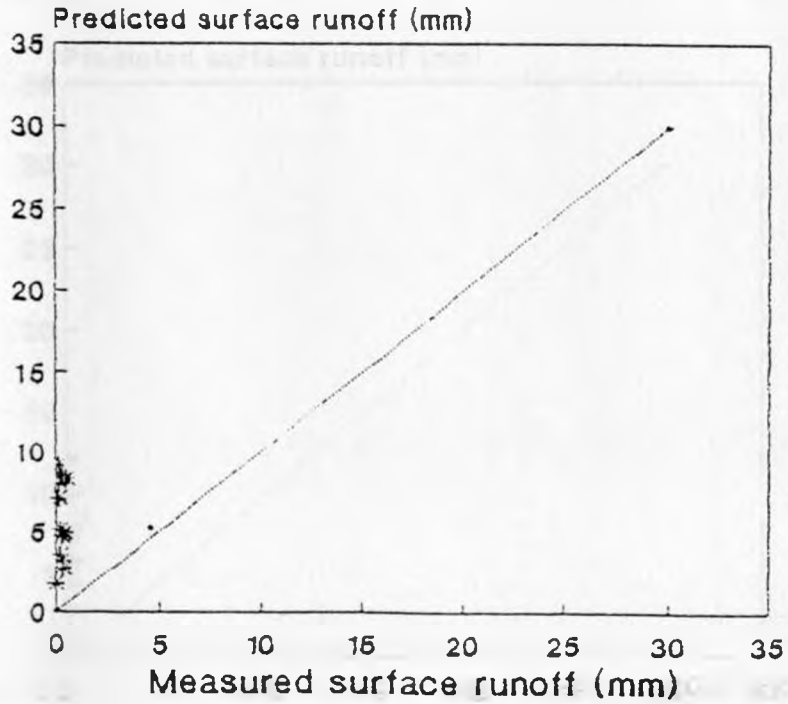

Fig. 4.2 Comparison of predicted surface runoff to measured for Sambret catchment based on the original Green-Ampt model using nomograph parameters and taking into account interception

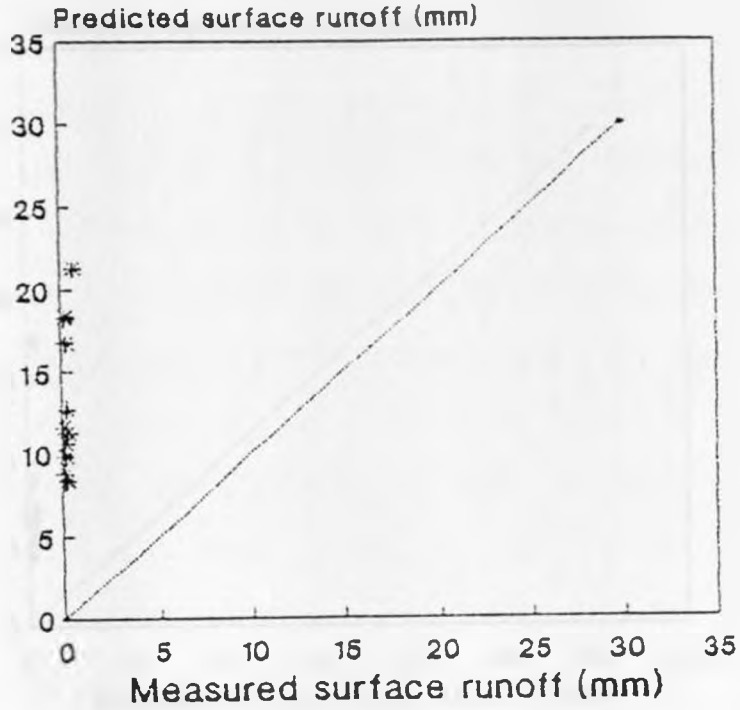

Fig. 4.3 Comparison of predicted surface runoff to measured for Sambret sub-catchment based on the original Green-Ampt model using nomograph parameters and assuming negligible interception

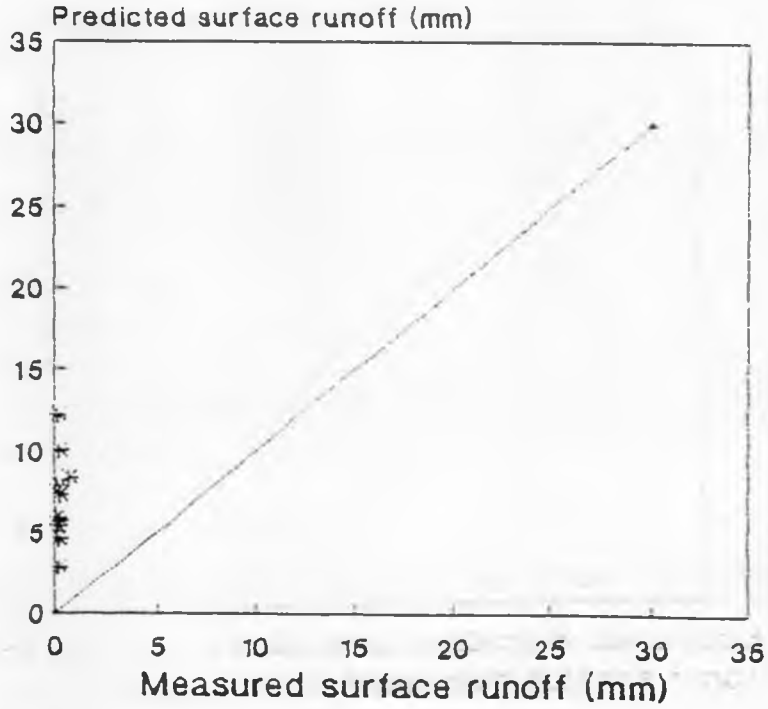

Fig. 4.4 Comparison of predicted surface runoff to measured for Sambret sub-catchment based on the original Green-Ampt model using nomograph parameters and taking into account interception

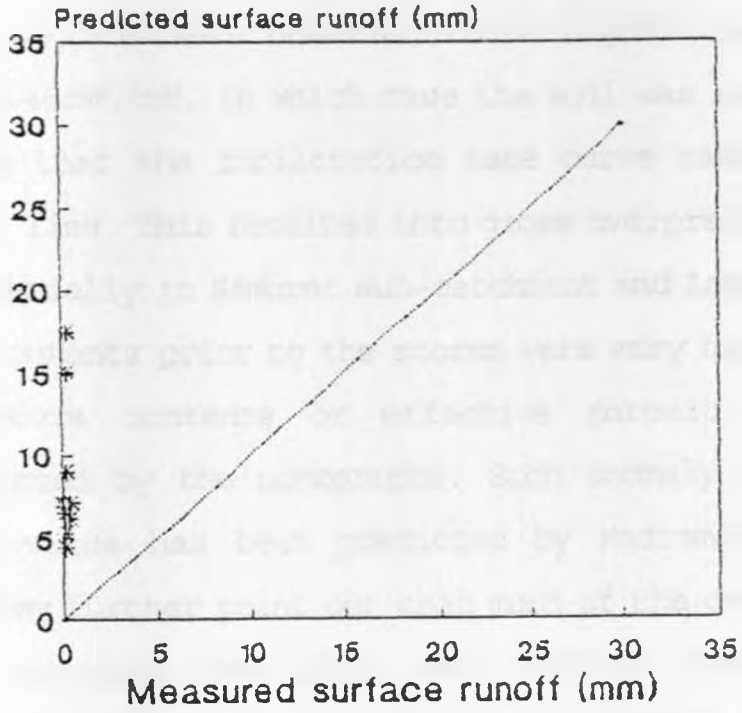

Fig. 4.5 Comparison of predicted surface runoff to measured for Lagan catchment based on the original Green-Ampt model using nomograph parameters and assuming negligible interception

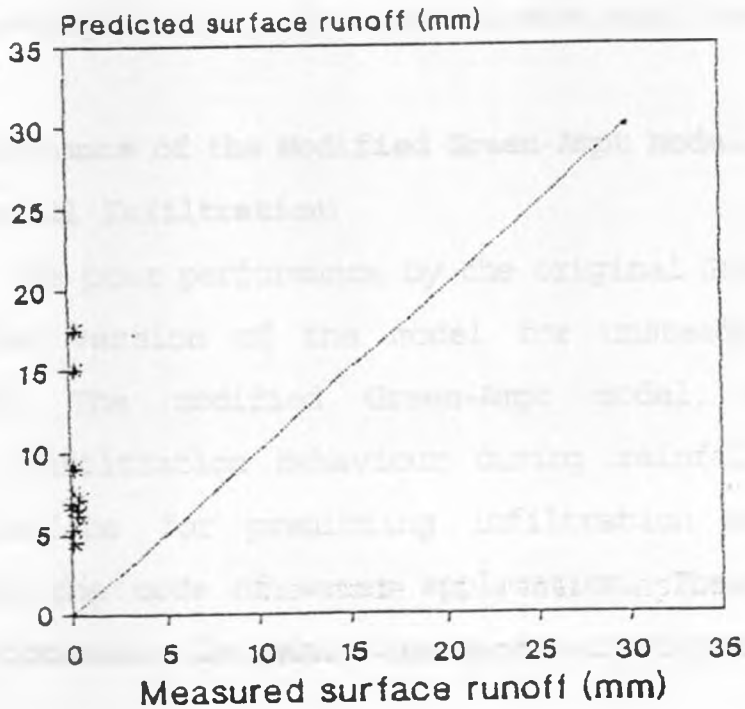

Fig. 4.6 Comparison of predicted surface runoff to measured for Lagan catchment based on the original Green-Ampt model using nomograph parameters and taking into account interception

Some values of measured antecedent moisture contents from the available records were observed to be higher than the nomograph value of 0.45cm³/cm³, in which case the soil was assumed saturated. This means that the infiltration rate curve takes the form of a horizontal line. This resulted into gross overprediction of surface runoff especially in Sambret sub-catchment and Lagan where the soil moisture contents prior to the storms were very high. The saturated soil moisture contents or effective porosity may have been underpredicted by the nomographs. Such anomaly in the nomograph predicted value has been predicted by Madramootoo and Enright (1989). They further point out that much of the data which form the basis of nomograph development were derived from coarse textured soils. The nomographs may not have been applicable in fine textured soils (e.g. clay). On the other hand, the available records on antecedent moisture contents may not be representative of the catchment average as only three sites were monitored.

4.1.2 Performance of the Modified Green-Ampt Model (Developed for Rainfall Infiltration)

In view of the poor performance by the original Green-Ampt model, the modified version of the model for unsteady rainfall was implemented. The modified Green-Ampt model, developed for predicting infiltration behaviour during rainfall events is a better technique for predicting infiltration behaviour where rainfall is the mode of water application. The modified model simulates correctly the behaviour of infiltration during rainfall

events. The surface runoff was predicted with and without considering interception. The results of analysis are presented in Tables 4.4 through 4.6 and Figs. 4.7 through 4.12 . Evidently again surface runoff was overpredicted for all the events in the three catchments whether interception was assumed negligible or taken into account.

4.1.3 Suspected Reasons for Overprediction

Despite implementing the modified version of Green-Ampt model, the predictions of surface runoff hardly improved. The poor predictability can be associated with the improper values of parameters such as K_s, θ_s, and S_{av} as has been noted elsewhere (Madramootoo and Enright, 1989). The value of saturated hydraulic conductivity (K_s) predicted from the nomographs is 0.005cm/h, where as the K_s value documented in texts (Chow et al., 1988) is 0.03cm/h for clay soils.

Table 4.4 Measured and predicted surface runoff for Samboret catchment based on the modified Green-Ampt model using nomograph parameters

Date	Rainfall mm	Antecedent Moisture Content (cm³/cm³)	Interception mm	Surface runoff Measured mm	Predicted Without Interception	Predicted With Interception
10-9-66	16.30	0.42	6.85	0.36	14.18	7.33
10-2-69	22.86	0.40	9.60	0.22	17.32	7.72
11-7-69	7.37	0.54	3.10	0.21	6.58	3.48
10-9-69	27.43	0.38	11.52	0.40	22.86	11.34
11-10-69	13.97	0.40	5.87	0.02	11.54	5.67
10-2-70	22.85	0.47	9.60	0.16	18.77	9.17
13-5-70	20.57	0.40	8.64	0.20	17.65	9.01
16-1-71	18.90	0.34	7.94	0.31	15.41	7.47
24-4-71	15.20	0.46	6.38	0.18	13.43	7.05
3-5-72	22.30	0.51	9.37	0.33	18.01	8.64
22-2-73	29.40	0.41	12.35	0.50	26.41	14.06

Table 4.5 Measured and predicted surface runoff for Sambret sub-catchment based on the modified Green-Ampt model using nomograph parameters

Date	Rainfall mm	Antecedent Moisture Content (cm^3/cm^3)	Interception mm	Surface runoff Measured mm	Predicted Without Interception	Predicted With Interception
10-2-66	12.20	0.50	3.66	0.12	11.57	7.91
10-3-66	13.00	0.52	3.99	0.30	11.28	7.29
12-4-66	9.40	0.55	2.82	0.13	8.74	5.92
10-2-70	43.18	0.39	12.95	0.70	36.41	23.46
10-4-70	22.35	0.47	6.71	0.26	19.87	13.16
24-4-70	20.40	0.52	6.12	0.21	18.31	12.19
10-2-70	17.60	0.41	5.28	0.18	14.61	9.33
10-4-70	20.80	0.44	6.24	0.23	19.41	13.17
13-1-72	17.50	0.39	5.24	0.21	11.61	6.37
25-10-72	18.40	0.33	5.52	0.22	12.43	6.91
15-1-73	23.20	0.37	6.96	0.30	16.51	9.55

Table 4.6 Measured and predicted surface runoff for Lagan catchment based on the modified Green-Ampt model using nomograph parameters

Date	Rainfall mm	Antecedent Moisture Content (cm^3/cm^3)	Interception mm	Surface runoff Measured mm	Predicted (mm) Without Interception	Predicted (mm) With Interception
21-10-66	14.29	0.49	4.29	0.08	11.20	6.91
21-11-66	19.05	0.43	5.72	0.16	17.63	11.91
5-3-67	17.50	0.42	5.25	0.40	13.65	8.40
21-8-67	21.59	0.39	6.48	0.46	16.95	10.47
22-8-67	27.0	0.49	8.10	0.35	25.64	17.54
21-4-69	12.95	0.53	3.89	0.16	10.46	6.57
21-5-69	27.80	0.44	8.34	0.30	25.24	16.90
21-7-69	15.24	0.51	4.57	0.22	13.61	9.04
29-3-74	17.0	0.42	5.10	0.10	14.48	9.38
30-5-74	11.50	0.46	3.45	0.09	10.99	7.54
29-6-74	17.80	0.39	5.34	0.13	14.65	9.31

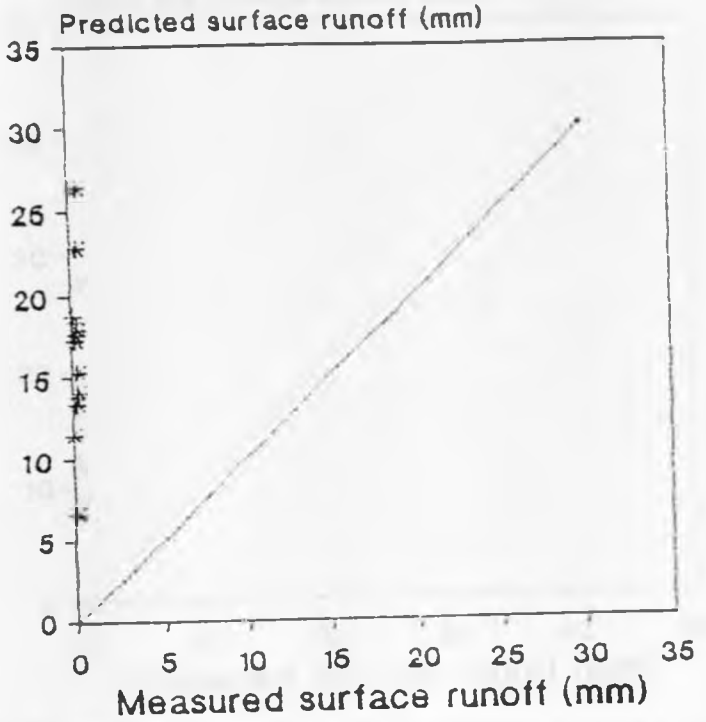

Fig. 4.7 Comparison of predicted surface runoff to measured for Sambret catchment based on the modified Green-Ampt model using nomograph parameters and assuming negligible interception

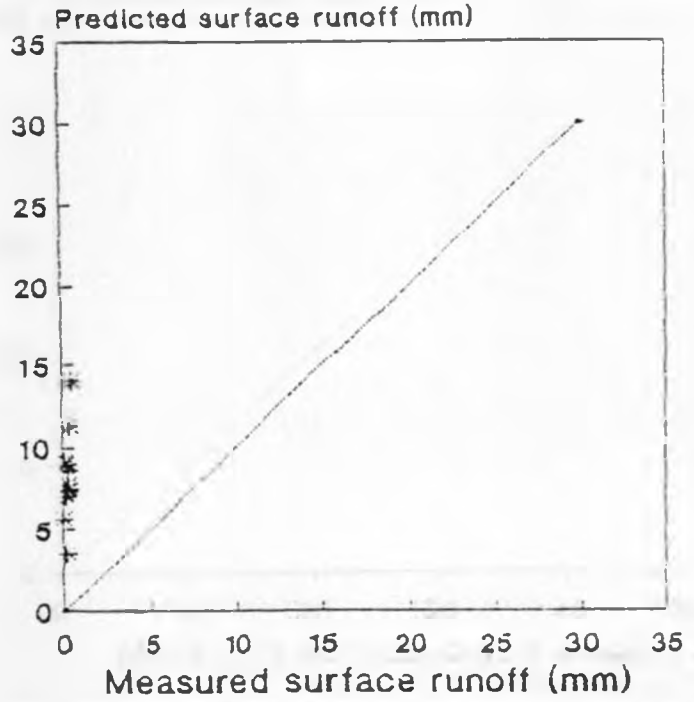

Fig. 4.8 Comparison of predicted surface runoff to measured for Sambret catchment based on the modified Green-Ampt model using nomograph parameters and taking into account interception

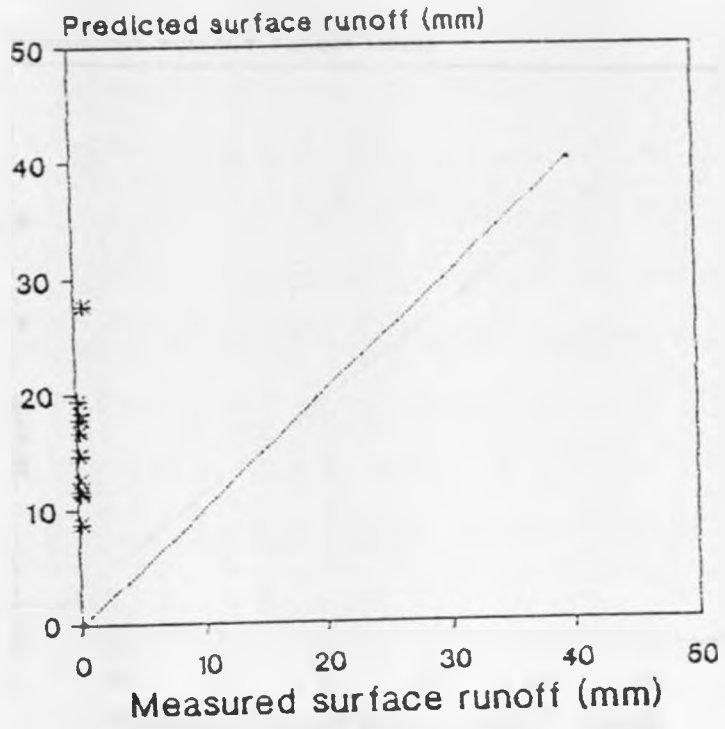

Fig. 4.9 Comparison of predicted surface runoff to measured for Sambret sub-catchment based on the modified Green-Ampt model using nomograph parameters and assuming negligible interception

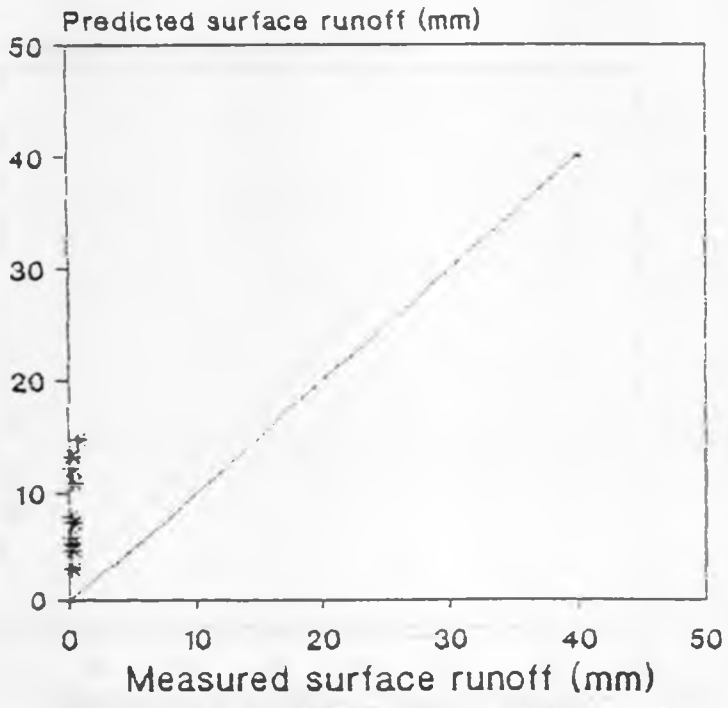

Fig. 4.10 Comparison of predicted surface runoff to measured for Sambret sub-catchment based on the modified Green-Ampt model using nomograph parameters and taking into account interception

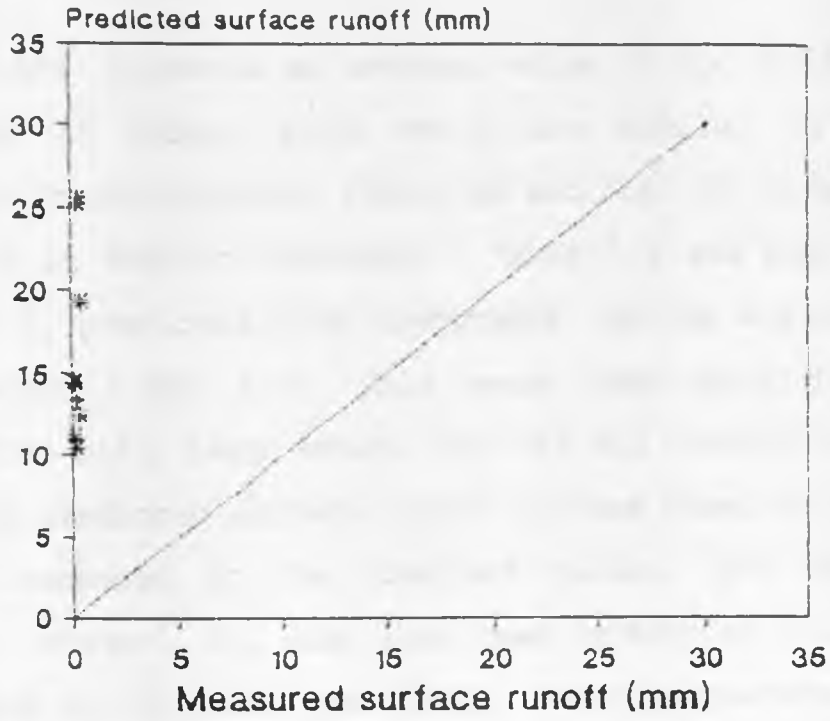

Fig. 4.11 Comparison of predicted surface runoff to measured for Lagan catchment based on modified Green-Ampt model using nomograph parameters and assuming negligible interception

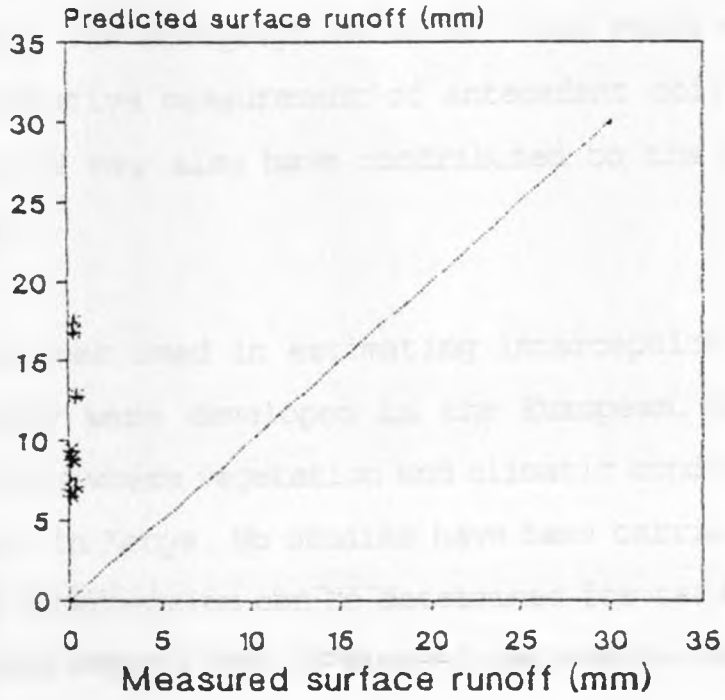

Fig. 4.12 Comparison of predicted surface runoff to measured for Lagan catchment based on the modified Green-Ampt model using nomograph parameters and taking into account interception

Miriti (1994) presents an average value of K_s= 12.03cm/h for the top layer of Kabete soils which are similar in texture and hydraulic characteristics (Table A2 and Fig. A2 in Appendix 4) to the soils in Sambret catchment (Table 3.2 and Fig. 3.1). A low value of K_s predicted from nomographs implies a reduced rate of infiltration (Eq. 2.8). This means less water from the rain infiltrates and a large amount runs off and therefore explains the very high predicted surface runoff volumes based on low values of K_s when compared to the observed values. The saturated soil moisture content, θ_s, has also been predicted too low by the nomographs as mentioned previously. Other parameters predicted by nomographs fall within the acceptable limits. For example the value of S_{av} i.e. the wetting front suction for clay soils is documented to lie in the range 6.39-156.5cm in the hydrologic texts (Chow et al., 1988). The nomograph value of 150cm falls within this range. Unrepresentative measurement of antecedent soil moisture obtained from records may also have contributed to the poor prediction by this model.

The techniques used in estimating interception in the catchments under study were developed in the European, American and Asian environments where vegetation and climatic conditions are different from those in Kenya. No studies have been carried out to find means by which interception can be determined for tea shrubs which is the predominant vegetation in Sambret catchment. Although methods are

available for estimating interception in forested areas, they were developed for catchments with climatic conditions different from those in Kenya. Hence the interception values used in analysis for Sambret, Lagan and Sambret sub-catchments may not represent the true situation. This might have contributed to the poor prediction of surface runoff when interception is considered.

Among the parameters considered as having resulted into poor prediction of surface runoff using the Green-Ampt model, the hydraulic conductivity (K_s) is the most variable and unpredictable. It is hard to establish an exact value for any given soil. Different methods of measurement also yield different values. The saturated soil moisture content for the soil of a given texture can be regarded as constant. It rarely varies with landuse. For the soils in Sambret catchment, the measured value is about $0.7cm^3/cm^3$. This was taken as the value for Sambret and Lagan catchments which are similar in texture and therefore expected to have the same value of porosity. The nomograph value of $0.45cm^3/cm^3$ is too low and should be discarded. Since the most suspected parameter in the Green-Ampt model appears to be the saturated hydraulic conductivity an attempt was made to establish a representative value of K_s for each of the catchments by an optimization exercise. The exercise was carried out as follows.

4.2 Optimization of Saturated Hydraulic Conductivity (K_s)

The exercise for optimization was begun using the K_s values ranging

from 0.01 upwards with a step of 0.01 until the predictions approached measured surface runoff. The measured value of θ_s was taken as 0.7cm³/cm³ as was retrieved from record as a measured value and the nomographic value (θ_s=0.45cm³/cm³) was discarded. However the value of the wetting front suction S_{av} was taken as 150cm from the nomographs without alteration. The soil moisture content, θ_i, were used in the same way as was used in the preceding sections. In case (with or without interception), the surface runoff was predicted with the modified Green-Ampt model for all the catchments under study. It was observed that for most of the events, the predicted surface runoff continued to drop as K_s was raised from 0.01 to 0.1 (Tables 4.7 through 4.13). The predicted surface runoff reached zero when K_s assumed the value of 0.1cm/h. Such a behaviour in runoff response suggested that an optimal value should lie within the range of 0.01 to 0.1cm/h. In order to determine the optimal value of K_s, the objective function J_{xs} was computed and plotted against K_s values rising from 0.01 with a step 0.01. A typical plot is shown in Fig. 4.13 which corresponds to Sambret catchment. The coordinates for the plot, i.e., abscissa (K_s) and ordinate (J_{xs}) are shown in Table 4.8. It can be seen that the plot dips at the value of K_s = 0.08cm/h and the minimum value of J_{xs} is 0.02. Therefore, the optimal value of K_s shall be regarded 0.08cm/h for the Sambret catchment without taking interception into account. The optimization results for all catchments with and without interception are shown in Tables 4.14 through 4.16. The optimized values of K_s are indicated summarized in Table 4.17.

Table 4.7 Measured and predicted surface runoff, obtained without considering interception for Sambret catchment, at limits between which the optimal value of K_s (cm/h) is expected

Date	Rainfall mm	Antecedent Moisture Content (cm^3/cm^3)	Interception mm	Surface runoff Measured mm	Predicted (mm) K_s=0.01	K_s=0.1
10-9-66	16.30	0.42	6.85	0.36	7.76	0
10-2-69	22.36	0.40	9.60	0.22	13.04	0
11-7-69	7.37	0.54	3.10	0.21	4.20	0
10-9-69	27.43	0.38	11.52	0.40	15.03	0
11-10-69	13.97	0.40	5.87	0.02	7.03	0
10-2-70	22.85	0.47	9.60	0.16	9.46	0
13-5-70	20.57	0.40	8.64	0.20	10.53	0
16-1-71	18.90	0.34	7.94	0.31	8.72	0
24-4-71	15.20	0.46	6.38	0.18	8.91	0
3-5-72	22.30	0.51	9.37	0.33	15.96	0
12-2-73	29.40	0.41	12.35	0.50	15.21	0
			Value of objective function (J_{xs})		625.19	0.26

Table 4.8 Variation of the objective function J_{xs} with saturated hydraulic conductivity within the range 0.01cm/h<=K_s<=0.1cm/h for Sambret catchment without interception

Saturated hydraulic conductivity (K_s) (cm)	Objective function (J_{xs}) (mm)
0.01	625.19
0.02	508.30
0.03	430.30
0.04	302.13
0.05	178.0
0.06	92.53
0.07	22.67
0.08	0.02
0.09	0.16
0.10	0.26

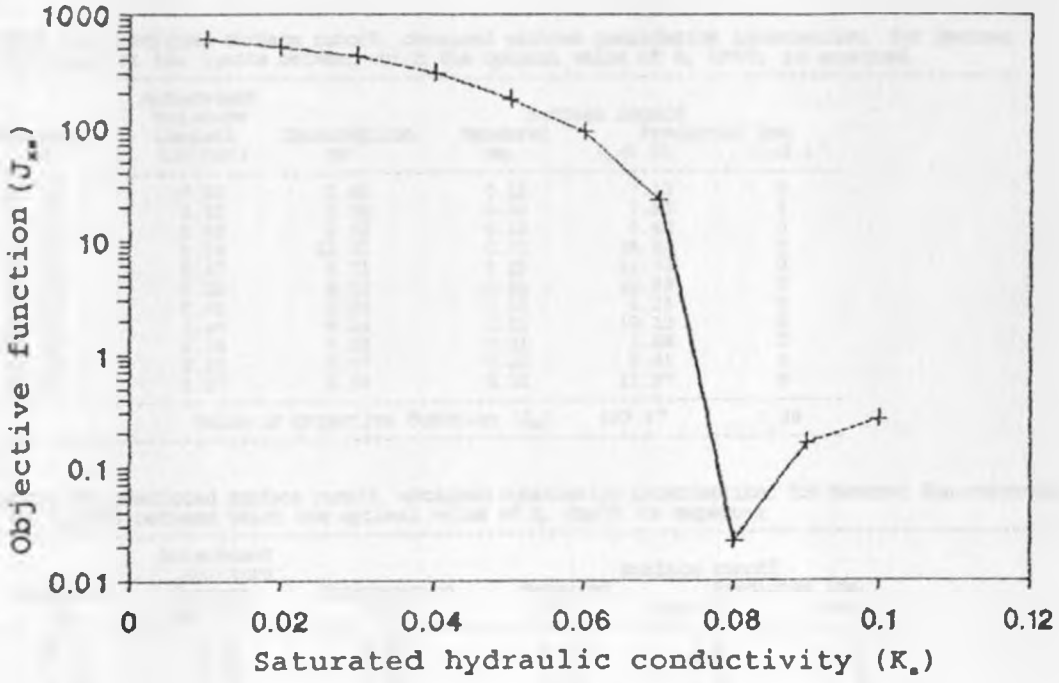

Fig. 4.13 Variation of objective function (J_{xs}) with saturated hydraulic conductivity (K_s) within the range $0.01<=K_s<=0.1$cm/h for Sambret catchment without considering interception

Table 4.9 Measured and predicted surface runoff, obtained considering interception, for Sambret catchment at the limits between which the optimal value of K_s (cm/h) is expected

Date	Rainfall mm	Antecedent Moisture Content (cm3/cm3)	Interception mm	Surface runoff Measured mm	Predicted (mm) K_s=0.01	K_s=0.1
10-9-66	16.30	0.42	6.85	0.36	0.91	0
10-2-69	22.86	0.40	9.60	0.22	3.44	0
11-7-69	7.37	0.54	3.10	0.21	1.10	0
10-9-69	27.43	0.38	11.52	0.40	3.51	0
11-10-69	13.97	0.40	5.87	0.02	1.16	0
10-2-70	22.85	0.47	9.60	0.16	0.81	0
13-5-70	20.57	0.40	8.64	0.20	0.82	0
16-1-71	18.90	0.32	7.94	0.31	0.78	0
24-4-71	15.20	0.46	6.38	0.18	0.43	0
3-5-72	22.30	0.51	9.37	0.33	6.59	0
12-2-73	29.40	0.41	12.35	0.50	2.90	0
			Value of objective function (J_{xs})		25.16	0.26

Table 4.10 Measured and predicted surface runoff, obtained without considering interception, for Sambret sub-catchment at the limits between which the optimal value of K_s (cm/h) is expected

Date	Rainfall mm	Antecedent Moisture Content (cm^3/cm^3)	Interception mm	Surface runoff Measured mm	Predicted (mm) K_s=0.01	K_s=0.1
10-2-66	12.20	0.50	3.66	0.12	7.13	0
10-3-66	13.30	0.52	3.99	0.30	7.92	0
12-4-66	9.40	0.55	2.82	0.13	5.42	0
10-2-70	43.18	0.39	12.95	0.70	28.24	0
10-4-70	22.35	0.47	6.71	0.26	12.73	0
23-4-70	20.40	0.52	6.12	0.21	10.98	0
15-1-71	17.60	0.41	5.28	0.18	8.38	0
26-6-71	20.80	0.44	6.24	0.23	10.13	0
31-1-72	17.50	0.39	5.25	0.21	7.66	0
25-10-72	18.40	0.33	5.52	0.22	9.46	0
15-1-73	23.20	0.37	6.96	0.30	12.97	0
			Value of objective function (J_{ss})		469.67	0.26

Table 4.11 Measured and predicted surface runoff, obtained considering interception, for Sambret Sub-catchment at the limits between which the optimal value of K_s (cm/h) is expected

Date	Rainfall mm	Antecedent Moisture Content (cm^3/cm^3)	Interception mm	Surface runoff Measured mm	Predicted (mm) K_s=0.01	K_s=0.1
10-2-66	12.20	0.50	3.66	0.12	3.47	0
10-3-66	13.30	0.52	3.99	0.3	3.93	0
12-4-66	9.40	0.55	2.82	0.13	2.60	0
10-2-70	43.18	0.39	12.95	0.70	15.29	0
10-4-70	22.35	0.47	6.71	0.26	5.32	0
23-4-70	20.40	0.52	6.12	0.21	4.86	0
15-1-71	17.60	0.41	5.28	0.18	3.10	0
26-6-71	20.80	0.44	6.24	0.23	3.89	0
31-1-72	17.50	0.39	5.25	0.21	2.41	0
25-10-72	18.40	0.33	3.94	0.22	3.94	0
15-1-73	23.20	0.37	6.96	0.30	6.01	0
			Value of objective function (J_{ss})		469.67	0.26

Table 4.12 Measured and predicted surface runoff, obtained without considering interception for Lagan catchment at the limits between which the optimal value of K_s (cm/h) is expected

Date	Rainfall mm	Antecedent Moisture Content (cm^3/cm^3)	Interception mm	Surface runoff Measured mm	Predicted (mm) K_s=0.01	K_s=0.1
21-10-66	14.29	0.49	4.29	0.08	8.45	0
21-11-66	19.05	0.43	5.72	0.16	12.0	0
22-8-67	17.50	0.42	5.25	0.40	11.41	0
22-8-67	21.59	0.39	6.48	0.46	13.50	0
22-8-67	27.0	0.49	8.10	0.35	16.41	0
21-4-69	12.95	0.53	3.89	0.16	8.64	0
21-5-69	27.80	0.44	8.34	0.30	16.43	0
22-7-69	15.24	0.51	4.57	0.22	10.91	0
29-3-74	17.0	0.42	5.10	0.10	11.61	0
30-5-74	11.50	0.46	3.45	0.09	4.94	0
26-6-74	17.80	0.39	5.34	0.13	9.98	0
			Value of objective function (J_{os})		666.4	0.22

Table 4.13 Measured and predicted surface runoff, obtained considering interception, for Lagan catchment at the limits between which the optimal value of K_s (cm/h) is expected

Date	Rainfall mm	Antecedent Moisture Content (cm^3/cm^3)	Interception mm	Surface runoff Measured mm	Predicted (mm) K_s=0.01	K_s=0.1
21-10-66	14.29	0.49	4.29	0.08	4.16	0
21-11-66	19.05	0.43	5.72	0.16	6.28	0
5-3-67	17.50	0.42	5.25	0.40	6.16	0
21-8-67	21.59	0.39	6.48	0.46	7.02	0
22-8-67	27.00	0.49	8.10	0.35	8.31	0
21-4-69	12.95	0.53	3.89	0.16	4.75	0
21-5-69	27.80	0.44	8.34	0.30	8.09	0
22-7-69	15.24	0.51	4.57	0.22	5.34	0
29-3-74	17.00	0.42	5.10	0.10	6.51	0
30-5-74	11.50	0.46	3.45	0.09	1.49	0
29-6-74	17.80	0.39	5.34	0.13	4.64	0
			Value of objective function (J_{os})		172.10	0.22

Table 4.14 Measured and predicted surface runoff at the optimized values of K_s (cm/h) for Sambret catchment

Date	Rainfall mm	Antecedent Moisture Content (cm3/cm3)	Interception mm	Surface runoff Measured mm	Predicted Without Interception (K_s=0.09cm/h)	Predicted With Interception (K_s=0.03cm/h)
10-9-66	16.30	0.43	6.85	0.36	0.29	0.31
10-2-69	22.86	0.40	9.60	0.22	0.17	0.41
11-7-69	7.37	0.54	3.10	0.21	0.13	0.18
10-9-69	27.43	0.38	12.52	0.40	0.37	0.45
12-10-69	13.97	0.40	5.87	0.02	0.00	0.20
10-2-70	22.85	0.47	9.60	0.16	0.21	0.22
23-5-70	20.57	0.40	8.64	0.20	0.18	0.28
15-1-71	18.90	0.34	7.94	0.31	0.28	0.26
24-4-71	15.20	0.46	6.38	0.18	0.21	0.14
3-5-72	22.30	0.51	9.37	0.33	0.30	0.38
12-2-73	29.40	0.41	12.35	0.50	0.41	0.46
			Value of objective function (J_{os})		0.02	0.18

Table 4.15 Measured and predicted surface runoff at the optimized values of K_s (cm/h) for Sambret sub-catchment

Date	Rainfall mm	Antecedent Moisture Content (cm^3/cm^3)	Interception mm	Surface runoff Measured mm	Predicted (mm) Without Interception (K_s=0.09cm/h)	Predicted With Interception (K_s=0.04cm/h)
10-2-66	12.20	0.50	3.66	0.12	0.09	0.20
10-3-66	13.30	0.52	3.99	0.30	0.12	0.27
12-4-66	9.40	0.55	2.82	0.13	0.21	0.18
10-2-70	43.18	0.39	12.95	0.70	0.92	0.91
10-4-70	22.35	0.47	6.71	0.26	0.51	0.31
23-4-70	20.40	0.52	6.12	0.21	0.32	0.29
15-1-71	17.60	0.41	5.28	0.18	0.42	0.22
26-5-71	20.80	0.44	6.24	0.23	0.11	0.21
31-1-72	17.50	0.39	5.25	0.21	0.14	0.25
25-10-72	18.40	0.33	5.52	0.22	0.16	0.24
15-1-73	23.20	0.37	6.96	0.30	0.20	0.30
			Value of objective function (J_{os})		0.09	0.32

Table 4.16 Measured and predicted surface runoff at the optimized values of K_s (cm/h) for Lagan catchment

Date	Rainfall mm	Antecedent Moisture Content (cm3/cm3)	Interception mm	Surface runoff Measured mm	Predicted Without Interception (K_s=0.09cm/h)	Predicted With Interception (K_s=0.05cm/h)
21-10-66	14.29	0.49	4.29	0.08	0.16	0.10
11-11-66	19.05	0.43	5.72	0.16	0.19	0.23
5-3-67	17.50	0.42	5.25	0.40	0.21	0.29
21-8-67	21.59	0.39	6.48	0.46	0.31	0.36
22-8-67	27.00	0.49	8.10	0.35	0.11	0.41
21-4-69	12.95	0.53	3.89	0.16	1.92	0.19
22-5-69	27.80	0.44	8.34	0.30	0.41	0.28
21-7-69	15.24	0.51	4.57	0.22	0.32	0.25
29-3-74	17.00	0.42	5.10	0.10	0.00	0.24
30-5-74	11.50	0.46	3.45	0.09	0.07	0.00
29-6-74	17.80	0.39	5.34	0.13	0.11	0.15
			Value of objective function (J_{xs})		1.81	0.20

Table 4.17 Summary of the optimized values of saturated hydraulic conductivity (K_s) for the catchments

Catchment	Optimized K_s (cm/h) value Without Interception	J_{xs}	With Interception	J_{xs}
Sambret	0.08	0.02	0.03	0.18
Sambret sub-catchment	0.09	0.09	0.04	0.02
Lagan	0.09	1.81	0.05	0.20

One can see that optimal values of K_s (Table 4.17) without interception are nearly constant for all the catchments. However, they tend to vary when the interception is taken into account. The variation of K_s is expected to vary in response to vegetal cover even for the same textural classification. Hence a need arises to validate the role of interception and subsequently the value of K_s. The results of validation exercise are described below.

4.3 Validation of Hydraulic Conductivity (K_s)

For each optimal value obtained, the goodness of fit was determined between the measured and predicted surface runoff. The criteria for determining this goodness of fit was based on the coefficient of determination (R^2). For each catchment, the value of K_s that results into a higher R^2 is taken as the valid one.

Fourteen storms were used for validation in the Sambret catchment. Of the two optimized values (K_s=0.08 and 0.03cm/h), a better quality of fit was obtained at K_s=0.03cm/h which pertains to the situation when interception is taken into account. The comparison of measured and predicted values is shown in Table 4.18 and Figs. 4.14 and 4.15 for both values of K_s. Also in Sambret sub-catchment fourteen storms were considered for the validation exercise. Of the two optimized values, 0.09cm/h and 0.04cm/h (without and with interception), The better quality of fit between the measured and predicted values of surface runoff was obtained for the latter value (0.04cm/h). The results are shown in Table 4.19 and Figs 4.16 and 4.17. In Lagan catchment, a better correspondence was obtained at K_s=0.05cm/h which corresponds to the situation in which interception is considered. The results of validation exercise are shown in Table 4.20 and Figs. 4.18 and 4.19.

Table 4.18 Measured and predicted surface runoff for Sambret catchment during validation of previously optimized values of saturated hydraulic conductivity (K_s)

Date	Rainfall mm	Antecedent Moisture Content (cm^3/cm^3)	Interception mm	Surface runoff Measured mm	Predicted (mm) Without Interception (K_s=0.08cm/h)	Predicted (mm) With Interception (K_s=0.03cm/h)
12-1-65	20.32	0.36	8.13	0.31	0.14	0.29
5-12-65	18.80	0.23	7.52	0.11	0.00	0.01
10-3-66	15.50	0.44	6.20	0.41	0.86	0.38
11-6-66	17.53	0.43	7.01	0.34	1.67	0.40
12-12-66	19.30	0.41	7.72	0.16	1.71	0.19
25-3-67	20.10	0.53	8.04	0.30	2.03	0.26
12-5-67	37.85	0.54	15.14	0.28	3.52	0.27
13-7-67	17.53	0.46	7.01	0.10	1.38	0.13
9-2-68	20.07	0.31	8.03	0.20	0.19	0.26
15-6-68	27.70	0.36	11.08	0.31	0.41	0.30
12-8-68	16.26	0.39	6.50	0.23	0.17	0.21
10-8-69	19.05	0.51	7.62	0.18	1.56	0.26
13-5-70	20.57	0.40	8.23	0.28	0.40	0.25
14-7-70	25.40	0.27	10.16	0.34	0.26	0.40

Table 4.19 Measured and predicted surface runoff for Sambret sub-catchment during validation of previously optimized values of saturated hydraulic conductivity (K_s)

Date	Rainfall mm	Antecedent Moisture Content (cm3/cm3)	Interception mm	Surface runoff Measured mm	Predicted Without Interception (K_s=0.09cm/h)	Predicted With Interception (K_s=0.04cm/h)
31-1-65	21.90	0.49	6.57	0.28	2.31	0.27
4-7-65	27.0	0.54	8.10	0.30	2.51	0.31
13-6-66	18.70	0.57	5.61	0.26	1.92	0.25
9-5-67	26.0	0.39	7.80	0.28	2.98	0.26
18-11-67	26.40	0.41	7.92	0.24	3.02	0.28
26-11-67	18.30	0.37	5.49	0.14	1.31	0.18
9-2-68	20.60	0.37	6.18	0.22	2.31	0.24
15-6-68	29.80	0.53	8.94	0.36	3.41	0.34
17-7-69	22.60	0.47	6.78	0.25	2.42	0.27
24-11-69	20.90	0.43	6.27	0.21	2.37	0.24
15-3-70	36.40	0.56	10.92	0.44	4.94	0.41
26-8-70	24.0	0.54	7.20	0.27	3.36	0.31
27-1-71	30.90	0.36	4.71	0.29	4.71	0.29
27-5-71	29.00	0.41	4.66	0.29	4.66	0.26

Table 4.20 Measured and predicted surface runoff for Lagan catchment during validation of previously optimized values of saturated hydraulic conductivity (K_s)

Date	Rainfall mm	Antecedent Moisture Content (cm^3/cm^3)	Interception mm	Surface runoff Measured mm	Predicted (mm) Without Interception (K_s=0.09cm/h)	Predicted (mm) With Interception (K_s=0.05cm/h)
3-3-65	22.61	0.23	6.78	0.32	2.98	0.27
1-1-66	14.22	0.36	4.27	0.20	2.74	0.21
3-2-66	13.21	0.31	3.96	0.15	1.89	0.17
1-5-66	24.13	0.47	7.24	0.26	3.41	0.30
7-3-67	22.86	0.51	6.86	0.31	2.41	0.29
2-3-69	17.78	0.55	5.33	0.20	3.01	0.25
9-2-70	11.60	0.41	3.48	0.18	0.42	0.15
9-12-70	27.69	0.10	8.31	0.30	1.42	0.28
2-5-71	18.0	0.62	5.40	0.24	1.94	0.23
0-7-71	17.0	0.51	5.10	0.25	2.41	0.20
1-12-71	14.48	0.52	4.34	0.16	1.96	0.17
4-2-72	12.80	0.35	3.84	0.20	0.98	0.19
8-2-72	14.20	0.21	4.26	0.13	1.22	0.14
9-5-73	10.0	0.56	3.00	0.15	0.91	0.10

The validation exercise supports the hypothesis that the interception is an important process in the rainfall-infiltration-runoff interaction in the catchments under study. The interception process influences the availability of the rainfall for infiltration significantly and cannot be regarded as negligible. The modest variations among the K_s values in the catchments is expected in view of the landuse and a crude procedure of accounting for the interception losses. In Sambret sub-catchment, the evergreen forest is mixed with bamboo whose interception behaviour must be different from those of pure evergreen forests. Hence the validated value of K_s tends to differ for Lagan and Sambret sub-catchment when interception is taken into account.

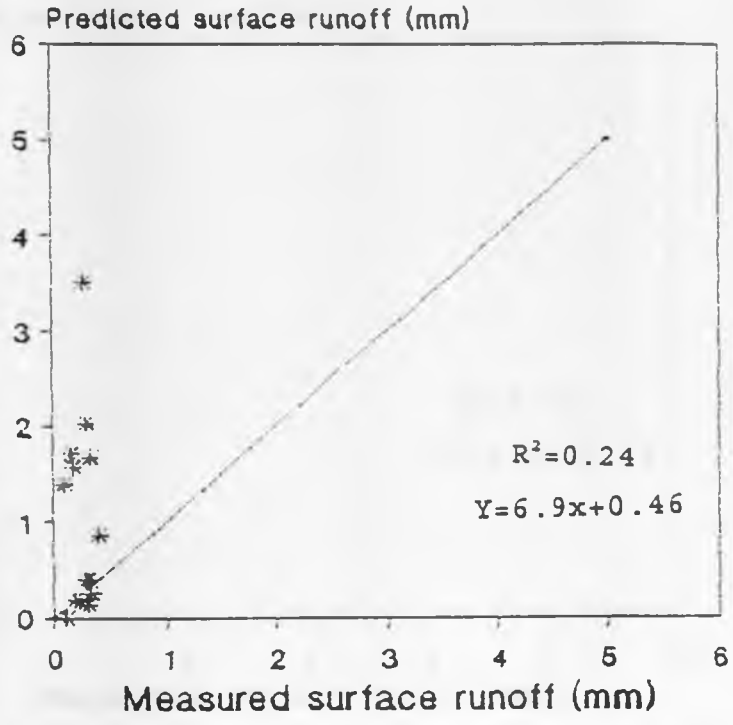

Fig. 4.14 Comparison of predicted surface runoff to measured for Lambret catchment during validation at K_s=0.08cm/h pertaining to the situation when interception is assumed negligible

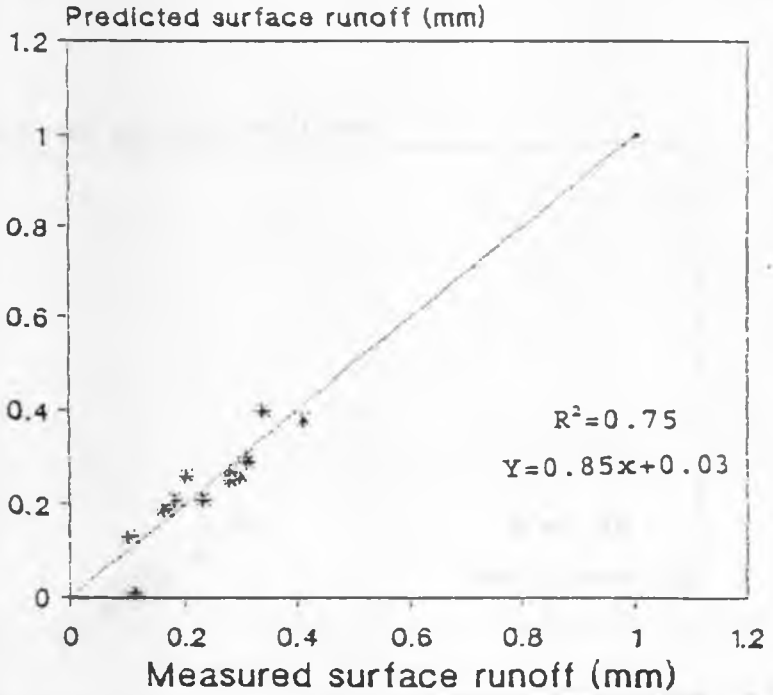

Fig. 4.15 Comparison of predicted surface runoff to measured at the validated value K_s=0.03cm/h pertaining to the situation when interception is taken into account

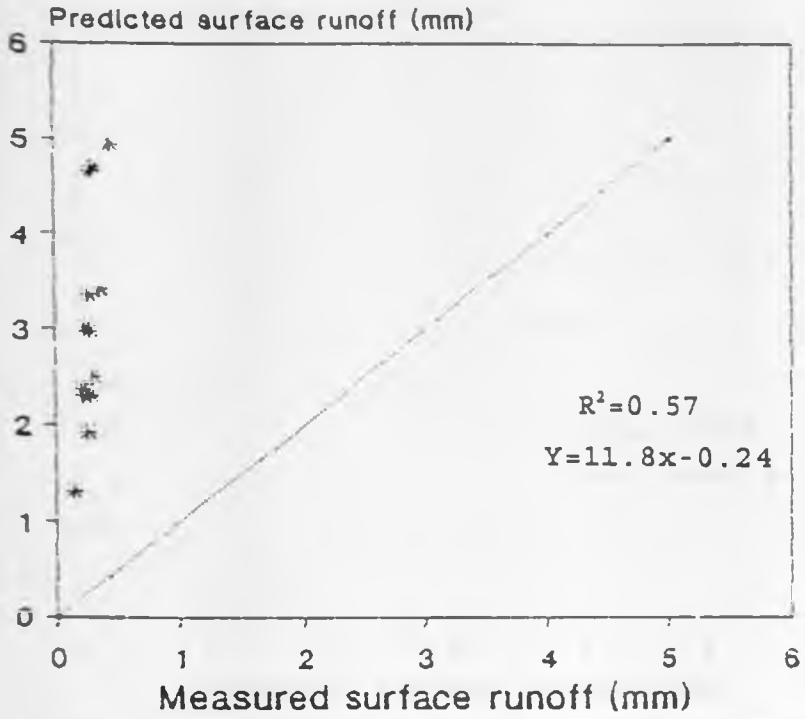

Fig. 4.16 Comparison of predicted surface runoff to measured for Embret sub-catchment at K_s=0.09cm/h pertaining to the situation when interception is assumed negligible

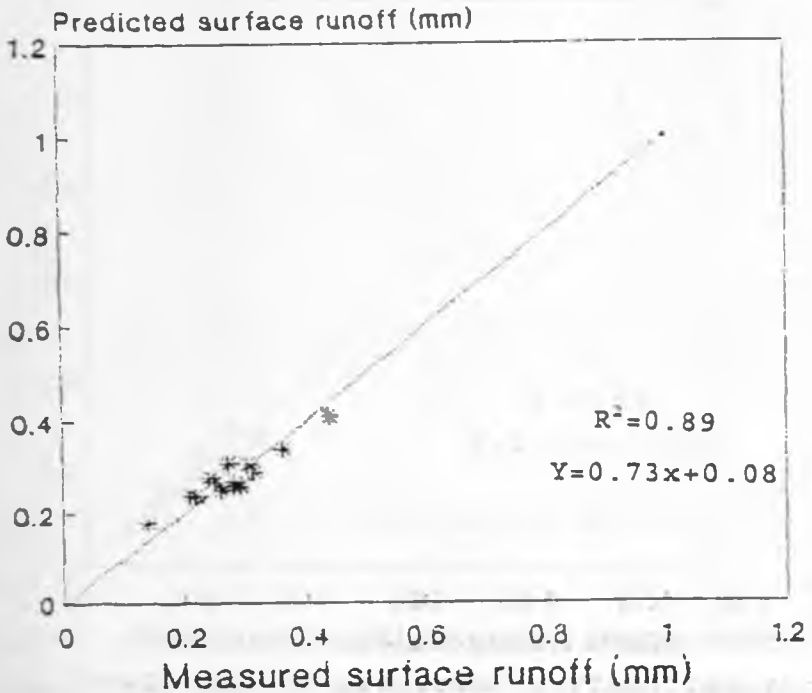

Fig. 4.17 Comparison of predicted surface runoff to measured for Embret sub-catchment at the validated value K_s=0.04cm/h pertaining to the situation when interception is taken into account

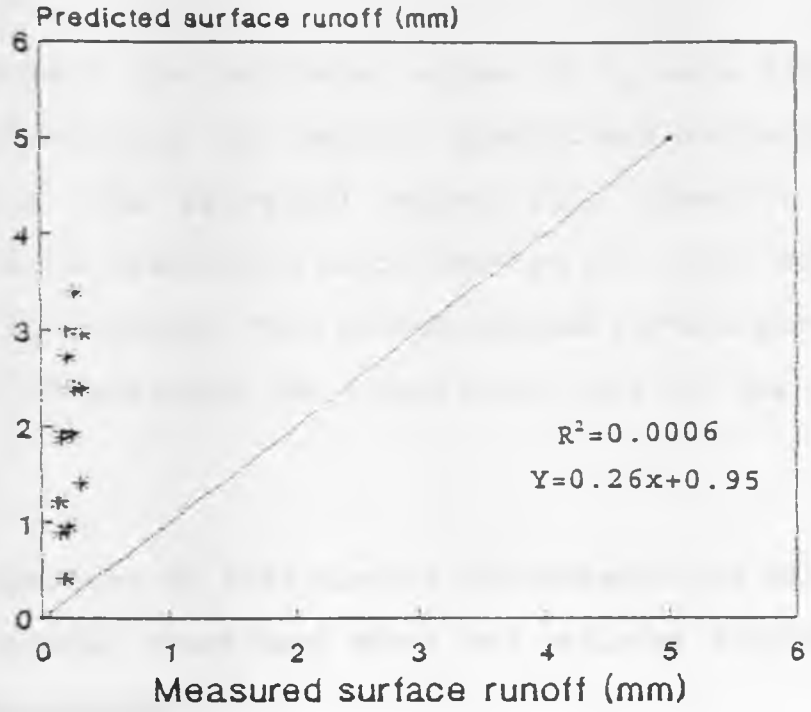

Fig. 4.18 Comparison of Predicted surface runoff to measured for Lagan catchment at K_s=0.09cm/h pertaining to the situation when interception is assumed negligible

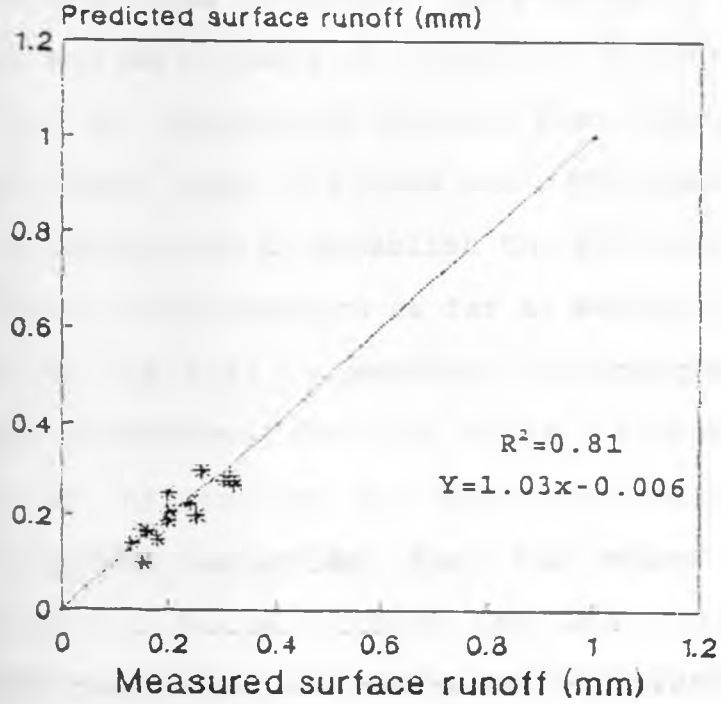

Fig. 4.19 Comparison of predicted surface runoff to measured for Lagan catchment at the validated value of K_s=0.05cm/h pertaining to the situation when interception is taken into account

In a nutshell the validated values of K_s were found as 0.03, 0.04, and 0.05cm/h for Sambret, Sambret sub-catchment and Lagan catchments. The aforesaid values fall close to the values documented in hydrologic texts (Chow et al., 1988) for clay soils which is K_s=0.03cm/h. This correspondence further strengthens the validity of analysis and significant role of the interception process.

4.4 Comparison of Infiltration Characteristics Based on the Original Green-Ampt Model and Cylinder Infiltrometer Measurements

A comparison was carried out on Kabete soils which are similar in texture and hydraulic characteristics (Table A2 and Fig. A2 in Appendix 4) to the soils in Sambret and Lagan catchments where this study was conducted. The purpose of this exercise is to compare the performance of concentric cylinder infiltrometers in relation to predictions derived from the physically based Green-Ampt model under the same soil and moisture conditions. This would enable one to establish the accuracy and reliability of concentric infiltrometers as far as determining infiltration behaviour of the soil in question is concerned. Based on the Green-Ampt parameters for the soils in question, the time variation of infiltration was determined using the Green-Ampt model for ponded conditions. Fig. 4.20 shows the infiltration characteristic curve so obtained. The final infiltration rate is 15mm/h. The plotted points represent infiltration rates derived by averaging the values obtained from predictions at three spots

on Kabete soil where infiltration measurements were also carried out using the double ring infiltrometers. It should be noted that at these sites initial moisture contents were different and were found as $0.18cm^3/cm^3$, $0.18cm^3/cm^3$ and $0.23cm^3/cm^3$. However the values of soil hydraulic parameters viz. θ_s, K_s, and S_{av} were nearly same. Fig. 4.21 shows the time variation of infiltration rate based on the cylinder infiltrometer measurements. Each point plotted on the graph of infiltration rate against time represents an average of three values derived from the readings taken at the three spots where the infiltration measurements were carried out. The final rate is about 36mm/h which is nearly three times as great in relation to Green-Ampt based value. Evidently, the infiltration rates measured by cylinder infiltrometers are very high as compared to the model predictions. Also it is expected that the infiltration rate decreases consistently with time so that when a curve is drawn through all the points in the infiltration rate Vs time graph, a smooth curve reflecting a gradual decrease of infiltration rate (f) with time (t) is obtained. This was only observed with the Green-Ampt model. With the infiltrometer measurements, the curve is smoothened to establish a trend of variation of infiltration rate with time. If the points were joined by lines during measurement by infiltrometers one may get infiltration rates behaving erratically.

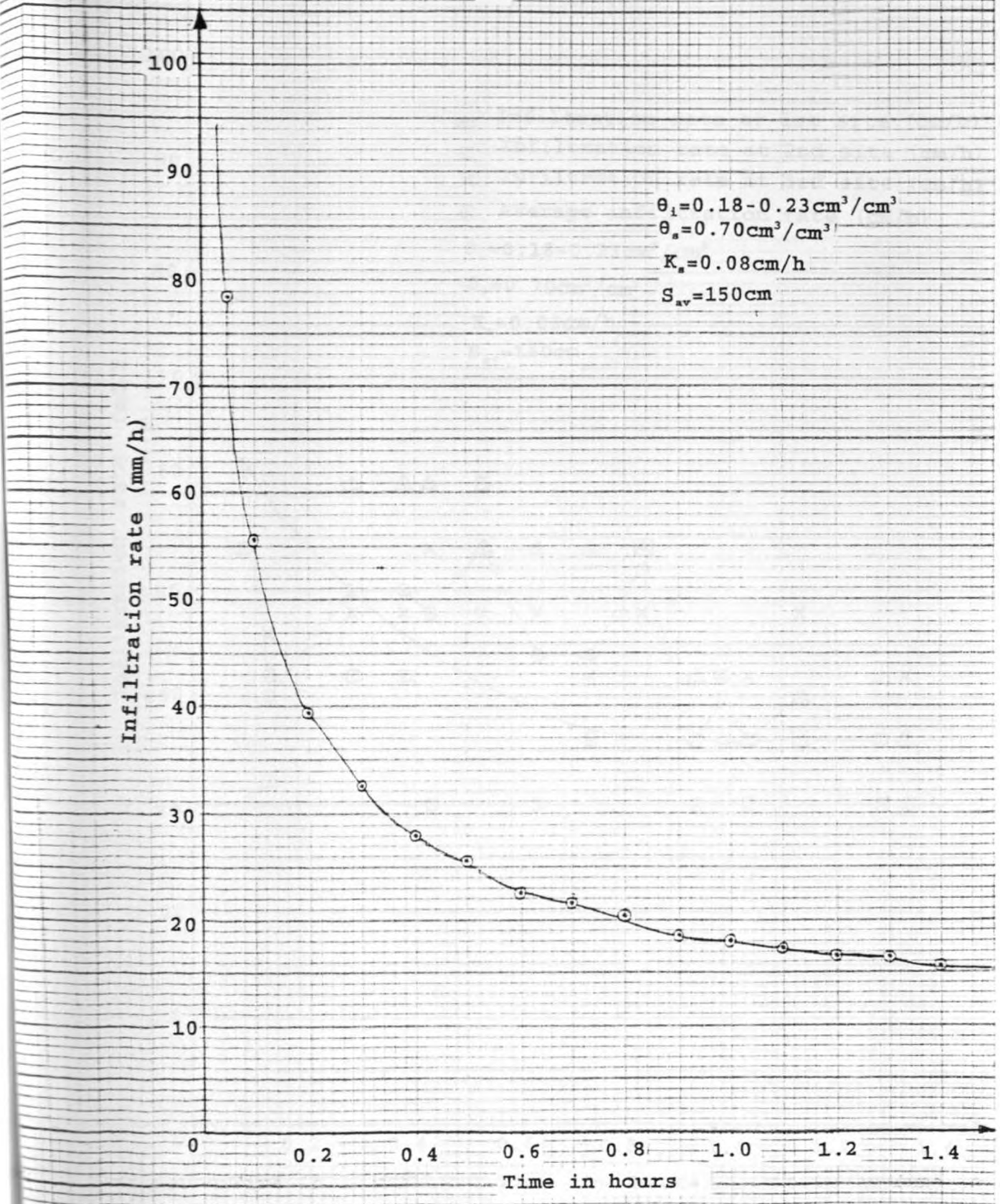

Fig. 4.20 Infiltration rate curve for Kabete soils derived from the original Green-Ampt model derived for ponded conditions

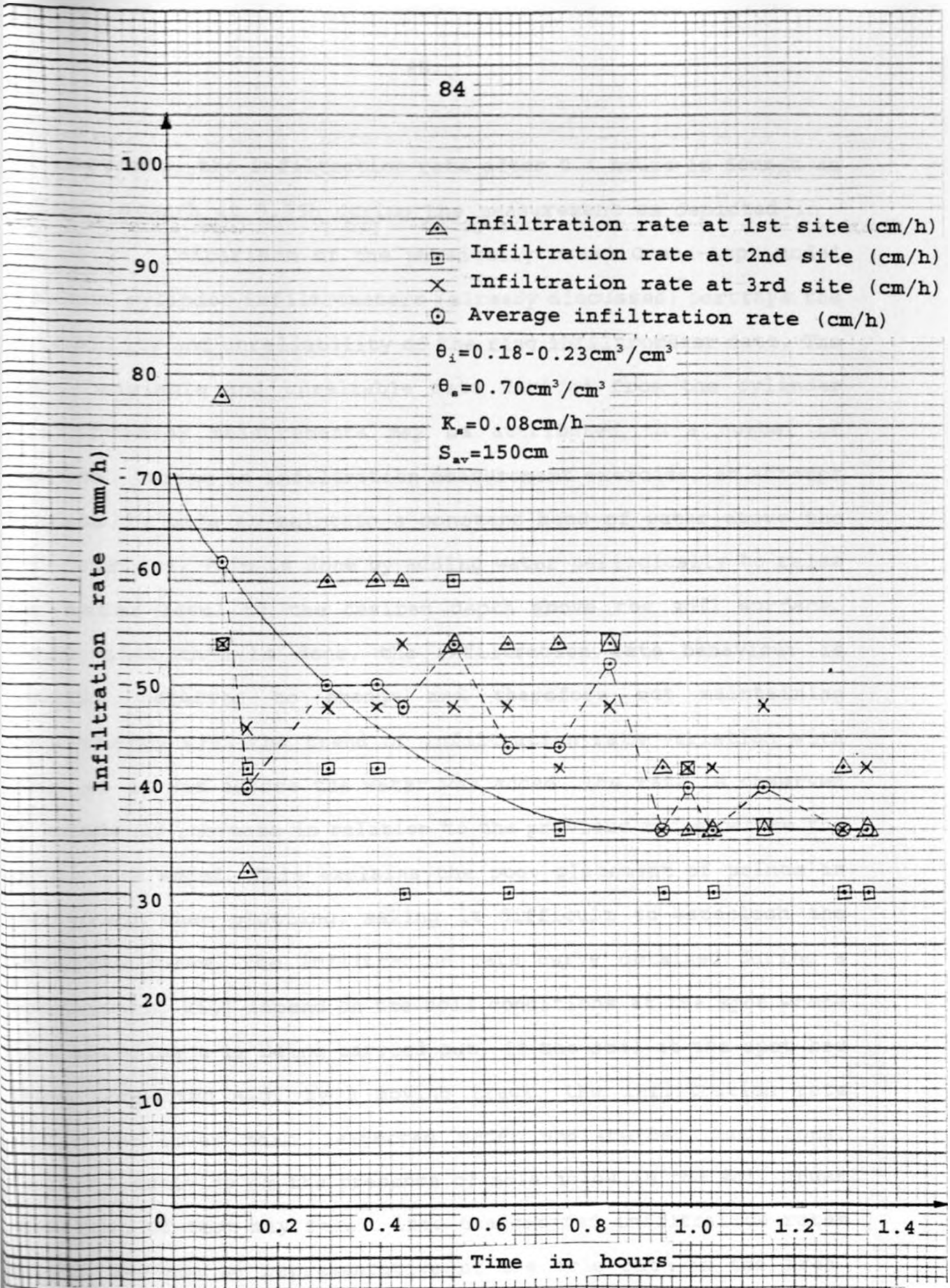

Fig. 4.21 Infiltration rate curve for Kabete soils derived from the double ring infiltrometer measurements

for instance, the infiltration rate after 0.4 hours is 50mm/h as against 64mm/h at 0.55h during the measurement as depicted in fig. 4.21. Comparison of the physically based Green-Ampt model with the cylinder infiltrometers (already discussed) portrays the variability and unreliability of the ring infiltrometer data. The high, variable and unreliable data derived from the cylinder infiltrometer measurements may be attributed to a number of reasons. During an infiltration measurement exercise, an attempt is usually made to maintain a constant head of water above the soil surface. This is done by adding water periodically to raise the water level to the desired depth above the soil surface. Every time this is done, the infiltration rate behaviour is usually observed to change and therefore not maintaining consistency with the trend of infiltration rate variation with time as it was before the water was added. The rate is observed to suddenly increase in relation to the previous rates before the water was added. This explains the poor placement of points in the graph when plotting, making it difficult to establish the accurate curve. The infiltration rate curve obtained during a measurement will depend on the soil conditions at the spot where the experiment is being carried out. If the soil at the spot had been compacted e.g. by a moving track, the infiltration rate would be lower than expected under undisturbed conditions. Termite activity or the presence of mole holes in the soil under the area of test may result into exaggerated infiltration rates which may not be representative of the true rate in the area. Another important source of error is associated with the

destruction of soil structure while cylinders are driven. Driving two cylinders by hammering certainly destroys the soils natural tilth and structure and hence the infiltration behaviour.

The Green-Ampt model for ponded conditions is physically based and predicts infiltration based on soil hydraulic parameters that can be estimated from texture. It gives a sensible estimate of the infiltration behaviour of the soil under study. It can therefore serve as a reliable standard for evaluating the performance of a technique for measurement. The model predictions are not subject to errors that are associated with cylinder infiltrometers e.g. those caused by water additions, poor techniques of driving the cylinders without disturbing the soils and human reading errors among others. The model, however depends on accurate determination of the parameters associated with the model.

5. CONCLUSIONS

The following conclusions may be drawn from the study.

1. The USDA-SCS texture based nomographs appear not to give reliable estimates of the Green-Ampt model parameters for the soils of the area under study. Only the wetting front suction, S_{av} (150cm) is reliably predicted. The saturated hydraulic conductivity (K_s=0.005cm/h), predicted from the nomographs was found to be far too low for the clay soils in Sambret and Lagan catchments. The saturated soil moisture content, θ_s, from the nomographs was also found out to be lower (0.45cm^3/cm^3) than would be expected for these soils. The measured value (0.7cm^3/cm^3) available from the records was much higher than the nomograph value.

2. After the optimization process and subsequently by validation, the saturated hydraulic conductivity (K_s) was found to be 0.03cm/h for Sambret catchment, 0.04cm/h for Sambret sub-catchment and 0.05cm/h for Lagan catchment. Since the value of K_s for all the catchments was obtained considering interception, the influence of interception in surface runoff prediction using the Green-Ampt model should be considered in all the three catchments.

3. The measured value of θ_s ($0.7 cm^3/cm^3$) may be used reliably for the catchments studied instead of the nomograph value of $\theta_s = 0.45 cm^3/cm^3$ which has been discarded as being too low for soils of the catchments studied. The measured values of antecedent soil moisture (θ_i) should be used with caution in the Green-Ampt model. Some of the measured values were unexpectedly high hence the need to select carefully the reliable values. The value of wetting front suction, S_{av}=150cm, (nomograph based) can be relied on for the catchments studied.

4. The double ring infiltrometers yield highly inflated, variable and unreliable infiltration data when compared to the data from physically based Green-Ampt model developed for ponded conditions. Such data should be used cautiously in hydrologic calculations.

6. RECOMMENDATIONS

The following recommendations may be made from the research carried out.

1. The nomographs for predicting effective porosity need modification before they can be used on Kenyan catchments. Since they were developed for coarse textured soils further work needs to be done for fine soils.

2. Derivation of hyetographs from rainfall charts, besides being tedious and time consuming also requires them to be available though daily rainfall records may be more common. There is need to develop techniques by which the time distribution of rainfall may be derived from daily rainfall data.

3. Records on measured antecedent moisture contents are rarely available and yet this is an important parameter in the Green-Ampt model. There is need to develop modelling techniques by which the moisture contents prior to a storm may be determined.

4. Better accuracy can be achieved by experimenting this kind of work on a microcatchment scale e.g. on runoff plots where the Green Ampt parameters can be easily determined with less cost and time.

5. Double ring infiltrometers when used to measure infiltration yield highly variable and unreliable results. Therefore there is need to test other types of infiltrometers which would simulate infiltration behaviour similar to actual flow of rainwater into the soils.

6. There is need to develop techniques by which interception loss can be determined for Kenyan catchments instead of relying on models developed elsewhere such as America and Europe where vegetation and climatic conditions differ from those in Kenya.

REFERENCES

Bhuja, L.R., R.R. Bruce, D.K. Cassel, W.J. Rawls. 1988. Field measurement and estimation of soil hydraulic properties and their spatial variability for modelling. In: Proceedings of International Symposium. ASAE. St. Joseph, Michigan:19-32.

Bouwer, H. 1966. Rapid field measurement of air entry value and hydraulic conductivity of soil as significant parameters in flow system analysis. Water Resour. Res., 2(4): 729-738.

Bradford, P.W., W.J., Rawls, D.L. Brakensiek, and J.R. Wight. 1990. Predicting runoff from rangeland catchments: a comparison of two models. Water Resour. Res., 26(4): 2401-2410.

Chiti, R.M. 1991. Effect of farmyard manure in soil surface sealing and crusting of disturbed topsoil - a case study of west Pokot, Kenya. M.Sc. Thesis, Department of Agricultural Engineering, University of Nairobi.

Chow, V.T., D.R. Maidment, and L.W.Mays. 1988. Applied Hydrology. Mc Grawhill book company, Newyork: 108-122.

Chu, S.T. 1978. Infiltration during an unsteady rain. Water Resour. Res., 14(3): 461-466.

Edwards, K.A. and J.R. Blackie. 1979. The Kericho research project. In: Hydrological Research in East Africa. E. Afr. Agr. for. J., 43: 44-50.

Edwards, K.A., J.R., Blackie, S.M., Cooper, G. Roberts and E.S. Waweru. 1976. Summary of hydrological data from the EAAFRO experimental catchments. E.A. Community, CPS, Printer,

Nairobi.

Bachene, C.K.K. 1995. Effect of Soil Erosion on Soil Properties and Crop Response in Central Kenya. Reports and Dissertations, 22. Swedish University of Agricultural Sciences, Uppsala, Sweden.

Hillel, D. 1982. Introduction to Soil Physics. Academic Press Inc., Sandiego, California: 211-234.

Kerfoot, O. 1962. The vegetation of Sambret and Lagan Catchments. In: Hydrological effects of changes in land use in some East African areas. E. Afr. Agr. for. J. (special issue), vol 27 (March). Government printer, Nairobi: page 23.

Madramootoo, C.A. and P. Enright. 1989. Prediction of surface runoff using Green-Ampt infiltration model and estimated soils parameters. Can. Agric. Eng., 32: 39-45.

Marshal, T.J. 1958. A relation between permeability and size distribution of pores. Journal of Soil Science, 9(1): 1-8.

Marshal, T.J., and J.W. Holmes. 1988: Soil Physics. Cambridge University Press, Newyork: 138-141.

Mein, R.G. and C.L. Larson. 1971. Modelling the infiltration component of the rainfall-runoff Process. Water Resour. Research Centre, Bulletin 43. University of Minnesota, Minnepolis, Minnesota.

Mein, R.G. and D.A. Farrel. 1974. Determination of wetting front suction in the Green-Ampt equation. Soil Sci. Soc. Amer. proc., 38: 872-876.

Michael, A.M. 1978. Irrigation Theory and Practice. Vikas publishing house P.V.T. LTD. Jagnpura. New Delhi: 465-472.

Miriti J.M. 1994. The effect of tillage, compost, and mulch on physical properties and crop yield. Unpublished M.Sc. thesis. Department of Agric Engineering, University of Nairobi.

Morel-Seytox, H.J. 1981. Application of infiltration theory for the determination of excess rainfall hyetograph. Water Resources Bulletin, 17(6): 1012-1022.

Mullem, J.A.V. 1991. Runoff and peak discharges using Green-Ampt infiltration model. Journal of Hydraulic Engineering. ASCE., 117(3): 354-370.

Mwaura, F.D.K. 1980. Spatial variability of infiltration rate in 0.3 ha field in Katumani Dryland Research Station. Post. grad. Dip. Report, Department of Agricultural Engineering, University of Nairobi.

Njuguna, S.N. 1979. Comparison of determination of infiltration parameters by means of double ring infiltrometer and analysis of furrow advance and intake in Mitunguu irrigation scheme, Meru district. post grad. dip. report, department of Agricultural Engineering, University of Nairobi.

Rawls, W.J. and D.L. Brakensiek. 1983. A procedure to predict Green-Ampt infiltration parameters. In: Advances in infiltration. Proceedings of the national conference on infiltration. ASAE, Chicago, Illinois: 102-112.

Scott, R.M. 1962. Summary of soil survey observations on the Sambret valley. In: Hydrological effects of changes in Land use in some East African areas. E. Afr. Agr. for. J. (special issue), vol 27 (March). Government printer, Nairobi: page 22

Sessanga, S.M. 1982. Soil water movement, retention, and release properties of selected soils of Kenya. M.Sc. thesis. Department of Soil Science. University of Nairobi.

Skaags, R.W. and R. Khaleel. 1982. Infiltration. In: Hydrologic modelling of small Watersheds. Haan, C.T., Johnson, H.P., Brakensiek, D.L. Eds. ASAE monograph Number 5. St. Joseph, Michigan: 121-165.

Slack, W.J. and C.L. Larson. 1981. Modelling infiltration: the key process in water management, runoff and erosion. In: Tropical Agricultural Hydrology. John Willey and Sons. Chichester, U.K: 433-450.

Viessman, W., G.Lewis and J.W. Knapp.1989. Introduction to Hydrology. Harper and Row publishers, Newyork:55-83.

Ward, R.C. 1975. Principles of Hydrology. McGrawhill Book Company (UK) Limited. Berkshire, England: 54-70.

Ward, R.C., and M. Robinson. 1989. Principles of Hydrology. McGraw-hill book company (UK) Limited. London: 54-78.

Wilson, E.M. 1974. Engineering Hydrology. The Macmillan Press LTD. London: 54-68.

Wisler, C.O and E.F. Brater. 1959. Hydrology. John Willey and sons, inc. NewYork: 31-56.

Yomota A., and M.N., Islam .1992. Kinematic analysis of flood runoff for a small upland field. Journal of hydrology, 137: 311-326.

APPENDIX 1

THE VEGETATION OF THE SAMBRET AND LAGAN EXPERIMENTAL CATCHMENTS

By O. Kerfoot, E.A.A.F.R.O.

The whole of Lagan, and most of Sambret are covered with either mature moist montane evergreen high forest or secondary growth derived from it. Above 7,500 ft. on Sambret, the forest is displaced by montane bamboo forest which, however, contains evergreen forest elements scattered through the matrix. The bamboo is very much thicker and covers wider limits of elevation in the SW. Mau forest than anywhere else on the range. This may be due to fire, disturbance by animals or man, or to the high rainfall experienced in this sector (between 70 and 90 in.). At the lower end of Sambret, elements of montane Acacia woodland and savanna appear, albeit sparsely. The immediate environs of the streams on both catchments are densely populated with more hydrophilous species which include the tree fern *Cyathea manniana*, the giant lobelia, *Lobelia gibberoa*, and a wild banana *Ensete ventricosum*.

The dominant and high forest species, reaching a height of over 70 ft. in favourable localities, are *Albizia gummifera*, *Polyscias fulva*, *Fagara macrophylla* (largely removed by logging operations), *Syzygium guineense* and *Casearia battiscombei*. These plants form an almost continuous canopy with a density of between 30-50 to the acre, and are usually reinforced at co- or sub-dominant level by *Pygeum africanum*, *Ekebergia rueppelliana*, *Nuxia congesta*, *Ficus* spp. and *Croton macrostachys*. Secondary or numerically subordinate members of the upper strata include *Turraea holstii*, *Trichilia volkensii*, *Podocarpus milanjianus*, *Hagenia abyssinica*, *Neoboutonia macrocalyx*, *Macaranga kilimandscharica*, *Dombeya goetzenii* and *Schefflera volkensii*. The understorey species are almost entirely comprised of evergreen rubiaceous genera under 30 ft. in height, such as *Pauridiantha holstii*, *Grumilea megistostieta* and *Galiniera coffeoides*, but very conspicuous members of this stratum include *Canophayngia johnstonii*, *Trema guineensis*, *Allophylus abyssinicus*, *Dracaena afromontana*, *Maytenus senegalensis*, and *Nymalos monospora*. These may be augmented on the lighter and secondary margins by *Maesa lanceolata* and *Hypericum revolutum*. The lowest stratum is occupied largely by Acanthaceous genera such as *Mimulopsis solmsii* and *M. arborescens*, but nettles are well represented, *Floerya aestuans*, *Urera hypselodendron* and *Elatostemma orientale* being the commonest. There is an abundance of sedges and ferns; and climbers and epiphytes include *Basella alba*, *Piper capense*, *Culcasia scandens*, *Melothria* spp., *Canarina abyssinica* and *Peperomia* spp.

The bamboo zone is dominated by *Arundinaria alpina* but forest trees include *Pygeum africanum*, *Podocarpus milanjianus*, *Ekebergia rueppelliana*, and *Myrica salicifolia*. *Myrica salicifolia* may noticeably invade patches of burnt or degraded bamboo at higher, colder altitudes and maintain themselves satisfactorily. The herb layer is poorly represented in this zone. None of the species represented on these catchments exceeds 90 ft. in height. *Albizia gummifera* is the tallest, and on an average, the most robust dominant with an optimum circumference at breast height of 70 in. The species of *Ficus* may exceed 60 ft. but are never abundant. In the bamboo zone, growth is generally more stunted and 50 ft. is the optimum for emergent forest trees. There is a marked tendency for the height of bamboos to increase above the 7,500 ft. contour, to a maximum of 40 ft.

Hydrologically, the vegetative cover is complete, for even where the upper canopy has been disturbed or removal of primary vegetation has left gaps, rapid colonization by secondary species has been effected.

Near the upper rim of the Sambret catchment there is a 20 acre "vlei" or enclosed drainage basin, which over-flows into the main stream when the depth of water exceeds approximately 2 ft. The vegetation here consists entirely of grasses, sedges and a few geophytes with composite herbs. Dominant grasses are *Calamagrostis epigejos* var. *capensis*, *Leersia hexandra*, *Echinochloa pyramidalis* and *Setaria trinervia*.

The margins of this zone are populated by an impoverished woody cover; species include *Bersama abyssinica* var. *abyssinica*, *Acacia lahai*, *Oncoba spinosa* and a variety of thicket genera. Growth of most of the trees at the fringe of the vlei is stunted.

The status of the S.W. Mau Forest in the Sambret area is open to debate. There is reason to believe that many of the dominant genera of the existing high forest area are of secondary origin and that possibly *Podocarpus milanjianus*, *Cassipourea malosana* and *Nuxia congesta* are most representative of the primary "climax" type.

APPENDIX 2

SUMMARY OF SOIL SURVEY OBSERVATIONS ON THE SAMBRET VALLEY

By R. M. Scott, E.A.A.F.R.O.

The vegetation survey indicated a very sharp transition from tall montane rain forest to bamboo at an altitude of some 7,500 ft. in the Sambret Valley. To investigate whether this was due to a change of soil type, a soil survey of the catchment was carried out.

The two main soils are deep friable clays and differ from each other only in that one has a thin ash-derived soil overlying it.

In the past an ash layer was laid down over the whole area on well-developed red soils derived from the phonolite. Since then the ash-derived soil remains only on the more protected sites.

The ash-derived overlay, which is not so bright red in colour, is easily recognized by the presence of a buried humic horizon of the underlying soil about 2 ft. below the surface. This buried humic horizon contains large pieces of charcoal and in one case a piece of obsidian, which may have been an artifact, showing that this humic layer was not caused by pedological processes but has been buried. The high organic matter content and the non-sticky nature of the clay in the soil above the buried humic layer supports this view.

The profile, with the ash-derived overlay, consists of a very dark brown to reddish brown high organic matt layer up to 5 in. thick passing into a dark reddish brown friable clay, non-sticky but slightly plastic, having many small pieces of charcoal and a high root density. This overlies at about 2 ft. a buried humic horizon dark reddish brown in colour which in turn passes at about 3 ft. into a dark red subangular blocky friable clay, sticky and plastic, showing clay skins on the ped surfaces.

In the deep red friable clays, the profile consists of a 3 in. reddish brown to dark brown organic matt layer over a dark red crumby to subangular blocky friable clay which is sticky and plastic. This passes at 24–36 in. into a dark red subangular blocky clay with clay skins.

Both types of soils are deep, an auger being put down to 11 ft. and no appreciable change being seen in the subsoil.

Chemically the soils are very similar. This one would expect since although the one soil type does not contain a noticeable ash overlay, in all probability it would have been contaminated with ash to a greater or lesser extent and both soils have been considerably leached.

It will be seen from Table II that these soils are very low in total exchangeable bases with a very low saturation and it may well be advantageous to apply fertilizers to obtain the optimum yields.

The soil types tend to be related to topography; there is no correlation between the soils and vegetation, and the soils do not account for the transition from forest to bamboo. The presence of large burned tree stumps among the bamboo suggests that it has invaded the area after destruction of the forest cover by fire.

TABLE II—ANALYSIS OF THE MAIN SOIL TYPE

Depth in inches	Mechanical Analysis %				pH	Carbon/Nitrogen Ratio			Exchangeable Bases with equivalent m.e./100 gm.						Exch. Hydrogen m.e./100 gm	Total Exch. Cations	% Sat.
	Organic	Sand	Silt	Clay		%C	%N	C/N	Ca	Mg	Mn	K	Na	Total			
0–2	20·8	38·6	2·0	40·0	5·5	10·4	0·914	14·8	6·70	2·80	0·25	1·41		11·2	16·2	27·4	40·8
2–8	14·3	35·3	4·3	46·1	5·0	7·14	0·616	15·4	1·15	1·02	0·05	0·64		2·9	17·8	20·7	13·8
8–18	6·1	29·5	10·5	53·9	5·3	3·06	0·294	13·9	0·01		0·006	0·29		0·3	14·3	14·6	2·3
18–30	7·6	35·9	11·4	45·1	5·9	*3·77	0·222	22·6	0·01			0·16		0·2	15·8	16·0	1·2
30–41	2·4	20·0	9·8	67·8	5·7	1·22	0·116	14·0	0·01		0·005	0·21		0·3	11·2	11·5	2·4
41–71	2·6	20·0	9·2	68·2	5·6	1·28	0·118	14·5	0·11		0·004	0·29		0·4	10·9	11·3	3·6

APPENDIX 3

DETERMINATION OF SURFACE RUNOFF FROM RAINFALL USING GREEN-AMPT INFILTRATION MODEL

EXAMPLE A1

Consider a hypothetical storm with intensity distribution presented in Table A1. Fig. A1 shows the storm hyetograph.

Table A1 Intensity distribution for a hypothetical storm

Time (h)	Intensity (mm/h)
0-0.5	11.4
0.5-3.4	15.0
3.4-6.0	13.0

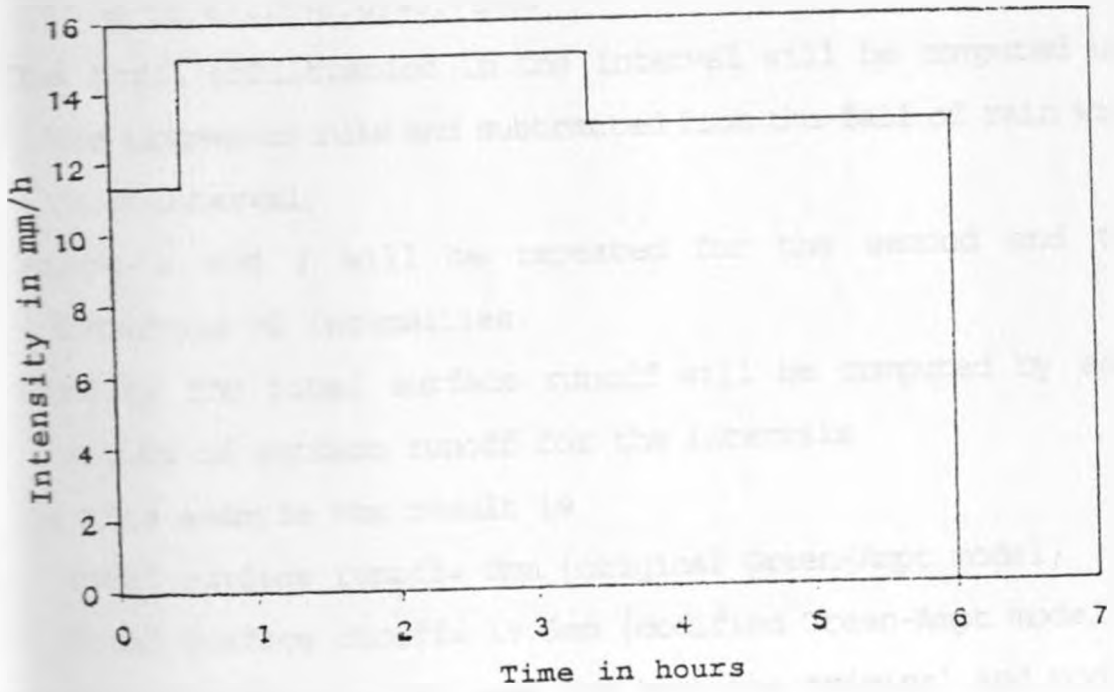

Fig. A1 Rainfall hyetograph for a hypothetical storm

Suppose surface runoff is to be predicted from the storm using Green-Ampt model. Let the model parameters be S_{av}=150cm, θ_s=0.7cm³/cm³ θ_i=0.36cm³/cm³, and K_s=0.1cm/h. The programme will determine the surface runoff as follows.

1. On running the programme, it will request for the Green-Ampt parameters to be entered. These are already mentioned.
2. The first intensity and its time limits will then be requested. These will be entered as

   To=0 {lower time limit}

   Tn=1.5 { Upper time limit}

   Intensity = 11.4mm/h

   the total fall of rain in the interval will be computed (i.e 11.4(1.5-0.0)=5.71mm.
3. The total infiltration in the interval will be computed using the trapezium rule and subtracted from the fall of rain within this interval.
4. Steps 2 and 3 will be repeated for the second and third intervals of intensities.
5. Finally the total surface runoff will be computed by adding values of surface runoff for the intervals
6. In this example the result is

   Total surface runoff= 0mm {original Green-Ampt model}

   Total surface runoff= 19.5mm {modified Green-Ampt model}

Note the procedure is the same for both the original and modified Green-Ampt model except that in the latter the time of ponding is determined.

APPENDIX 4

ME SOIL CHARACTERISTICS OF KABETE SOILS

ble A2 Texture and porosity for Kabete soils (adapted from Sessanga, 1982)

pth	Sand %	Silt % class	Clay % content	Textural	Saturated soil moisture
-6	13.53	24.46	62.01	clay	0.70
-36	8.01	1.66	67.25	clay	0.68
-66	8.01	22.57	69.33	clay	0.65

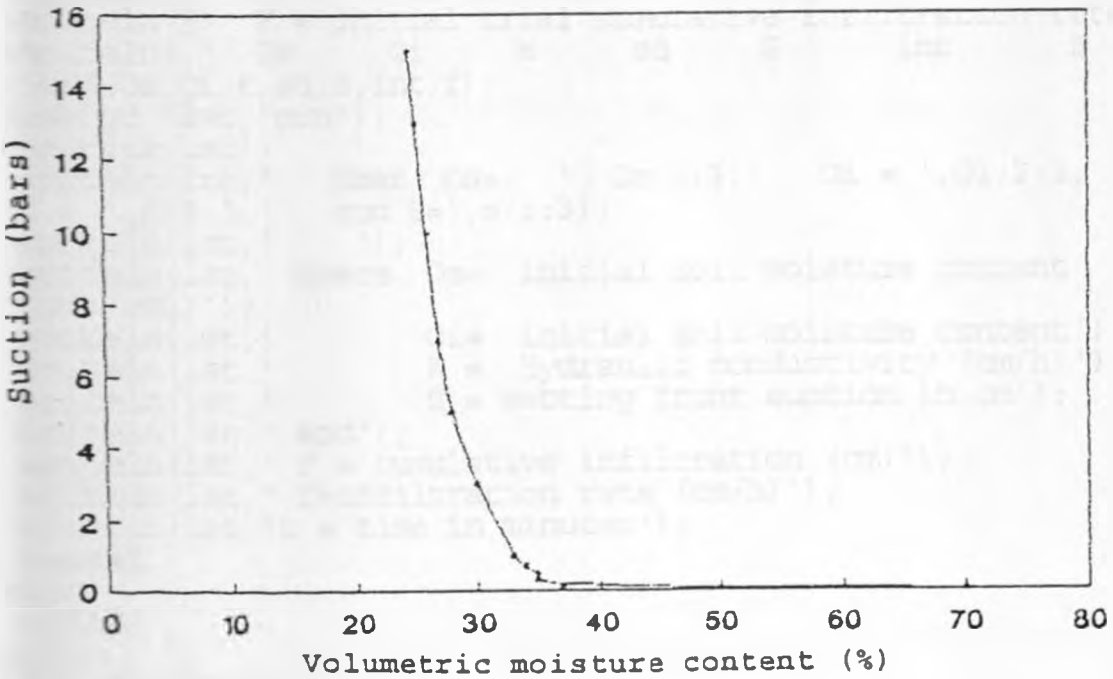

ig. A2 Soil moisture characteristic curve for Kabete soils

APPENDIX 5

COMPUTER PROGRAMS

```
Program GreenAmpt (input,output);
{This program works out the time distribution of
 infiltration rate and cumulative infiltration for
 the original Green-Ampt model given,the model parameters}
 Var
 lst:text;
 Os,Oi,k,s,t,F,pr,d,br,l,r,add,diff,inf,int,sd:real;
Begin
 t:=0;
 writeln ('enter Os    Oi    k    sd    s     int    F');
 writeln ('      ');
 writeln (' Os  =  saturated soil moisture content');
 writeln( ' Oi  =  initial moisture content');
 writeln('  k  =  saturated hydraulic conductivity');
 writeln('  sd =   storm duration in minutes');
 writeln('  s  =  wetting front suction');
 writeln('  int =  time interval in minutes');
 writeln ('  F = initial trial cumulative infiltration rate');
 writeln( '  Os     Oi     k     sd     S      int      F ');
 read(Os,Oi,k,sd,s,int,f);
 assign (lst,'prn');
 rewrite(lst);
 writeln(lst,'   When  Os=   ', Os:1:3,'   Oi = ',Oi:2:3, '
 K = ',K:3:3,'   and S=',s:3:3);
 writeln(lst,'    ');
 writeln(lst,' where  Os=  initial soil moisture content
 (cm3/cm3)');
 writeln(lst,'        Oi=  initial soil moisture content');
 writeln(lst,'        K =  Hydraulic conductivity (cm/h)');
 writeln(lst,'        S = wetting front suction in cm');
 writeln(lst,' and');
 writeln(lst,' F = cumulative infiltration (cm)');
 writeln(lst,' f=infiltration rate (cm/h)');
 writeln(lst,'t = time in minutes');
  Repeat
Begin
  repeat
Begin
  pr:=S*(Os-Oi);
  d:=F/pr;
  br:=1+d;
  l:=pr*ln(br);
  r:=(k*t)/60;
  add:=abs(l+r);
  diff:=abs(F-add);
  F:=add;
```

```
end;
   until diff<=0.00001;
   inf:=k*(1+pr/F);
   write(lst);
   writeln(lst,' at t=',t:2:2,'    F=',F:5:8,'    f=',inf:3:8);
end;
   t:=t+int;
   until t>sd;
   close(lst);
end.
```

```
PROGRAM GREENAMPTTp;
{This program works out the time distribution
of infiltration rate and cumulative infiltration using
the Green-Ampt model modified for rainfall infiltration}
VAR
lst:text;
P,Sav,Os,Diff,Oi,Ks,F,R,Sd,int,D,Fp,Tp,Ts,t,s,B,Rt,Lt,A,
inf,stop:Real;
begin
repeat
BEGIN
 Writeln('enter Sav   Os    Oi   Ks    F    R   Sd
 int  s  stop');
 writeln(' Sav=wetting front suction in cm');
 writeln(' Os = saturated water content in cm3/cm3');
 writeln(' Ks = hydraulic conductivity (cm/h)');
 writeln('  F = cumulative infiltration (cm)');
 writeln('  R = initial rainfall intensity (cm/h)');
 writeln(' Sd = storm duration (hrs)');
 writeln('int = time interval for plotting in hrs');
 Read(Sav,Os, Oi,Ks,F,R,Sd,int,s,stop);
 assign(lst,'prn');
 rewrite(lst);
 writeln(lst,'When  Sav=',Sav:3:3,'    Os=',Os:3:3,'
 Oi=',Oi:3:3,'
 Ks=',Ks:3:3,'  and R=', R:4:6);
 P:=Sav*(Os-Oi);
 D:=R/Ks;
 Fp:=P/(D-1);
 tp:=Fp/R;
 Ts:=(Fp-(P*ln(1+Fp/P)))/Ks;
 writeln(lst,'then tp=',tp:3:3,'   ts=',ts:3:3,'  and');
 t:=tp;
 Repeat
       Repeat
  B:=1+(F/P);
  Rt:=P*ln(B);
  Lt:=ks*(t-tp+Ts);
  A:=abs(Lt+Rt);
  F:=A;
  Diff:=F-A;
  until abs(Diff)<=0.0001;
  Inf:=Ks*(1+(P/F));
  Writeln(lst,'when t=',t:3:4, '      F=',F:3:4,'
  f=',  INF:3:4);
  t:=t+int;
  until  t>Sd;
  close(lst);
end;
  until s=stop
end.
```

```
program surfacerunoffgreenampt(input,output);
{this program predicts surface runoff from rainfall
using the original
green-Ampt model derived for ponded conditions}
var
lst:text;
sum1,totsro,pr,os,oi,k,sd,s,sro,t0,tn,f,int,intr,t,d,br,
rint,r,add,diff,inf,fo,fn,sum2,intf,intsro,totr,tsro:real;
begin
sum2:=0;
sum1:=0;
totsro:=0;
totr:=0;
writeln('enter    Os,     Oi,     K,     Sd,     S,   F,   int');
writeln('where  Os=saturated water content in cm/h');
writeln('       Oi=initial water content in cm3/cm3');
writeln('         K=hydraulic conductivity at natural saturation
cm/h');
writeln('      Sd=storm duration in minutes');
writeln('      S=wetting front suction in cm');
writeln('      F=initial trial cumulative infiltration in cm');
writeln('     int = time interval in minutes for computation');
read(os,oi,k,sd,s,f,int);
assign(lst,'prn');
rewrite(lst);
Oi:3:3,'cm3/cm3   K=',K:3:3,'cm/h   S=',S:3:3,'cm');
repeat
writeln('enter   to,  tn and   rintensity');
readln(t0,tn,rint);
t:=t0;
intr:=(rint*(tn-t0))/60;
repeat
repeat
pr:=s*(os-oi);
d:=f/pr;
br:=1+d;
l:=pr*ln(br);
r:=k*t/60;
add:=abs(l+r);
diff:=abs(f-add);
f:=add;
until diff<=0.000001;
inf:=k*(1+pr/f)*1/6;
sum1:=sum1+inf;
if t=t0 then fo:=inf;
if t=tn then fn:=inf;
t:=t+int;
until t=tn+1;
sum2:=sum1-fo-fn;
intf:=(int/2)*(fo+fn+(2*sum2));
```

```
intsro:=intR-intf;
if intsro<0 then intsro:=0;
totR:=totR+intR;
totsro:=totsro+intsro;
until tn=sd;
writeln(lst,'when total rainfall =',totr:4:6);
writeln(lst,'total surface runoff =',totsro:4:6);
close(lst)
end.
```

```
PROGRAM GRNAMPLATEST; {This program predicts surface
  runoff from a rainfall event using the Green-Ampt
  model derived for rainfall infiltration.}
  VAR
  lst:text;
  Sav,Os,Oi,Ks,fu,prR,R,ti,P,F2,t2,I,S,D,Fp,Br,tp,ts,F,
  tn,t0,B,Rt,Di,t,t1,inf,sum1,fo,fn,sum2,intf,rint,intr,
  intsro,totR, totsro,RO,sro,tR:real;
begin
  totr:=0;
  sum1:=0;
  intR:=0;
  totsro:=0;
  writeln('enter  Sav  Os    Oi    Ks     PrR
  R     ti-1    t2    I   S');
  read(Sav,Os,Oi,Ks,PrR,R,ti,t2,I,S);
  assign(lst,'prn');
  rewrite(lst);
  writeln({lst,}'when    Sav=',Sav:3:3,'     Ks=',Ks:3:3,'
  Os=',Os:3:3);
  writeln({lst,}'    Oi=',Oi:3:3,'     R=',R:3:3,'
  S=',S:3:3,'       PrR=',PrR:3:3);
  P:=Sav*(Os-Oi);
  D:=R/Ks;
  Fp:=P/(D-1);
  Br:=(Fp-PrR);
  tp:=ti+(Br/R);
  ts:=((Fp-(P*ln(1+Fp/P)))/Ks);
  F:=Fp;
  tn:=t2;
  t0:=0;
  if r<ks then writeln('equation invalid');
  If tp>t2  then writeln ('tp exceeds');
  Repeat
    Repeat
      B:=1+(F/P);
      Rt:=P*ln(B);
      Di:=(F-Rt)/Ks;
      t:=Di+tp-ts;
      If F=Fp+I then t1:=t;
      inf:=Ks*(1+P/F);
      If t<=t2 then F2:=F;
      If F<F2  then sum1:=0
      else sum1:=sum1+inf;
      If t<=tn then fn:=inf;
     {writeln(lst, ' when t=',t:3:3, '  F= ' ,F:3:3,
      ' f=', inf:3:3);}
      F:=F+I;
    until t>=tn;
     fu:=inf;
     sum1:=sum1-fu;
```

```
 sum2:= (sum1-fo-fn);
 If tn=t2 then intf:=0
 else  intf:=((t1-tp)/2)*(fo-fn+(2*sum2));
 intsro:=intR-intf;
 if intsro<0 then intsro:=0;
 totR:=totR+intR;
 totsro:=totsro+intsro;
 writeln('enter to   tn   rint');
 read(t0,tn,rint);
 intR:=Rint*(tn-t0);
 fo:=fn;
 sum1:=fo+inf;
 sum2:=0;
until t0=tn;
 RO:=(R*(t2-tp))-(F2-Fp)-(S);
 SRO:=(totsro+RO)*10;
 TR:=((totR)+(R*(t2-ti))+PrR)*10;
 writeln( {lst,}'when total rainfall=',TR:3:5);
 writeln({lst,}'total surface runoff=',sro:3:5);
{ writeln(lst,'tp=',tp:3:5);
 writeln(lst,'ts=',ts:3:5);
 writeln(lst,'F2=',F2:3:5);
 writeln(lst,'Fp=',Fp:3:5);
 writeln(lst,'RO=',RO:3:5);
 writeln(lst,'fo=',fo:3:5);
 writeln(lst,'fn=',fn:3:5);
 writeln(lst,'sum1=',sum1:3:5);
 writeln(lst,'sum2=',sum2:3:5);
 writeln(lst,'t1=',t1:3:5);
 writeln(lst,'intf=',intf:3:5);
 writeln(lst,'inf=',inf:3:5);
 writeln(lst,'intsro=',intsro:3:5);}
 close(lst);
end.
```